Aus dem Institut für Pharmakologie

der Universitätsmedizin

der Johannes Gutenberg-Universität Mainz

„Effects of Glucocorticoids on Vascular NADPH Oxidases and endothelial NO Synthase“

Dissertation

zur Erlangung des Grades

„Doktor der Naturwissenschaften“

am Fachbereich

Biologie

der Johannes Gutenberg-Universität

Mainz

Silke Tobias

geb. in Temeschburg

Mainz, August 2012

„Logik bringt Dich von A nach B, Phantasie überall hin.“

(Albert Einstein)

Für meine Familie

Tag der Prüfung: 29. Oktober 2012

I hereby declare that this submission is my own work and that, to the best of my knowledge and belief, it contains no material previously published or written by another person nor material which to a substantial extent has been accepted for the award of any other degree or diploma of the university or other institute of higher learning, except where acknowledgment has been made in the text.

Mainz, 14. August 2012

Silke Tobias

Index

Figures

Tables

Abbreviations

A549/8	human alveolar epithelium-like lung carcinoma cell line
A7r5	rat thoracic aorta smooth muscle cell line
ACh	acetylcholine
ACTH	adrenocorticotropic hormone
ANOVA	analysis of variance
ATP	adenosin triphosphate
BCA	bicinchoninic acid
BH_2	7,8-dihydrobiopterin
BH_4	(6R)-5,6,7,8-tetrahydrobiopterin
BP	blood pressure
bpm	beats per minute
BSA	bovine serum albumin
cDNA	complementary desoxyribonucleic acid
cGMP	cyclic guanosine monophosphate
^{125}I-cGMP	radioactively labeled cyclic guanosine monophosphate
CaM	calmodulin
CM	cytokine mix (IFN-γ, IL-1β, TNF-α)
COX	cyclooxygenase
CRF	corticotropin-releasing factor
C_T	threshold cycle
ctl	control
DBP	diastolic blood pressure
DEPC	Diethyl pyrocarbonate
DEX	dexamethasone
dH_2O	distilled water
DHFR	dihydrofolate reductase
DNA	desoxyribonucleic acid
DMEM	Dulbecco's modified Eagle's medium
DMNQ	2,3-Dimethoxy-1,4-Naphthochinone (redox cycler)
DMSO	dimethyl sulfoxide
dNTP	deoxynucleotide triphosphate

DPBS	Dulbecco's phosphate buffered saline
DTE	dithioerythritol
DUOX	Dual Oxidase
EA.hy 926	fusion of human alveolar epithelium-like lung carcinoma cells (A549/8) cell line with human umbilical vein endothelial cells (HUVEC) - cells were kindly provided by Cora-Jean S. Edgell, University of North Carolina at Chapel Hill, USA
E. coli	*Escherichia coli*
EDRF	endothelium-derived relaxing factor
EDTA	ethylenediaminetetraacetic acid
e.g.	for example (abbr. of Latin "exempli gratia")
eNOS	endothelial NO synthase
ER	endoplasmatic reticulum
et al.	and others (abbr. of Latin "et alia")
FACS	fluorescence-activated cell sorting
FAD	flavin adenine dinucleotide
FCS	fetal calf serum
GC	glucocorticoid
GCH1	GTP cyclohydrolase I
GC-HT	glucocorticoid-induced hypertension
GPx	glutathione peroxidase
GR	glucocorticoid receptor
GTP	guanosine triphosphate
GTPCH	GTP cyclohydrolase I (encoded by the gene GCH1)
h	hour(s)
H_2DCFDA	dichlorodihydrofluorescein diacetate
H_2O_2	hydrogen peroxide
HAT	hypoxanthine-aminopterin-thymidine
HBSS	Hank’s Balanced Salt Solution
HCASMC	human coronay artery smooth muscle cells (primary cells)
HPLC	high-performance liquid chromatography
HR	heart rate
HT	hypoxanthine-thymidine
HUVEC	human umbilical vein endothelial cells

IBMX	3-isobutyl-1-methylxanthine
ICAM-1	intercellular adhesion molecule 1
i.e.	that is (abbr. of Latin "id est")
IL-6	interleukin 6
iNOS	inducible NO synthase
L-012	8-amino-5-chloro-7-phenylpyrido[3,4-d]pyridazine-1,4-(2H,3H) dione
LB	lysogeny broth
L-NAME	N^G-nitro-L-arginine methyl ester (NOS inhibitor)
LPS	lipopolysaccharide
mg	milligram
min	minute(s)
mN	millinewton
MP	milk powder
mRNA	messenger-RNA
NaCl	sodium chloride
NADPH	reduced nicotinamide adenine dinucleotide phosphate
NF-κB	nuclear Factor 'kappa-light-chain-enhancer' of activated B-cells
ng	nanogram
nm	nanometer
nNOS	neuronal NO synthase
NO	nitric oxide
NOLA	N-nitro-L-arginine
NOS	nitric oxide synthase
Nox	homolog proteins of the NADPH-oxidase subunit $gp91^{phox}$
NOXO1	Nox Organizer Protein 1
NOXOA1	Nox Activator Protein 1
OD	optical density
PBS	phosphate buffered saline
PCR	polymerase chain reaction
phox	phagocyte oxidase
PLB	passive lysis buffer
PMA	phorbol-12-myristate-13-acetate
rcf	relative centrifugal force

RFL-6	fibroblasts from fetal rat lungs that express soluble guanylyl cyclase but do not express eNOS - cells were obtained from ATCC (# CCL-192)
RIA	radioimmunoassay
RNA	ribonucleic acid
RNase	ribonuclease
RNS	reactive nitrogen species
ROS	reactive oxygen species
rpm	rotations per minute
RT	room temperature
RT-PCR	reverse transcription PCR
qRT-PCR	quantitative “real-time” PCR
SBP	systolic blood pressure
SDS	sodium dodecyl sulfate
SDS-PAGE	SDS polyacrylamide gel electrophoresis
sec	second(s)
SEM	standard error of the mean
siRNA	small interfering RNA
SNP	sodium nitroprusside
SOD	superoxide dismutase
TAE	buffer solution containing tris base, acetic acid & EDTA
TBP	TATA-Box binding protein
TBS	tris buffered saline
TBST	tris buffered saline + tween
TNF-α	tumor necrosis factor α
UTR	untranslated region
UV	ultraviolet
VEGF	vascular endothelial growth factor
VPR	Volume Pressure Recording
WKY	Wistar Kyoto (rat strain used for *in vivo* experiments)
XDH	xanthine dehydrogenase
XO	xanthine oxidase
XOR	xanthine oxidoreductase

1 Introduction

1.1 Oxidative Stress and Its Impact on the Cardiovascular System

Evolving from the ATP-providing reaction from molecular oxygen (O_2) and hydrogen (H_2) to water (H_2O), radical and non-radical oxygen species like superoxide (O_2^-) are highly chemically instable (Thannickal and Fanburg, 2000). They feature unpaired electrons and thus a very high reactivity. Reactive oxygen species (ROS), including superoxide (O_2^-), hydrogen peroxide (H_2O_2), hydroxyl anion (OH^-), and reactive nitrogen species, such as nitric oxide (NO) and peroxynitrite ($ONOO^-$), are biologically important O_2 derivatives that are fundamental in vascular biology through their oxidation / reduction (redox) potential (Touyz and Schiffrin, 2004).

All vascular cell types (endothelial cells, vascular smooth muscle cells, and adventitial fibroblasts) produce ROS, primarily via cell membrane-associated NADPH oxidase. ROS participate in growth, apoptosis and migration of vascular smooth muscle cells, in the modulation of endothelial function, including endothelium-dependent relaxation and expression of pro-inflammatory phenotype, and in the modification of the extracellular matrix (Fortuño *et al.*, 2005).

Oxidative stress is no longer perceived as a simple imbalance between the production and scavenging of ROS (where prooxidants overwhelm antioxidant capacity) but as a dysfunction of enzymes involved in ROS production. NADPH oxidases are at the center of these events, underlying the dysfunction of other oxidases including NOS uncoupling, xanthine oxidase and mitochondrial dysfunction (Schramm *et al.*, 2012). Being of strong pathophysiological relevance, oxidative stress can cause random cell damage and is able to initiate intracellular signaling pathways that can lead to cell death (Slater, 1995). Oxidative stress and associated oxidative damage are mediators of vascular injury and inflammation in many cardiovascular diseases, including hypertension, atherosclerosis, hyperlipidemia and diabetes. Increased generation of ROS has been demonstrated in experimental and human hypertension (Touyz and Schiffrin, 2004). Affected vessel cells unavoidably undergo structural and functional

pathophysiological changes. Finally those modifications cause endothelial dysfunction and cardiovascular diseases (Cai and Harrison, 2000).

1.2 NADPH Oxidases – Important ROS Producers in the Vasculature

Within the last years on molecular level various enzymes could be identified, which scientists today hold responsible for the development of oxidative stress in diverse tissues (Geiszt, 2006). Some of those enzymes show a striking homology to the phagocytic NADPH oxidase and are now known as Nox family. Scientists assume that oxidative stress coming from NADPH oxidases induces the release of ROS produced by other enzymatic systems (Brandes and Kreuzer, 2005; Griendling, 2004) like xanthine oxidase (McNally *et al.*, 2003). NADPH oxidases are the only known enzyme family with the sole function to produce ROS (Altenhöfer *et al.*, 2012).

NADPH oxidases are multimeric protein complexes with six trans-membrane spanning alpha helices with cytosolic N- and C-termini. They consist of up to three cytosolic subunits ($p47^{phox}$, $p67^{phox}$ and $p40^{phox}$), a regulatory G-protein (Rac1 or Rac2) and a membrane-bound cytochrome b558 reductase domain (Figure 1.1). The cytochrome b558-domain is built up of two proteins: one smaller α-subunit ($p22^{phox}$) and a bigger catalytic β-subunit ($gp91^{phox}$). The latter contains flavin and iron groups as well as binding sites for NADPH and molecular oxygen. The β-subunit is needed to assure electron transport over the cell membrane by transferring electrons from NADPH to molecular oxygen (Bengtsson *et al.*, 2003). An increased expression of NADPH oxidases significantly contributes to the pathogenesis of cardiovascular diseases.

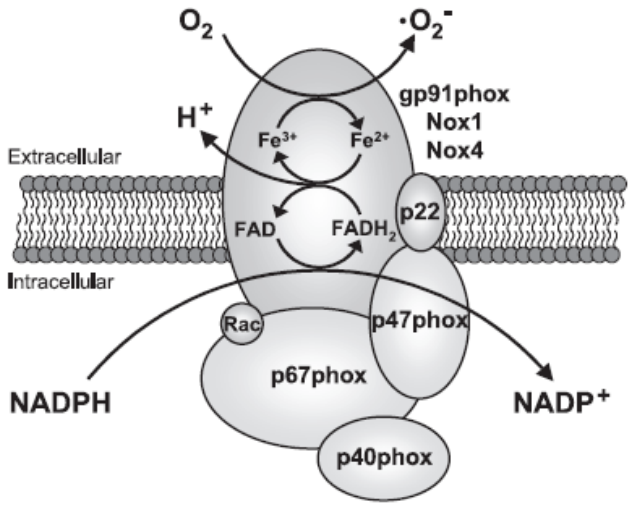

Figure 1.1: Biochemistry and general structure of NADPH oxidases. The electron flow (displayed by arrows) leads from the reduced form of nicotinamide adenine dinucleotide (NADPH) to flavine adenine dinucleotide (FAD), followed by iron (Fe) and eventually gets transferred to molecular oxygen (O_2) whereby superoxide (O_2^-) is produced. (Bengtsson *et al.*, 2003)

NADPH oxidases are located in the plasma membrane as well as within the membrane of phagosomes. Different Nox isoforms enable electron transfer across biological membranes (Bedard and Krause, 2007). After the catalytic subunit gp91^{phox} / Nox2 was first discovered in phagocytes, numerous other homologs could be identified in various cells and tissues (Figure 1.2). The Nox family consists of seven members, Nox1–5, and two dual oxidases (DUOX), DUOX1 and DUOX2. Of those, Nox1, 2, 4, and 5 have been implicated in vascular diseases (Altenhöfer *et al.*, 2012).

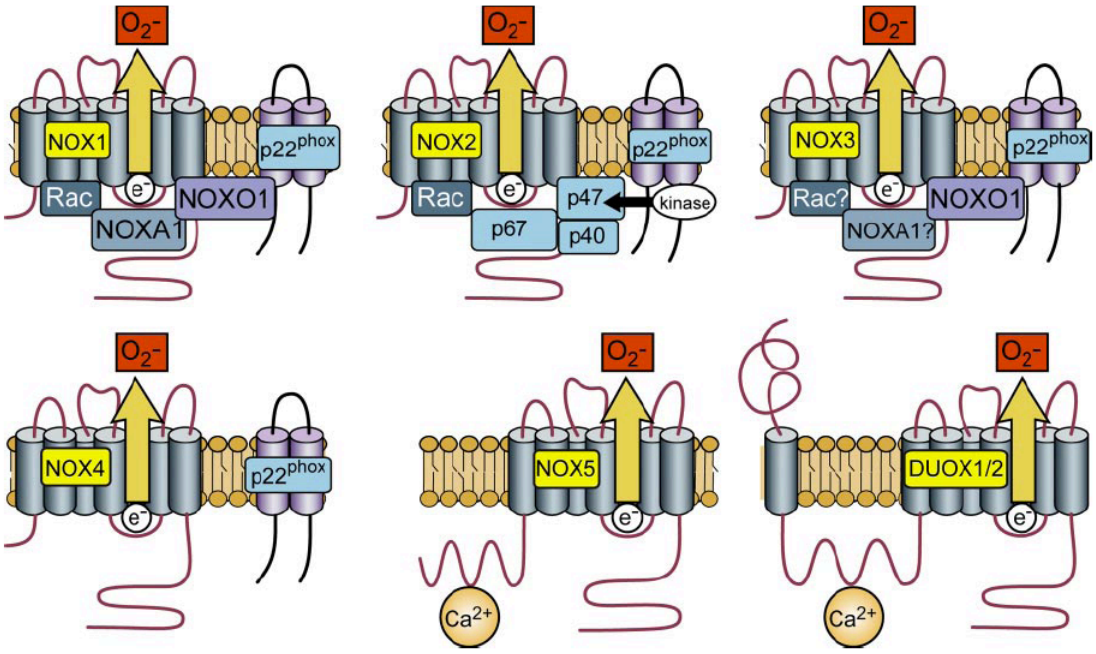

Figure 1.2: Activation of Nox isoforms.
Members of the Nox family have a similar structure and enzymatic function but differ in their mechanisms of activation. **A**: Nox1 activity requires p22^{phox}, NOXO1 (or possibly p47^{phox} in some cases) and NOXA1, and the small GTPase Rac. **B**: Nox2 requires p22^{phox}, p47^{phox}, p67^{phox}, and Rac; p47^{phox} phosphorylation is required for Nox2 activation. Although not absolutely required, p40^{phox} also associates with this complex and may contribute to activation. **C**: Nox3 requires p22^{phox} and NOXO1; the requirement for NOXA1 may be species dependent, and the requirement of Rac is still debated. **D**: Nox4 requires p22^{phox}, but in reconstitute systems it is constitutively active without the requirement for other subunits. However, in native Nox4-expressing cells, activation, possibly including Rac, has been described. **E** and **F**: Nox5, DUOX1, and DUOX2 are activated by Ca^{2+} and do not appear to require other subunits. (Bedard and Krause, 2007)

NADPH oxidases are the main source of ROS in the vascular system. There are four Nox isoforms located in the vessel walls (Griendling, 2004; Lassègue and Clempus, 2003).

Table 1.1: Expression of Nox subunits in the cardiovascular system.
(*only human; EC = endothelial cell; ND = not determined; VSMC = vascular smooth muscle cell)

	Nox1	Nox2	Nox3	Nox4	Nox5
VSMCs from conduit vessels	+	–	–	+++	+*
VSMCs from resistance vessels	–	+	ND	ND	ND
EC	+	+	ND	++++	+*
Cardiac myocytes	ND	++	ND	+	ND
Cardiac fibroblasts	+	+	ND	+++	ND

(Griendling, 2004)

1.2.1 Nox1

Nox1 was the first described homolog of Nox2. Those two isoforms share 60 % amino acid sequence identity (Bedard and Krause, 2007). So far one alternative splice variant (Nox1v) has been identified, lacking exon 11. This exon encodes amino acids predicted to participate in the binding of NADPH; thereby the lack of this region diminishes the ability of Nox1v to generate ROS (Geiszt and Leto, 2004). $p22^{phox}$, NOXO1 (or $p47^{phox}$) and NOXA1 (or $p67^{phox}$) seem to be essential for a functional Nox1 enzyme (Lambeth, 2004; Bedard and Krause, 2007). The predicted sizes of Nox1 and Nox1v are 65 kDa and 59 kDa respectively; however the commonly observed bands of this protein in SDS-PAGEs are 50-65 kDa (Dikalova *et al.*, 2005; Arnold *et al.*, 2007; Cui *et al.*, 2006). Of note is that immunodetection of Nox proteins is not well established and available antibodies differ in their immunoreactivity. Thus, also subcellular localization of endogenous Nox1 is controversially described. Most of the studies with recombinant Nox1 protein show localization within cell membranes, particularly in the plasma membrane (Helmcke *et al.*, 2009; Chen *et al.*, 2008; Ambasta *et al.*, 2004). Using immunofluorescence microscopy, also endogenous Nox1 protein displayed surface distribution along cellular margins (Hanna *et al.*, 2004). Nox1 was found in many different types of cells and tissue. Nevertheless, the highest expression level of Nox1 was detected in colon epithelium and in a cell line derived from colorectal carcinoma (Bánfi *et al.*, 2003). ROS derived from the Nox1 enzyme are involved in Ras-dependent malignant transformation (Mitsushita *et al.*, 2004). The transformation mechanism

may involve Nox1-derived ROS triggering mutagenesis in oncogenes or tumor suppressor genes, and an action of Nox1-derived ROS as intracellular mediators in the regulation of proliferation (Kamata, 2009; Mitsushita *et al.*, 2004). Relevant ROS targets related to growth and transformation may include p42/p44 mitogen activated protein kinase (MAPK) (Schäfer *et al.*, 2003), p38 MAPK (Wang *et al.*, 2007), signal transducers and activators of transcription (STAT) (Nakajima *et al.*, 2004), vascular endothelial growth factor (VEGF) (Arbiser *et al.*, 2002), Akt1 (alias protein kinase B) (Esposito *et al.*, 2003), nuclear factor kappa-light-chain-enhancer of activated B cells (NF-κB) (Chandel *et al.*, 2000; Dodd *et al.*, 2010) and activator protein-1 (AP-1) (Wu *et al.*, 2005). This aspect is also very important in different cardiovascular diseases. On the other hand, many signaling mediators have been shown to induce Nox1. ROS generation mediated by Nox1 can be triggered by platelet-derived growth factor (PDGF), epidermal growth factor (EGF), prostaglandin F2α (PGF2α) (Fan *et al.*, 2005a; Fan *et al.*, 2005b; Katsuyama *et al.*, 2005; Park *et al.*, 2004) and by angiotensin II (ang II) (Lassègue *et al.*, 2001). The molecular mechanism of Nox1 activation by these factors includes signaling cascades leading to increased mRNA expression or activation of NADPH oxidase subunits.

1.2.2 Nox4

Of the catalytic NADPH oxidase subunits, Nox4 is the most widely distributed isoform (Altenhöfer *et al.*, 2012). The enzyme could be identified strongly expressed in the kidney, why it was initially referred to as “Renox” by Leto and co-workers (Geiszt *et al.*, 2000). There the enzyme functions as “oxygen sensor” and thereby is involved in the regulation of the erythropoietin synthesis (Geiszt, 2006). In addition to the kidney Nox4 is also expressed in numerous other tissues and cells like heart, pancreas, skeletal muscle, ovaries, testes, but also endothelial cells, smooth muscle cells and fibroblasts (Krause, 2004). In endothelial cells Nox4 is even the most abundant Nox isoform (Table 1.1). In the vascular system it seems to be involved in genesis and progression of human coronary atherosclerotic disease (Sorescu *et al.*, 2002). Nox4 builds a functional complex in combination with $p22^{phox}$ which constitutively produces superoxide (Ambasta *et al.*, 2004). The knockdown of Nox4 or $p22^{phox}$ reduced endothelial ROS production in HUVECs (Ago *et al.*, 2004; Kuroda *et al.*, 2005). However, for its enzymatic function this complex does not need any further cytosolic subunits like NOXO1 and NOXA1 or $p47^{phox}$ and $p67^{phox}$ (Brandes and Kreuzer, 2005).

Martyn *et al.* were able to show that not even the GTPase Rac is necessary for the regulation of Nox4 (Martyn *et al.*, 2006). Suppression of Nox4 via antisense oligonucleotides led to a reduced superoxide production in endothelial cells (Ago *et al.*, 2004; Kuroda *et al.*, 2005). Additionally, in patients with endothelial dysfunction, a strong correlation between Nox4 expression, ROS production and the extent of the present dysfunction in those vessels could be demonstrated (Guzik *et al.*, 2004). Elevated Nox4 expression could also be observed in early stages of atherosclerotic lesions (Sorescu *et al.*, 2002). In smooth muscle cells Nox4 is located in the ER and the nucleus (Hilenski *et al.*, 2004; Pedruzzi *et al.*, 2004). ROS production in this cell type is strongly dependent on the expression level of Nox4. For instance, a 65 % down-regulation of Nox4 mRNA led to a drop in superoxide production of 41 %, without having any influence on the expression of Nox1 (Ellmark *et al.*, 2005). It is known that Nox4 is involved in the genesis of superoxide within inflammatory processes. An elevated mRNA and protein expression as well as increased superoxide production could be demonstrated in human aortic smooth muscle cells after TNF-α treatment (Moe *et al.*, 2006). The role of Nox4 in the proliferation of smooth muscle cells is uncertain. Very likely it is comparable to other Nox isoforms and enforces proliferation. TGF-β1 increased the expression of Nox4 as well as the ROS-dependent proliferation in pulmonary artery smooth muscle cells. This effect could partially be inhibited by Nox4 siRNA (Sturrock *et al.*, 2006).

1.3 Uncoupled eNOS as ROS Producer

In 1989 an enzyme was described for the first time, that produces nitric oxide (NO) in a calcium-dependent manner and uses L-arginine as substrate: the NO synthase (NOS) (Förstermann *et al.*, 1989; Moncada *et al.*, 1989). Depending on the tissue, this reaction is catalyzed by one of three different NOS isoforms - neuronal NO synthase (nNOS, NOS I), inducible NO synthase (iNOS, NOS II), endothelial NO synthase (eNOS, NOS III) (Förstermann *et al.*, 1994). eNOS is a constitutively expressed enzyme whose activity is calcium-dependent (Förstermann and Kleinert, 1995). It was first isolated out of bovine aortic endothelial cells (Förstermann *et al.*, 1991); later on it could be detected in human endothelial cells as well (Janssens *et al.*, 1992). Immunohistochemical analyses revealed eNOS being present in various types of endothelial cells of arterial and venous origin (Pollock *et al.*, 1993) but it could also be detected in numerous other mammalian cells like cardiac myocytes and thrombocytes

(Michel and Feron, 1997), certain neurons of the brain, in syncytiotrophoblasts of human placenta, and in kidney tubular epithelial cells (Förstermann and Sessa, 2011).

1.3.1 Physiological and Protective Effects of eNOS

The functional NOS is built up of two monomers, each subunit consisting of a reductase domain and an oxygenase domain, which are connected via a zinc-thiolate cluster (Figure 1.3). Monomers and isolated reductase domains can bind calmodulin (CaM), which stimulates the electron transfer within the reductase domain. However, monomers are unable to bind the cofactor (6R-)5,6,7,8-tetrahydrobiopterin (BH_4) or the substrate L-arginine and cannot catalyze NO production (Förstermann and Münzel, 2006). The presence of heme allows NOS dimerization. Heme is the only cofactor that is absolutely required for the formation of active NOS dimers. Heme also is essential for the interaction between reductase and oxygenase domains and for the interdomain electron transfer from the flavins to the heme of the opposite monomer (Förstermann and Münzel 2006).

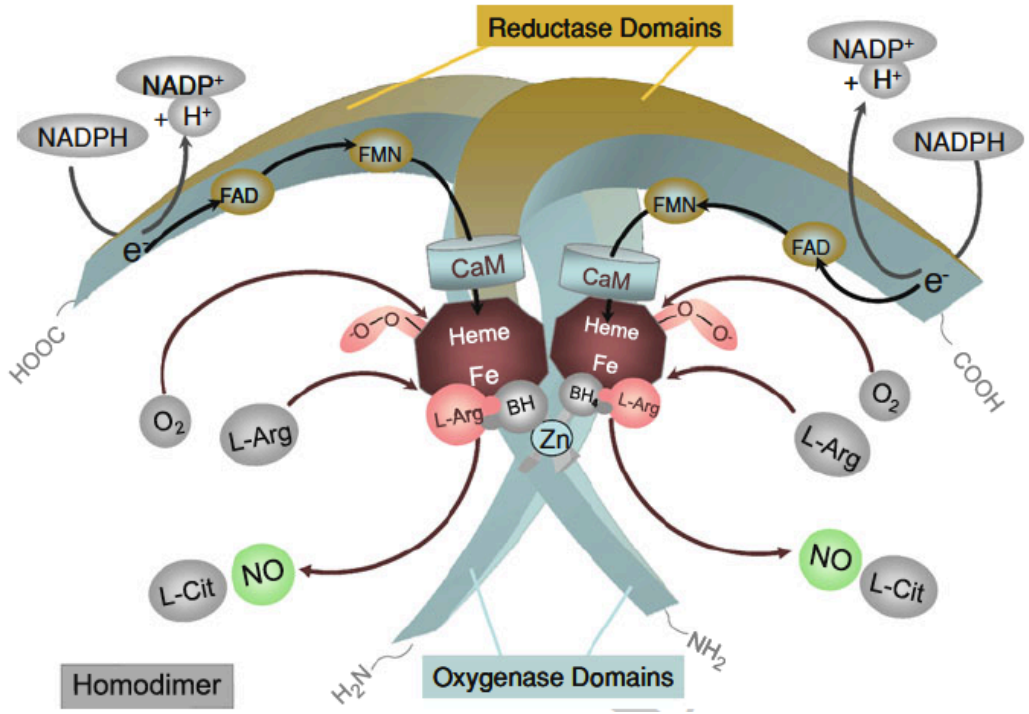

Figure 1.3: Structure and catalytic mechanisms of the functional endothelial NO synthase. (Förstermann and Li, 2012) See text above for further information.

The N-terminal oxygenase domain of the first monomer interacts with the C-terminal reductase domain of the second monomer. The oxygenase domain carries the prosthetic heme group and binds BH_4, molecular oxygen and the substrate L-arginine. The reductase domain binds nicotinamide adenine dinucleotide phosphate (NADPH), flavin adenine dinucleotide (FAD) and flavin mononucleotide (FMN) (Förstermann *et al.* 1994). NADPH releases electrons that are passed on from the first monomer over the interconnected elements FAD, FMN and CaM to the heme group and transferred into the oxygenase domain of the second monomer. Within the oxygenase domain the molecular oxygen is reduced and L-arginine as substrate gets hydroxylated. The intermediate N^{ω}-OH-L-arginine is generated, which decays into NO and citrulline in an oxidation reaction (Stuehr *et al.* 2001). L-citrulline is formed as a by-product.

NO derived from eNOS is a homeostatic regulator of numerous essential cardiovascular functions. NO produced by eNOS dilates all types of blood vessels by stimulating soluble guanylyl cyclase and increasing cyclic GMP in smooth muscle cells (Rapoport *et al*., 1983; Ignarro *et al*., 1987). Deletion of the eNOS gene leads to elevated blood pressure (Huang *et al*., 1995). Besides its ability to inhibit platelet aggregation and adhesion to the vessel wall, it also prevents proliferation of smooth muscle cells (Alheid *et al*., 1987; Busse *et al.*, 1987). Furthermore endothelium-derived NO has an anti-atherosclerotic effect. It can inhibit leucocyte adhesion to the vessel wall, which is an early event in the development of atherosclerosis. Thus, NO may protect against the onset of atherogenesis (Kubes *et al*., 1991). Also anti-inflammatory effects mediated by NO are known as well as the ability to stimulate angiogenesis (Dimmeler *et al*., 1999b). eNOS expressed by bone marrow stromal cells influences recruitment of stem and progenitor cells. Reduced systemic NO bioactivity seen in ischemic heart disease may therefore contribute to impaired neovascularization (Aicher *et al*., 2003). In patients with ischemic cardiomyopathy the NO bioavailability is typically reduced, also indicating a fundamental role of NO in neovascularization. Pre-treatment of bone marrow cells from these patients with 4-fluoro-N-indan-2-yl-benzamide (AVE9488), an enhancer of eNOS expression and activity, significantly increased eNOS expression and activity (Wohlfahrt *et al*., 2008; Sasaki *et al*., 2006).

1.3.2 Impact of NO on the Endothelium

Nitric oxide (NO) is the smallest known signaling molecule (Förstermann *et al.*, 1995). Its relevance was highly valued with the Nobel Prize for physiology and medicine in 1998. Awardees were the scientists Furchgott, Ignarro and Murad. First and foremost they received the prize for the research in NO signal transduction. Furchgott and Zawadzki were the first ones to describe endothelial-dependent relaxation of isolated vessels after application of acetylcholine (Furchgott and Zawadzki, 1980). Subsequent studies revealed EDRF (endothelium-derived relaxing factor) as trigger for the observed relaxation, which stimulates the activity of the soluble guanylyl cyclase (Furchgott *et al.*, 1984). Ferid Murad found out that NO is a potent stimulator of the soluble guanylyl cyclase (Murad *et al.*, 1978) before 1988 when Furchgott and Ignarro, independently from each other, could show that EDRF and NO are identical (Furchgott, 1988; Ignarro *et al.*, 1988).

NO plays a crucial role in cardiovascular homeostasis and in the pathogenesis of cardiovascular disease. The bioactivity of NO in the vessel wall is dependent on several factors: eNOS expression, supply of eNOS with substrate and cofactors, phosphorylation status and presence of ROS that can deactivate NO (Searles 2006). Beside its relevance as inhibitor of thrombocyte adhesion and aggregation (Alheid *et al.*, 1987; Busse *et al.*, 1987), inhibition of leukocyte adhesion by NO could be demonstrated later as well (Kubes *et al.* 1991). Furthermore, DNA synthesis, mitogenesis and proliferation of smooth muscle cells are inhibited by NO (Garg 1989; Hogan and Cerami 1992; Nakaki *et al.*, 1990).

NO as a vasodilating factor is crucial for blood pressure regulation. Huang *et al.* could show that eNOS knockout mice develop hypertension and possess a decreased NO-mediated vasodilation (Huang *et al.*, 1995). NO generated by eNOS has anti-atherosclerotic functions that could be verified in animal models as well (Li and Förstermann, 2000). Pharmacological inhibition of eNOS in rabbits (Cayatte *et al.*, 1994) and mice (Kauser *et al.*, 2000) as well as the additional deletion of the eNOS gene in ApoE knockout mice (Kuhlencordt *et al.*, 2001) led to an accelerated development of atherosclerosis.

1.3.3 eNOS Expression and Uncoupling under Pathological Conditions

Cardiovascular risk factors and vascular disease are associated with an elevated ROS production (Cai *et al.*, 2001; Patterson *et al.*, 2000). There are several enzyme systems that can potentially produce ROS in the vessel wall, including NADPH oxidases, xanthine oxidase, enzymes of the mitochondrial respiratory chain and uncoupled eNOS (Mueller *et al*. 2005). An increased degradation of NO by its reaction with superoxide could be observed in vascular disease, due to enhanced oxidative stress. However, oxidative stress has also been shown to convert eNOS from an NO-producing enzyme to an enzyme that generates superoxide. This process is known as eNOS uncoupling. Mechanisms involved in eNOS uncoupling include oxidation of the cofactor BH_4, depletion of L-arginine and accumulation of endogenous methylarginines. More recently, S-glutathionylation of eNOS has been proposed as yet another mechanism leading to eNOS uncoupling (Förstermann and Sessa, 2011). Numerous diseases of the cardiovascular system lead to changes also in eNOS expression. Animals with an increased cholesterol level showed an elevated expression of the enzyme, probably indicating a compensatory mechanism. An atherogenic diet induced an increase in eNOS expression in New Zealand rabbits (Kano *et al.*, 1999). Nevertheless, levels of bioactive NO and thus endothelium-dependent vasorelaxation were clearly decreased, probably through NO inactivation via ROS or eNOS uncoupling (Li *et al.*, 2002). In late phases of atherosclerosis, eNOS expression was diminished. This could be shown in humans (Oemar *et al.*, 1998) as well as pigs (Stulak *et al.*, 2001) and guinea pigs (Schwemmer *et al.*, 2000). Also in diabetes mellitus a decreased vasorelaxation with limited availability of bioactive NO was described, whereas eNOS expression was unchanged or elevated (Hink *et al.*, 2001; Kobayashi and Kamata, 2001). During progression of hypertension a biphasic eNOS regulation becomes apparent. Comparable to the different stages of atherosclerosis, in early phases eNOS expression is unchanged or slighty increased whereas it appears massively decreased at later time-points (Li *et al.*, 2002). Plasma levels of cGMP and NO species (NO_2^-, NO_3^-) were lowered in hypertensive patients (Takase *et al.*, 2000). Thus, also here eNOS functionality was reduced and NO was inactivated by ROS respectively (Berry *et al.*, 2001; Zalba *et al.* 2001). During cardiac insufficiency both eNOS mRNA and protein level were elevated in human myocardial cells (Stein *et al.*, 1998). However, in vascular cells of rats (Comini *et al.*, 1996) a reduced expression could be observed.

1.3.4 Mechanisms of eNOS Uncoupling

When eNOS is uncoupled, the production of NO is omitted and ROS are generated instead (Figure 1.4). Superoxide produced by an uncoupled eNOS could be demonstrated both in cell culture experiments (Pritchard *et al.*, 1995) as well as *in vivo* experiments (Cosentino and Lüscher, 1999; Kerr *et al.*, 1999; Mollnau *et al.*, 2002). Antioxidants on the one hand can prevent eNOS uncoupling and on the other hand are able to inactivate produced superoxide radicals.

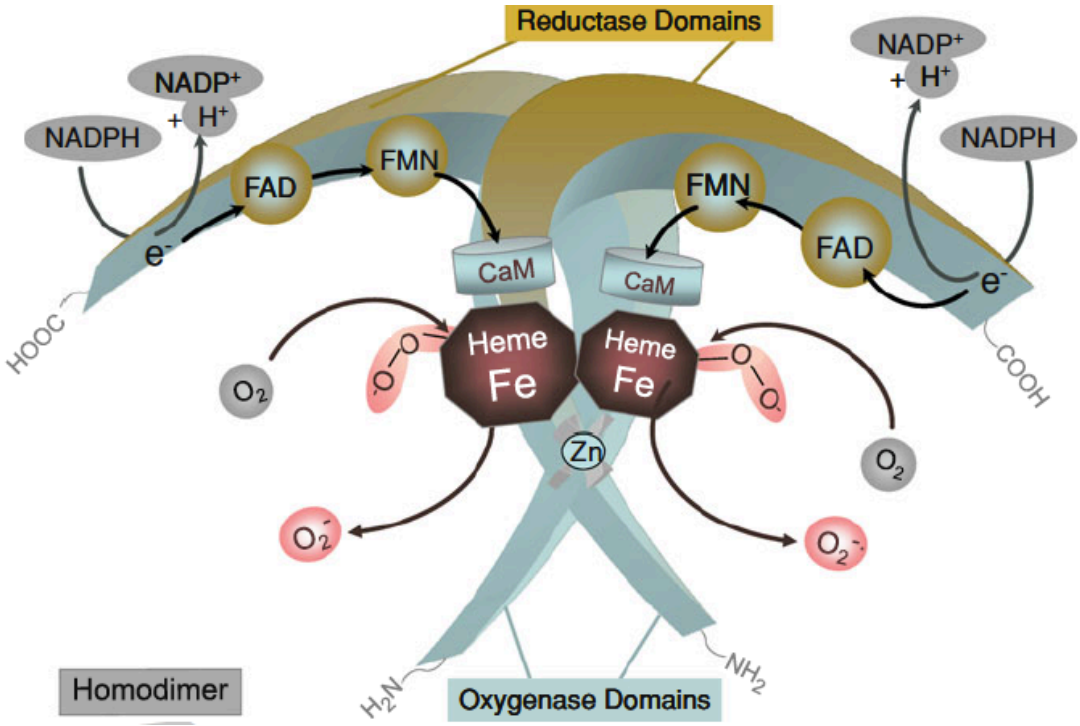

Figure 1.4: The uncoupled eNOS. (Förstermann and Li, 2012) See text for further information.

There are several factors of importance for eNOS uncoupling. A diminished supply of eNOS with its substrate L-arginine can lead to uncoupling. Local lack of arginine occurs in human cells e.g. when arginase II expression or activity is increased (Bachetti *et al.*, 2004; Ming *et al.*, 2004). Such an increase could be demonstrated in lung endothelium of patients suffering from pulmonary hypertension (Xu *et al.*, 2004). Production of NO and L-citrulline is highly dependent on intracellular concentration of the essential cofactor BH_4 (Werner-Felmayer *et al.*, 1993). There are two causes possible for decreased BH_4 concentrations: On the one hand ROS can increase BH_4 oxidation

(Laursen *et al.*, 2001), on the other hand the *de novo* synthesis of BH_4 can be reduced (Moat *et al.*, 2006). Superoxide reacts with NO to form $ONOO^-$, which in turn oxidizes BH_4 to trihydrobiopterin (BH_3^-) and dihydrobiopterin (BH_2) (Werner *et al.*, 2003; Förstermann and Sessa, 2011) (Figure 1.5). In several animal models depletion of BH_4 and a subsequent eNOS uncoupling (Hong *et al.*, 2001; Shinozaki *et al.*, 1999) could be demonstrated. Peroxynitrite also oxidizes the zinc-thiolate cluster of eNOS and for this reason causes the loss of central zinc cations with subsequent eNOS dimer destabilization (Zou *et al.*, 2002). Monomers are unable to bind the cofactor BH_4 or the substrate L-arginine and cannot catalyze NO production (Förstermann and Münzel, 2006).

Accordingly to mechanisms that lead to eNOS uncoupling, there are ways to regenerate the enzyme back to a coupled status. Drexler *et al.* showed that in patients with hypercholesterolemia, coronary microcirculation could be improved by L-arginine supplementation (Drexler *et al.*, 1991). Reduced BH_4 levels can be countered with supplementation of the cofactor itself or by addition of folic acid. In this way, patients with hypercholesterolemia, essential hypertension and diabetes also profit from BH_4 treatment, as well as chronic smokers (Heitzer *et al.*, 2000a; Heitzer *et al.*, 2000b; Higashi *et al.*, 2002; Stroes *et al.*, 1997). Vitamin C supports the regeneration from BH_2 to BH_4. This led to improved endothelial function in patients with chronic heart failure (Heitzer *et al.*, 2001) and to an enhanced endothelium-dependent vasodilation in diabetes patients (Ting *et al.*, 1996).

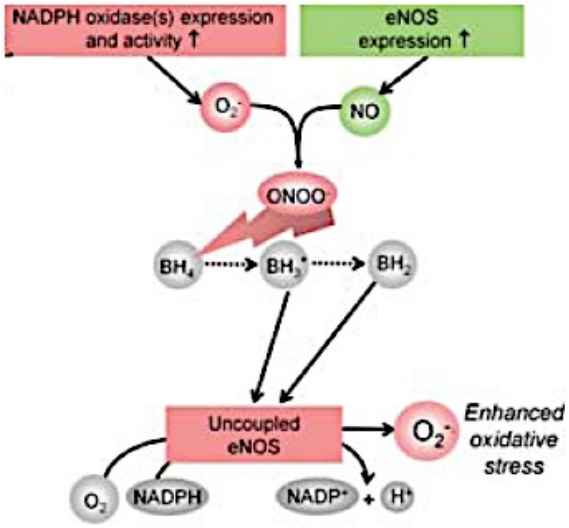

Figure 1.5a: BH_4 hypothesis for eNOS uncoupling. The products of NADPH oxidases and eNOS, O_2^- and NO, rapidly recombine to form peroxynitrite ($ONOO^-$). This can oxidize the essential cofactor of eNOS tetrahydrobiopterin (BH_4) to trihydrobiopterin radical (BH_3^+) which in turn can disproportionate to the quinonoid dihydrobiopterin (BH_2). As a consequence, O_2 reduction by eNOS is uncoupled from NO formation, and a functional eNOS is converted into a dysfunctional O_2^- generating enzyme that contributes to vascular oxidative stress. (Förstermann and Sessa, 2011)

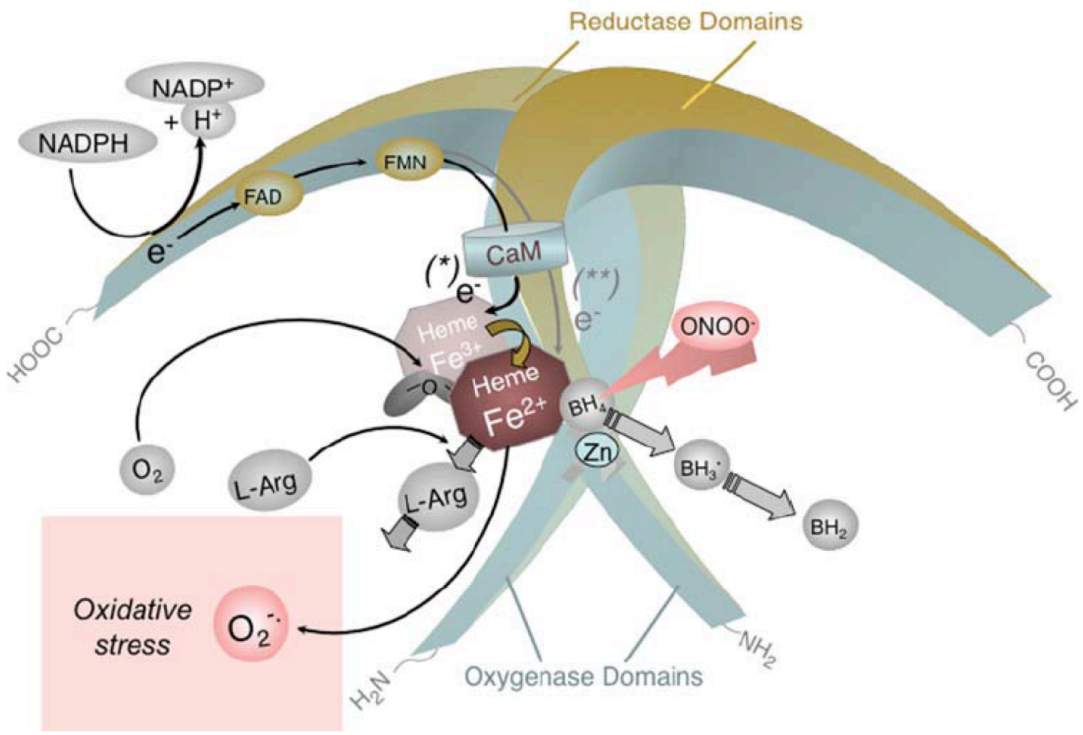

Figure 1.5b: BH_4 hypothesis for eNOS uncoupling. Oxidation of BH_4 by $ONOO^-$ results in biologically inactive products such as the BH_3^+ radical or BH_2 that also reduces the affinity of the substrate L-arginine (L-Arg) to NO, and eNOS catalyzes the uncoupled reduction of O_2, leading to the production of superoxide (O_2^-). (Förstermann, 2010)

1.3.5 Role of BH_4 in eNOS Functionality

Endothelial BH_4 availability is a crucial regulator of eNOS activity and enzymatic coupling *in vivo* (Bendall *et al.*, 2005). It is the stoichiometric relationship between the cofactor BH_4 and eNOS rather than the absolute BH_4 level that is important for eNOS functionality - coupled or uncoupled. Even in the absence of increased oxidative stress, eNOS overexpression in the endothelium without concomitant increase in BH_4 concentration can result in eNOS uncoupling (Bendall *et al.*, 2005).

In normal vascular tissue the vast majority of vascular BH_4 is present in the endothelium (Tiefenbacher *et al.*, 2000). BH_4 is synthesized from guanosine 5'-triphosphate (GTP) via a *de novo* pathway catalyzed by the rate-limiting enzyme GTP cyclohydrolase I (GCH1). Alternatively, the synthesis of BH_4 can occur via the so-called salvage pathway from BH_2 back to BH_4 by an enzyme named dihydrofolate reductase (DHFR) (Alp and Channon, 2004). BH_4 functions as both an allosteric and redox cofactor for eNOS, stabilizes the enzyme and improves the L-arginine binding affinity. In the

catalytic cycle of NO synthesis BH_4 provides the second electron to the heme of eNOS (Li and Förstermann, 2009). BH_2, as a partially oxidized analog of BH_4, has no eNOS cofactor activity and is unable to prevent ROS formation by eNOS (Gao *et al.*, 2007). Since BH_2 competes with BH_4 for eNOS binding, it might even lead to enhanced superoxide formation from eNOS in the presence of saturating L-arginine concentration (Vásquez-Vivar *et al.*, 2002). Crabtree *et al.* even postulated that for eNOS functionality BH_4 / BH_2 ratio may be more important than the absolute BH_4 concentration. BH_4 and BH_2 bind eNOS with equal affinity and BH_2 can rapidly and efficiently replace BH_4 in pre-formed eNOS-BH_4 complexes (Crabtree *et al.*, 2008). Thus, probably diminished intracellular BH_4 / BH_2, rather than BH_4 depletion *per se*, is the molecular trigger for NO insufficiency.

1.4 Glucocorticoids and Their Impact on the Cardiovascular System

Glucocorticoids (GCs) are steroid hormones that are synthesized in the adrenal cortex without previous storage but generated and released into the blood as required. Deriving from the anterior pituitary, the adrenocorticotropic hormone (ACTH) stimulates glucocorticoid secretion and itself is controlled by the corticotropin-releasing factor (CRF) (Munck *et al.*, 1984). Increasing blood concentrations of endogenous or exogenous GCs as well as stress intervene in this regulatory circuit via negative feedback (Sendelbeck and Yates, 1970). Therefore, an elevated GC level inhibits the release of CRF. Because of the missing stimulus for ACTH flow, the synthesis of endogenous cortisol is inhibited. In the regulation of essential physiological processes, including immune response, energy metabolism, electrolyte balance, blood pressure and stress response, GCs play an essential role. The action of GCs is mediated by the glucocorticoid receptor (GR). The GR is a DNA-binding transcription factor of the nuclear receptor superfamily and nearly ubiquitously expressed (Bookout *et al.*, 2006). Upon activation of the GR by endogenous or synthetic GCs it undergoes a structural conformational change that drives translocation from the cell cytoplasm into the nucleus (Biddie *et al.,* 2012). Once in the nucleus, the ligand-bound GR is available to interact with regulatory elements, where it is known to enhance and repress transcription of hundreds of target genes (So *et al.,* 2007; John *et al.*, 2009).

Chronic excessive activation of GR induces obesity, insulin resistance, glucose intolerance, dyslipidemia and hypertension. Subtle abnormalities of the hypothalamic pituitary adrenal axis and / or of tissue sensitivity to GCs are also associated with these cardiovascular risk factors in patients with the metabolic syndrome. Furthermore, GCs have direct effects on heart and blood vessels, mediated by both glucocorticoid and mineralocorticoid receptors (Walker, 2007). These effects influence vascular function, atherogenesis and vascular remodeling following intra-vascular injury or ischemia. Synthetic GCs, such as dexamethasone (DEX), play a fundamental role in the treatment of inflammatory diseases.

GCs are known to reduce eNOS mRNA and protein expression in human endothelial cells caused by transcriptional inhibition as well as mRNA destabilization (Wallerath *et al*., 1999). Since this effect is preventable by a GR-antagonist, the inhibition of eNOS expression should be mediated via glucocorticoids receptors. However, the human eNOS promoter does not feature an intact „glucocorticoid response element“ (GRE). Analyses revealed that GCs concentration-dependently decreased the binding affinity of the transcription factor GATA to eNOS promoter. The observed down-regulation of eNOS could also be demonstrated *in vivo*. Oral DEX treatment diminished eNOS mRNA level in several endothelium-rich organs in rats. Furthermore, plasma levels of NO_2^- / NO_3^- (NO oxidation products) were reduced to the same extent as well as endothelium-dependent vasodilation. In addition, a significant increase in blood pressure could be observed in DEX-treated animals (Wallerath *et al*., 1999). In $eNOS^{-/-}$ mice glucocorticoids had no effect on the blood pressure (Wallerath *et al*., 2004).

2 Objective of Research

Glucocorticoids (GCs) are important hormones in the regulation of metabolic homeostasis. Synthetic GCs, such as dexamethasone (DEX), play a fundamental role in the treatment of inflammatory diseases. There are numerous side effects of a GC therapy including the development of hypertension. In the pathogenesis of hypertension oxidative stress is a crucial factor. However, the source of this elevated superoxide production is unknown. Vascular diseases are often attended by elevated oxidative stress and NADPH oxidases (Nox) are the main source of reactive oxygen species (ROS) in the vascular system. An increased expression of Nox enzymes significantly contributes to the pathogenesis of cardiovascular diseases, thus a participation of this enzyme family in GC-induced oxidative stress seems likely. Hence, it should be investigated if NADPH oxidases are the source of this elevated ROS production stimulated by GCs. Glucocorticoid-induced hypertension (GC-HT) has been shown to be associated with an imbalance between nitric oxide (NO) and superoxide (O_2^-). In previous studies an influence of GCs on elevated blood pressure and concomitant downregulation of eNOS expression *in vivo* could be shown. In $eNOS^{-/-}$ mice GCs had no effect on the blood pressure. Also *in vitro* glucocorticoid treatment led to reduced eNOS expression. DEX, a potent synthetic glucocorticoid, is commonly used for studies of the generic effects of GCs in different disease states and various biological pathways. In this study it should be analyzed if an uncoupling of the endothelial NO synthase (eNOS), a key mediator of vascular homeostasis, may contribute to DEX-induced oxidative stress. Because BH_4 availability is a crucial regulator of eNOS activity and enzymatic coupling, the impact of DEX on this cofactor should be investigated. Alterations in the production of BH_4 contribute to GC-HT and an understanding of the mechanisms may provide new therapeutic options. Therefore it was important to further study the two pathways of BH_4 synthesis and the rate-limiting enzymes involved (GCH1 and DHFR) after DEX treatment. It should be analyzed if modifications in the supply of BH_4 through GCs eventually lead to eNOS uncoupling and thereby elevate oxidative stress.

3 Material and Methods

All chemicals used were purchased from the manufacturers Roth, Sigma-Aldrich or AppliChem unless stated otherwise. Cell culture and general laboratory material from Greiner and Eppendorf was used.

3.1 Molecular Cloning

3.1.1 Maintenance of Bacterial Glycerol Stocks

Genetically modified *E.coli* were stored as glycerol stocks (20 to 30 % glycerol (v/v) in LB medium) at -80 °C. For expansion of glycerol stock, LB medium was inoculated using autoclaved toothpicks and incubated over night at 37 °C at 250 rpm on a tilted platform.

3.1.2 Restriction of Plasmid DNA

Plasmid DNA was cut with the help of restriction enzymes (purchased from New England Biolabs). Restrictions allow the characterization of plasmid DNA as well as the preparation of DNA fragments for cloning. For analytical digestions 0.1-1 µg of plasmid DNA together with 1 U of enzyme was mixed with the appropriate buffer (depending on the used buffer, with or without BSA) up to a total volume of 10 µl, choosing temperature and incubation time according to the manufacturer's protocol. For preparative restrictions 5-10 µg of DNA were used and therefore the total volume had to be adjusted to 50 µl. Characterization of the DNA and control of the restriction digestion occurred via agarose gel electrophoresis.

3.1.3 Agarose Gel Electrophoresis

To control the restriction digestion, agarose gels were used in which the percentage of agarose was depending on the fragment size. TAE (50x: 2 M tris-acetate, 0.05 M EDTA, pH 7.6-7.8) was used as running buffer and agarose solvent. To be able to subsequently detect the DNA 5 ng / ml of the intercalating dye ethidium bromide (Roth) was added to the gel. For electrophoresis samples were combined with DNA sample buffer and applicated on the gel. Electrophoresis was performed with a voltage of 4-5 V / cm. Via fluorescence (UV transilluminator) it was possible to differentiate and identify the distinct DNA fragments in comparison to a DNA ladder with fragments of familiar sizes.

3.1.4 Elution of DNA Fragments out of Agarose Gels

DNA fragments of a certain size were specifically isolated via separation on an agarose gel and visualized with a UV transilluminator. The DNA fragment of interest was cut out of the gel. To prevent DNA damage a low UV intensity was chosen and the UV exposition was as short as possible. The including DNA was eluted from the gel with the QIAquick – Gel Extraction Kit (Qiagen) following the manufacturer's protocol.

3.1.5 Ligation of DNA

Ligation of cut plasmid DNA with DNA fragments of interest was performed after the protocol of the Quick Ligation™ Kit (New England Biolabs). 50 ng of vector were combined with a 3-fold molar excess of insert. The volume was adjusted to 10 µl with dH_2O. After adding 10 µl of 2x Quick Ligation Reaction Buffer and 1 µl of Quick T4 DNA Ligase the combination was mixed thoroughly, centrifuged briefly and subsequently incubated at room temperature for 5 min. The ligation mix was chilled on ice until transformation or stored at -20 °C until further use.

3.1.6 Heat Shock Transformation

To 50 µl competent *E.coli* either 10 ng of plasmid DNA or 5 to 10 µl of ligation mixture was added and incubated for 30 min on ice. After a heat shock (45 sec, 42 °C) and successive incubation on ice (2 min) bacteria were incubated on 37 °C for 1 h with 250 µl LB media (for 500 ml: 5 g tryptone, 2.5 g yeast extract, 5 g NaCl, pH 7.5) prior to plating. Plates were incubated upside down at 37 °C over night.

3.1.7 Cultivation of Bacteria

Bacterial media were autoclaved and supplemented with antibiotics prior to use. For a preparatory culture 4 ml LB media (supplemented with appropriate antibiotics) were inoculated with a single colony and incubated for at least 8 h at 37 °C and 250 rpm on a shaking device. Subsequently 100 ml LB media (supplemented with appropriate antibiotics) were inoculated with the preparatory culture and incubated at 37 °C and 250 rpm over night.

3.1.8 Plasmid Preparation

The bacterial culture was transferred into matching tubes and pelleted by centrifugation at 5000 x g and 4 °C for 15 min. Plasmids were isolated from the bacteria according to the manufacturer's protocol (peqGOLD XChange Plasmid Maxi-EF Kit, PEQLAB Biotechnologie GmbH). The DNA pellet was re-dissolved in an appropriate volume of TE-EF buffer or sterile deionized H_2O-EF.

3.2 Cell Culture

3.2.1 Cultivation of Eukaryotic Cell Lines

Cultivation of adherent cells occurred in an incubator at 37 °C, 5 % CO_2-saturation and 100 % atmospheric moisture in corresponding cell culture dishes. Required solutions and cell culture media were held at room temperature for about an h or pre-warmed for 20 min at 37 °C prior to use. Depending on the cell line, culture medium was changed every 2-3 days. Particular culture media, their compositions and additives are listed below (Table 3.1 and 3.2). When reaching 70-80 % confluence cells were split. Then, the used culture medium was extracted and cells were washed with 10 ml PBS. 1 ml of 1x trypsin / EDTA solution was used to detach the cells from the bottom of the cell culture flask. Cells were then resolved in fresh complete medium and an aliquot was used for further cultivation. Depending on the requirements, the rest of the cells were counted and seeded in corresponding cell culture dishes or microplates for planned experiments. Since EA.hy 926 cells are a permanent cell line, for experiments described in this dissertation cells were used until passage 30.

Table 3.1: Media for cultivation of EA.hy 926 cells.

media	composition
HAT	1 % L-Glutamine (100x) 1 % Penicillin / Streptomycin (100x) 2 % HAT Supplement (50x) 1 % Sodium Pyruvate (100x) 10 % FCS
HT	1 % L-Glutamine (100x) 1 % Penicillin / Streptomycin (100x) 2 % HT Supplement (50x) 1 % Sodium Pyruvate (100x) 10 % FCS

Table 3.2: Equipment, material, chemicals for cultivation of endothelial cells.

equipment, chemicals, material	manufacturer
Dulbecco's modified Eagle's medium (DMEM)	Sigma
Earle's Medium 199 (M 199)	Invitrogen
DPBS (1 x), (-) $CaCl_2$, (-) $MgCl_2$	Invitrogen
L-Glutamine (100x)	Invitrogen
HAT Supplement (50x)	Invitrogen
HT Supplement (50x)	Invitrogen
Sodium Pyruvate (100x)	Invitrogen

Fetal Calf Serum (FCS)	PAA Laboratories
Penicillin / Streptomycin (100x)	Invitrogen
Trypsin / EDTA	PAA Laboratories
Cell Culture Dishes	Greiner Bio-One
Microscope	Olympus
Incubator	Heraeus

3.2.2 Freezing and Thawing of Eukaryotic Cells

For permanent conservation cells were frozen in fresh FCS that additionally contained 10 % DMSO (Roth) (1 ml of cell suspension per 1.5 ml Greiner cryogenic storage vial). Cells were washed with PBS and trypsinized. Resuspended in 10 ml of PBS the cells were transferred to a 15 ml Greiner tube and centrifuged for 5 min at 900 x g. Cells were resuspended in prepared FCS / DMSO solution and portioned out. Confluent cells out of one 75 cm^2 cell culture flask could be divided onto three cryotube vials. Those vials were frozen at -80 °C first and transferred to liquid nitrogen (-196 °C) for enduring storage the next day.

To use frozen cells the cryogenic storage vials were warmed up at 37 °C and directly transferred to 5 ml of fresh complete medium. To get rid of the DMSO-containing medium the cell suspension was centrifuged (5 min at 900 x g), the pellet resuspended in 5 ml of fresh rich medium and plated out on a cell culture flask.

3.2.3 Cell Amount Determination

To ensure an even distributed amount of cells for the experiment, cells were counted using a Neubauer counting chamber. A sample of the cell suspension was pipetted into the chamber, which is divided into four large squares (area: 1 mm² each, height: 0.1 mm, resulting in a volume of 1 mm² x 0.1 mm = 0.1 µl), each of them again divided into 16 small squares. When the cover glass was applied correctly (formation of Newton's rings) there was a defined volume within the chamber. The average number of live cells in 4 large squares was counted and multiplied by the factor 10^4 to get the number of cells per ml of cell suspension. Potentially generated dilutions had to be included in the calculation. After determination of the amount of cells within the suspension it was possible to sow out the cells on a cell culture dish in a certain density, according to the planned experiments.

3.2.4 Stimulation of Cells

Incubation of cells with a certain stimulus was performed in well plates. Cells were sowed out on appropriate dishes and confluently cultivated. On the day of the experiment the stimulation was started with a particular substance, according to the experimental conditions. Controls were incubated in the corresponding solvent in adequate concentration. To stop the incubation after a defined period of time the substance was gently aspirated off the cells, which were then directly put into a box of liquid nitrogen and frozen at -80 °C until further use.

3.2.5 Transient Transfection of Plasmids in Eukaryotic Cells

In order to perform promoter assays cells were transfected with certain plasmids, which carry the promoter of interest. Nanofectin (PAA Laboratories GmbH) was used as a transfection reagent, following the manufacturer’s protocol given for transfection in 24-well plates. For optimal transfection conditions the cells had to be be 60 % confluent. For each well 1 µg of DNA was diluted with 150 mM NaCl to a final volume of 50 µl. In a second tube 3.2 µl of Nanofectin was diluted with 150 mM NaCl to a final volume of 50 µl. In the next step the Nanofectin solution was added to the same volume of DNA solution. After a 30 min incubation time at RT the Nanofectin / DNA

mixture was added dropwise to the serum containing medium in each well. Two h after transfection start 500 µl serum containing medium was added to double the volume of liquid. Four h after transfection start the procedure was stopped (due to observed cytotoxicity if applied over night) by removing the transfection complexes and replacing them with fresh serum-containing medium.

3.3 Gene Expression Analyses

3.3.1 Isolation of RNA

Isolation of total RNA was done using peqGold TriFast™ (peqLab Biotechnologie GmbH) which is a ready-to-use reagent that allows simultaneous extraction of RNA, DNA and proteins based on an optimized guanidinium thiocyanate / phenol-method.

To lyse cells grown in a monolayer 1 ml TriFast™ was added to a 3.5 cm diameter dish directly in a culture dish, passing the cell lysate through a pipette several times. The amount of TriFast™ needed is based on the area of the culture dish (1 ml per 10 cm^2) and not on the number of cells. An insufficient amount of TriFast™ could result in contamination of the isolated RNA with DNA. Phase separation, RNA precipitation, wash steps and RNA solubilization were performed following the manufcturer's protocol. The dried RNA pellet was diluted in 30-50 µl DEPC H_2O and frozen at -80 °C until further use.

To efficiently isolate RNA out of rat aorta with TriFast™, the tissue samples were homogenized first with the help of a ceramic mortar. Samples were homogenized in 1 ml TriFast™ per 50-100 mg of tissue. Phase separation, RNA precipitation, wash steps and RNA solubilization were performed following the manufcturer's protocol. The dried RNA pellet was diluted in 30-50 µl DEPC H_2O and frozen at -80 °C until further use.

3.3.2 Determination of RNA Concentration

To determine the concentration and purity of isolated nucleic acids, the optical density (OD) of an aqueous solution had to be defined via UV absorbtion measurement. OD values of RNA were measured at 260 nm and 280 nm. The 260 / 280-ratio allows evaluating the purity of the RNA solution since proteins, especially aromatic amino acids, absorb light at 280 nm. Therefore, nucleic acid solutions free of proteins do have an $OD_{260/280}$ ratio of 1.8 to 2.0.

Photometric determination of the RNA concentration was done with the NanoDrop™ ND-1000 spectrophotometer (peqLab Biotechnologie GmbH).

3.3.3 Reverse Transcription

To determine the level of gene expression at the time of the RNA isolation, RNA had to be converted into cDNA (complementary DNA) first. cDNA then could be used as a template for the following quantitative “real time” PCR analyses.

For cDNA syntheses the High Capacity cDNA RT Kit (Applied Biosystems) was used, following the manufacturer’s protocol and PCR was performed in an thermal cycler (iCycler from Bio-Rad Laboratories GmbH).

Table 3.3: Reverse transcription – reaction mixture (20 µl).

Reagents	Volume (µl)
10x RT Puffer	2
25x dNTP Mix (100 mM)	0,8
10x RT Random Primers	2
MultiScribe Reverse Transcriptase	1
H_2O	4,2
Template RNA (< 2 µg)	10

Table 3.4: RT-PCR temperature scheme.

Temperature (°C)	Time (min)
25	10
37	60
37	60
85	5
4	∞

3.3.4 Polymerase Chain Reaction (PCR)

With the help of the PCR (polymerase chain reaction) it is possible to amplify a specific (section of a) gene of interest. DNA fragments that have to be analyzed are amplified with the help of specific oligonucleotides (primer). Consisting of several repeating cycles, various single steps (denaturation, primer annealing and elongation) had to be performed at defined temperatures within a thermal cycler. Hydrogen-bonds of double-stranded DNA break during denaturation at 95 °C. Hybridization of oligonucleotides (primer annealing) occurs at lower, primer specific temperatures and allows an attachment of oligos to the now single-stranded DNA. The polymerization (elongation) of nucleic acids is the terminal step. On their 3'-end primers are extended complementary to the template by a thermostable Taq polymerase. Since those single steps are repeated periodically, this procedure amplifies the DNA fragment of interest.

3.3.5 Quantitative “Real Time” PCR (qRT-PCR)

Via quantitative PCR it is possible to display the expression rate of a corresponding mRNA. With this method one can verify differential gene expression. qRT-PCR enables the detection of amplified cDNA in „real time“ by the use of fluorescent signals. Proportionality between the fluorescent signal and the number of cDNA copies allows to determine the sample’s concentration – the higher the concentration of a specific mRNA or cDNA within the solution, the earlier the corresponding PCR product accumulates. For qRT-PCRs in the present work SYBR® Green JumpStart™ Taq ReadyMix™ (Sigma-Aldrich) was used as fluorescent dye, which is a cyanin dye and able to intercalate with double-stranded DNA. The resulting DNA-dye complex absorbs blue light at a wavelength of 494 nm and emits green light at 521 nm. Using the iCycler (iCycler iQ™ Multi-Color Real Time PCR Detection System, BioRad Laboratories GmbH) the software generates an amplification curve during the PCR procedure and calculates C_T-values („threshold cycle“). The C_T-values indicate a certain PCR cycle within the exponential phase of the amplification, where the amplification curve strides a threshold limit value. At this point a clear increase in fluorescence can be detected. Subsequently the relative expression level of the genes of interest were calculated. By comparing the gene of interest to a constitutively expressed housekeeping gene (TBP or Pol II a) the C_T-value was normalized.

Table 3.5: qRT-PCR mixture (20 µl).

Reagents	Volume (µl)
SYBR Green Super-Mix	10
Primer for (10 pM)	0,2
Primer rev (10 pM)	0,2
H_2O	5,6
Template cDNA (40 ng)	4

Table 3.6: qRT-PCR temperature scheme.

Temperature (°C)	time	cycle
95	30 sec	
95	30 sec	2
95	3 min	
95	15 sec	35
60	30 sec	
72	30 sec	
95	30 sec	
60	30 sec	
60	10 sec	8

Table 3.7: Equipment, chemicals, material used for PCR.

equipment, chemicals, material	manufacturer
Microseal® 'B' Film	BioRad Laboratories GmbH
0.2 ml reaction tubes (ThermoTube PCR Tubes)	peqLab Biotechnologie
SYBR® Green JumpStart™ Taq ReadyMix™	Sigma-Aldrich
High Capacity cDNA RT-Kit	Applied Biosystems
iCycler	BioRad Laboratories GmbH
96-well microplates	peqLab Biotechnologie

Table 3.8: Human oligonucleotides (primer) for quantitative RT-PCR.

Primer	Sequence
hu_Nox1_FWD	5’- AAG CCG ACA GGC CAC AGA T -3’
hu_Nox1_REV	5’- CCC CCC TTT TTC TCA TCA TGA -3’
hu_Nox2_FWD	5’- CACCAATCTGAAGCTCAAAAAGATCTAC -3’
hu_Nox2_REV	5’- CATCTGGCTCTCCAGCAGTTG -3’
hu_Nox4_FWD	5’- TTT TCT CAG GCG TGC ATG TG -3’
hu_Nox4_REV	5’- CAT TCA GTT CAA CAA AGT CTT CAC TGT -3’
hu_p22phox_FWD	5’- TCC GGC CTG ATG CTC ATC -3’
hu_p22phox_REV	5’- AAT GGA GTA GGC ACC AAA GTA CCA -3’
hu_TBP_FWD	5’- GCC GCC GGC TGT TTA ACT -3’
hu_TBP_REV	5’- ACG CCA AGA AAC AGT GAT GCT -3’
hu_Pol IIa_FWD	5’- GCT ATA AGG TGG AAC GGC ACA T -3’
hu_Pol IIa_REV	5’- ACC CGA TGC CCC ATC AT -3’
hu_GCH1_FWD	5’- TCA GTG TGT GTC TGC AGA ACC A-3’
hu_GCH1_REV	5’- TGT CTT CCA CCG TCA GTT CAT T -3’
hu_DHFR_FWD	5’- TCC TCC CGC TGC TGT CA -3’
hu_DHFR_REV	5’- GCC GAT GCC CAT GTT CTG-3’
hu_eNOS_FWD	5’- CAC CAG GAA GAA GAC CTT TAA AGA -3’
hu_eNOS_REV	5’- TCA CTC GCT TCG CCA TCA C -3’
hu_SOD1_FWD	5’- CTC TCA GGA GAC CAT TGC ATC A -3’

hu_SOD1_REV	5’- CCT GTC TTT GTA CCT TCT TCA TTT CCA -3’
hu_XDH_FWD	5’- TGA CAT TGC CAA GGT AAC CA -3’
hu_XDH_REV	5’- AGT GGT CTT GAG GGC TGA GA -3’
hu_TXN1_FWD	5’- AAG TCA AAT GCA TGC CAA CAT -3’
hu_TXN1_REV	5’- GCT TTT CCT TAT TGG CTC CAG -3’

Table 3.9: Rat oligonucleotides (primer) for quantitative RT-PCR.

Primer	Sequence
rat_Nox1_FWD	5’- ACC CCC TGA GTC TTG GAA GTG -3’
rat_Nox1_REV	5’- GGG TGC ATG ACA ACC TTG GT -3’
rat_Nox4_FWD	5’- CTG TCC TGA ACC TCA ACT GCA G -3’
rat_Nox4_REV	5’- TGT GAT CCG CGA AGG TAA GC -3’
rat_p22phox_FWD	5’- TAC CTG ACC GCT GTG GTG AAG -3’
rat_p22phox_REV	5’- GCA GTA AGT GGA GGA CAG CCC -3’
rat_SOD1_FWD	5’- GTC GTC TCC TTG CTT TTT GC -3’
rat_SOD1_REV	5’- TCT GCT CGA AGT GAA TGA CG -3’
rat_SOD2_FWD	5’- CCA AAG GAG AGT TGC TGG AG -3’
rat_SOD2_REV	5’- TTG GAC TCC CAC AGA CAC AG -3’
rat_SOD3_FWD	5’- GAC CTG GAG ATC TGG ATG GA -3’
rat_SOD3_REV	5’- GGA CCA AGC CTG TGA TCT GT -3’

rat_GPx1_FWD	5’- TCG AAC CCG ATA TAG AAG CCC -3’
rat_GPx1_REV	5’- CAC CAA GCC CAG ATA CCA GG -3’
rat_XDH_FWD	5’- GCC TTC ACA CCA AGA TGG TT -3’
rat_XDH_REV	5’- GGG ACG GTG TTA GTG CTT GT -3’
rat_Cat_FWD	5’- ACA TGG TCT GGG ACT TCT GG -3’
rat_Cat_REV	5’- CCA TTC GCA TTA ACC AGC TT -3’
rat_Pol IIa_FWD	5’- CGT ATC CGC ATC ATG AAC AGT G -3’
rat_Pol IIa_REV	5’- TGC ACC GCA GGA AAA CAT C -3’
rat_GCH1_FWD	5’- TGT GTA TGG TCA TGC GAG GT -3’
rat_GCH1_REV	5’- GAG GAA CTC CTC CCG AGT CT -3’
rat_eNOS_FWD	5’- GGA GGT TCA CCG CGT GC -3’
rat_eNOS_REV	5’- GAC GCT GGT TGC CAT AGT GAC -3’
rat_COX1_FWD	5’- CCT CTG TAC CCA AAG ACT GTC C -3’
rat_COX1_REV	5’- AAG TGT TGT GCA AAG AAA GCA A -3’
rat_COX2_FWD	5’- CAG ATG CTA TCT TTG GGG AGA C -3’
rat_COX2_REV	5’- CAC CCT TTC ACA TTA TTG CAG A -3’
rat_DHFR_FWD	5’- GTC TAC CAG GAA GCC ATG AAT C -3’
rat_DHFR_REV	5’- CAG TAG GAC TTG GGA GCA TGT T -3’
rat_TXN1_FWD	5’- TCC AAT GTC GTG TTC CTT GA -3’
rat_TXN1_REV	5’- ACC AGA GAA CTC CCC AAC CT -3’

rat_TXN2_FWD	5’- CGT TTT GTC CTT GTG GGT CT -3’
rat_TXN2_REV	5’- GTA GGA GGT GCT CAG GAT GC -3’

Table 3.10: qPCR (Thermo Fisher).

Temperature (°C)	Time	Cycle
95	30 sec	
95	30 sec	2
95	15 min	
95	15 sec	35
60	30 sec	
72	30 sec	
95	30 sec	
60	30 sec	

3.4 Protein Analyses

3.4.1 Isolation of Protein

After stimulation of cells for protein analyses the supernatant was evacuated. The samples were stored at -80 °C until further processing. All of the following steps were performed on ice. The cells were incubated for 10 min in Triton-X lysis buffer and then scraped off the plate and transferred into an Eppendorf reaction tube. After 15 min of incubation on ice cells were centrifuged at 13000 rpm and 4 °C for 10 min. The supernatant was transferred into a fresh reaction tube, the pellet was discarded.

3.4.2 Determination of Protein Concentration

BCA-Assay (Bicinchoninic Acid-Assay)

Measurement of the total protein concentration in the resulting supernatant was performed with BCA assay. It is a sensitive and easy method for protein detection that has been reported to be insensitive to interference by a number of substances disrupting the Bradford assay. The assay makes use of a color change that results from complexes formed between monovalent Cu^{+} ions and two molecules of bicinchonicic acid. There are two reactions that depend on the presence of proteins or polypeptides that reduce the bivalent Cu^{2+} ions to monovalent Cu^{+} ions: The temperature-independent oxidation of cysteine, tyrosine and tryptophan residues and the temperature-dependent reaction of peptide bonds with Cu^{2+} that is less prevalent at an incubation temperature of 37 °C. The extinction of the formed complexes is proportional to the protein concentration. A 96-well plate was used as a reaction vessel with 100 µl of water-diluted sample or BSA mixed with 100 µl of a 50:1 BCA / $CuSO_4$ solution per well. A BSA dilution series with 0.5, 1, 5, 10, 20, 30, 40 and 50 µg of BSA / 100 µl served as a calibration line. After 30 min of incubation at 37 °C the extinction at 595 nm was measured using an absorbance microplate reader. Protein concentration of the samples was calculated from the calibration line.

Bradford Assay

To determine the protein concentration of samples prepared for luciferase assay, the Bradford assay was used. This is a colorimetric protein assay, based on an absorbance shift of the dye Coomassie Brilliant Blue G-250 in which under acidic conditions the red form of the dye is converted into its blue form to bind to the protein being assayed. The binding of the protein stabilizes the blue form of the Coomassie dye. Thus the amount of the complex in solution is a measure for the present protein concentration and can be calculated by use of an absorbance microplate reader. A clear 96-well plate was used as a reaction vessel with 100 µl of water-diluted sample (1:10) mixed with 100 µl of 40 % Bradford reagent (BioRad Laboratories GmbH) per well. A BSA dilution series with 0.25, 0.5, 1, 1.5, 2, 2.5, 3, 3.5, 4 and 5 µg of BSA / 100 µl served as a calibration line. After 5 min of incubation at RT the absorbance was measured. Unlike other protein assays, the Bradford protein assay is less susceptible to interference by various chemicals that may be present in protein samples. An exception is an elevated concentration of detergent like sodium dodecyl sulfate (SDS). SDS is a common detergent that can be found in protein extracts prepared for western blot performance because it is used to lyse cells by disrupting the membrane lipid bilayer. For this reason measurements of protein concentration in samples used for western blots were done by BCA assay.

3.4.3 Protein Concentration via Precipitation

If the protein concentration was not high enough to perform adequate western blots, methanol-chloroform-precipitation was performed for quantitative recovery of proteins. Therefore 100 µl of protein sample was pipetted into a 1.5 ml Eppendorf tube and 400 µl of methanol was added. After vortexing and briefly spinning down to collect the sample, 100 µl of chloroform was added and the sample again well vortexed. Another quick spin was followed by mixing the sample with 300 µl of H_2O and separating the phases by centrifugation (5 min, 13000 rpm at RT). Since proteins concentrate at the interphase, the upper layer was carefully removed and discarded after centrifugation. In the next step proteins were precipitated by adding 300 µl of methanol to the tube, vortexing and spinning down for 5 min and 13000 rpm at RT. After the removal of the supernatant the pellet was dried and resuspended in the buffer of choice.

3.4.4 SDS-PAGE

The separation of proteins was performed by means of the discontinuous SDS polyacrylamide gel electrophoresis (SDS-PAGE) using the Mini-Protean 3 system (BioRad Laboratories GmbH). A separating gel of 1.5 mm thickness and a chosen percentage of acrylamide (depending on the protein of interest) was layered with H_2O. Before casting a stacking gel, the H_2O was removed.

Chamber and gels were assembled as described by the manufacturer's protocol. 3 µl of a prestained protein ladder (PageRuler^{TM}, #SM0671, Fermentas Life Sciences) was loaded on each gel as molecular weight standard. A volume of 20 µl per sample was loaded into a single pocket and the gels were run on a constant voltage of 140 V. Gels were subjected to western blotting once the bromophenol blue reached the lower end of the gel.

3.4.5 Western Blot Analysis

Electrophoretic Transfer

Proteins were transferred from the SDS-gel onto a nitrocellulose membrane (Whatman, PROTRAN® nitrocellulose transfer membrane, pore size 0.2 µm). Nitrocellulose membranes were incubated in transfer buffer for 15 min, blotting paper and blotting pads pre-soaked in transfer buffer. The "western blot sandwich" was assembled according to the protocol. Proteins were transferred at a constant current of 90 mA, over night at 4 °C.

Immunological Detection of Proteins on Nitrocellulose Membranes

After the electrophoretic transfer, membranes were rinsed briefly in TBS (0.5 M tris-base, 9 % NaCl, pH 7.6) and blocked for at least 1 h at RT in blocking buffer (5 % non-fat dry milk in TBST). Primary antibody diluted in blocking buffer was applied over night at 4 °C or for at least 1 h at RT. After 4 washing steps in TBST (0.05 % Tween 20 in TBS), HRP-conjugated secondary antibodies were applied for at least 1 h, followed by four washing steps with TBST. Membranes were exposed using the Enhanced Chemiluminescence Detection Kit (PerkinElmer).

Table 3.11: List of antibodies used for western blot analyses.

1st Antibody	Dilution	Company
mouse anti-eNOS	1 : 2 000 in 1 % BSA	BD Transduction (#610297)
rabbit anti-serine[117]	1 : 2 000 in 5 % BSA	Cell Signaling (#9571S)
mouse anti-GCH1	1 : 1 000 in 5 % MP	Abnova (H00002643-M01)
mouse anti-DHFR	1 : 5 000 in 5 % MP	BD Transduction (#610697)
mouse anti-Tubulin	1 : 200 000 in 5 % MP	Sigma-Aldrich (#T7816)
rabbit anti-GAPDH	1 : 20 000 in 5 % MP	Epitomics (#2251-1)
2nd Antibody	**Dilution**	**Company**
goat anti-rabbit	1 : 5 000 in 5 % MP	Sigma-Aldrich (#A9169)
rabbit anti-mouse	1 : 5 000 in 5 % MP	Sigma-Aldrich (#A9044)

Densitometric Evaluation of Band Intensities

For the quantification of the western blots only non-saturated, developed blot images were used. Blots were scanned using the BioRad Molecular Imager ChemiDoc™ XRS Imaging System. Intensities of individual bands were quantified with the “Quantity-one” software (BioRad Laboratories GmbH).

3.5 Luciferase Reporter Assay

3.5.1 Luciferase Reporter Vectors

Firefly Luciferase Reporter Vector - pGL3-Basic

The pGL3-Basic Vector lacks eukaryotic promoter and enhancer elements. Expression of luciferase activity in cells transfected with pGL3-Basic is dependent on the insertion of a functional promoter upstream *lux*+.

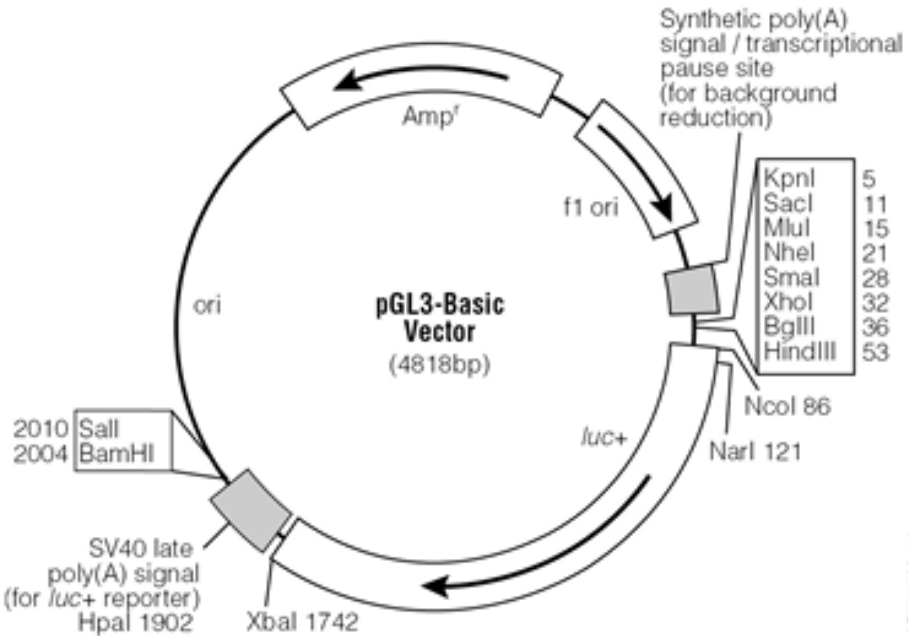

Figure 3.1: Firefly Luciferase Reporter Vector – pGL3-Basic.

Renilla Luciferase Reporter Vector – pLightSwitch

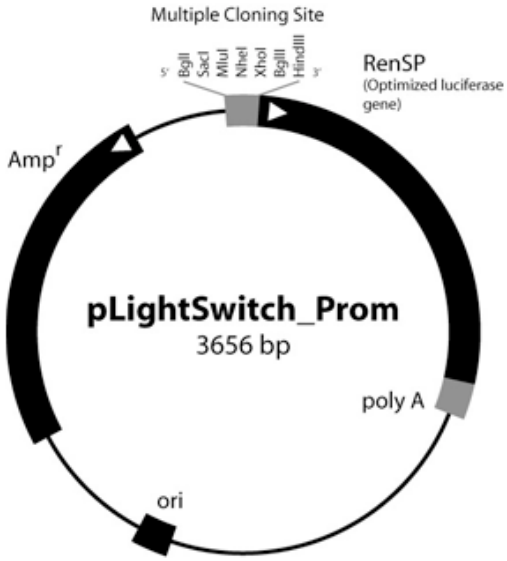

Figure 3.2: *Renilla* Luciferase Reporter Vector – pLightSwitch.
Commercially available from SwitchGear.

3.5.2 Preparation of Cell Extracts

After transient transfection (see 3.2.4) and incubation with a certain stimulus cells were washed with PBS and lysed with Passive Lysis Buffer (PLB, Promega, #E1941). Using a 24-well plate, 200 µl of 1x PLB were added to each well and incubated on a shaker at RT for 15 min. Samples were transferred to 1.5 ml Eppendorf tubes followed by a 15 min centrifugation step at 13000 rpm and 4 °C. The supernatant was collected, transferred into a new tube and stored at -80 °C for further analyses. The pellet (being composed of cell debris) was discarded.

3.5.3 Measuring Luciferase Activity

The luciferase enzyme used most frequently for reporter gene technology is derived from the coding sequence of the *luc* gene cloned from the firefly *Photinus pyralis*. The firefly luciferase enzyme catalyzes a reaction using D-luciferin and ATP in the presence of oxygen and Mg^{2+} resulting in light emission. The luciferase reaction is quantitated using a luminometer that measures light output. The total amount of light measured during a given time interval is proportional to the amount of luciferase reporter activity in the sample. The assay has been improved by including coenzyme A in the reaction that provides a longer, sustained light reaction with greater sensitivity.

Because the firefly and *Renilla* luciferases are of distinct evolutionary origins, they have dissimilar enzyme structures and substrate requirements. *Renilla* luciferase is a protein derived from the sea pansy *Renilla* reniformis and utilizes oxygen and coelenterazine to generate light emission. Similar to firefly luciferase, the luminescent reaction catalyzed by *Renilla* luciferase provides high sensitivity.

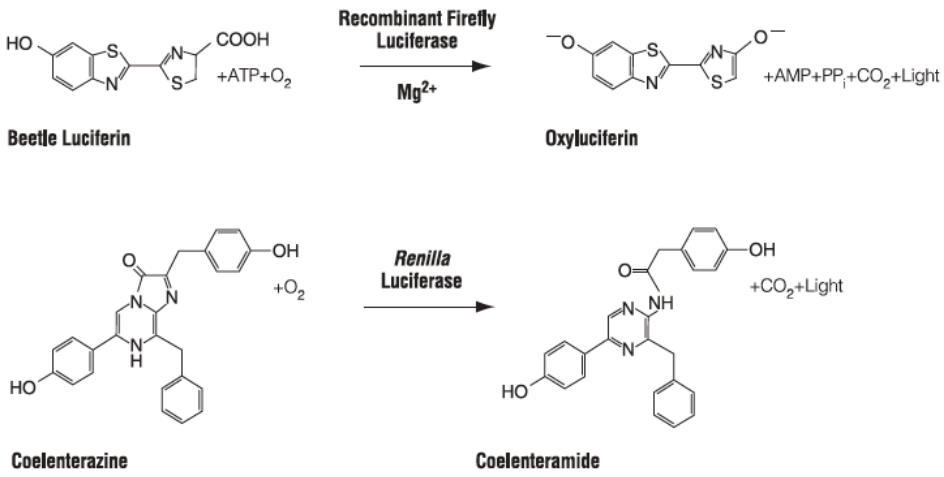

Figure 3.3: Bioluminescent reactions catalyzed by firefly and *Renilla* luciferases.
(source: Promega)

3.6 ROS-Detection

To detect the intra- and extracellular production of reactive oxygen species, cells were allocated on 96-well microplates (2.5 x 10^4 cells / well) one day prior to the start of the experiment.

For chemiluminescence measurements (plate reader from Berthold-Technologies LB 960) white 96-well microplates with clear bottom were used (µClear®-Plates, Greiner). To measure ROS via fluorescence (BMG Fluostar Optima) cells had to be allocated on black 96-well microplates with clear bottom (µClear®-Plates, Greiner).

3.6.1 Fluorescence

After incubation with a certain stimulus cells were washed with pre-warmed (37 °C) HBSS (Hank's Balanced Salt Solution, + $CaCl_2$, + $MgCl_2$, Gibco) followed by a 30 min incubation step with the detergent H_2DCFDA (2.5 µM) from Invitrogen at 37 °C. Cells were again washed with HBSS (37 °C) and covered with pure HBSS or HBSS in combination with a substance like L-NAME or DMNQ for the measurement, depending on the experimental setting. ROS development was monitored for up to 12 h within the plate reader (excitation: 485 nm, emission: 530 nm).

3.6.2 Chemiluminescence

To measure the production of ROS after stimulation with a certain substance the cells needed to be washed with HBSS (37 °C) and incubated with L-012 (100 µM, Wako) for 20 min at 37 °C. L-012 is a luminol derivative, which is a highly sensitive chemiluminescence probe and more active than luminol. After incubation with the dye, there was no additional washing step needed, the detergent was not taken off the microplate for the measurement. Subsequently the development or ROS was monitored for up to 12 h within the plate reader (Centro LB 960, Berthold Technologies).

3.6.3 Fluorescence-Activated Cell Sorting (FACS)

Alternatively to the above described methods in 96-well microplates, ROS were also measured using the FACSCalibur™ flow cytometer (BD Biosciences). The fluorescent dye H_2DCFDA was used again. EA.hy 926 cells were seeded into 24-well plates to 80 % confluence before treatment. After incubation with an experiment-specific substance cells were washed with PBS. Subsequently cells were incubated with H_2DCFDA in HBSS (2.5 µM) for 30 min at 37 °C in the dark. Afterwards cells were washed again with PBS and trypsinized. Medium was added to stop the enzymatic reaction and cells were collected in a 1.5 ml tube. After a 4-min centrifugation at 350 x g and 4 °C the supernatant was discarded. The cell pellet was washed with cold PBS and centrifuged a second time. The received cell pellet was resuspended in 300 µl PBS and transferred to a FACS-tube (5 ml BD Falcon Polystyrene Round-Bottom Tube, BD Biosciences) for analysis.

3.7 BH_4-Detection (HPLC)

Detection of BH_4 levels in DEX treated cells by HPLC was kindly performed by Alice Habermeier (AG Closs, Institut für Pharmakologie, Universitätsmedizin der Johannes Gutenberg-Universität Mainz). After DEX-treatment in 6-well plates EA.hy 926 cells were washed twice with ice-cold PBS+ (PBS+ = 50 ml PBS + 50 µl DTE + 10 µl Pefabloc®). Cells were scraped off the wells with ice-cold PBS++ (PBS++ = PBS + 5 nM Neopterin) and identical samples were pooled. HPLC analyses were performed with phosphate buffer (50 mM, pH 3.0) as eluent in appropriate columns (125/4 Nucleosil SA 100-5 mm, Macherey-Nagel) at 25 °C and a flow rate of 1.20 ml / min. Equipment from Bischoff was used as well as the Hitachi fluorescence detector 8470 (excitation: 350, emission: 450 nm). Evaluation was done with the help of MCDAcq Integrator software from Bischoff.

3.8 RFL-6 Reporter Cell Assay

The RFL-6 reporter cell assay is a sensitive method to quantify the amount of endogenous NO produced by endothelial cells. In this assay RFL-6 fetal rat lung fibroblasts were used as reporter cells. Those cells are rich in soluble guanylyl cyclase but do not express NO synthases. When activated by NO the soluble guanylyl cyclase catalyzes the formation from GTP to cGMP. The amount of formed cGMP is proportional to the quantity of activating NO. In these experiments the supernatant of stimulated or non-stimulated endothelial cells were the source of NO for RFL-6 cells. As controls the RFL-6 cells were either treated with the NO-donor linsidomine (SIN-1) to measure the maximal cGMP formation or left untreated to measure the cGMP baseline.

The cGMP concentration in RFL-6 cells was measured in a radioimmunoassay. Cell lysate from RFL-6 cells was incubated with radioactively labeled cGMP (^{125}I-cGMP) and an antibody targeting cGMP. The formation of either cGMP-antibody-complexes or radioactively labeled ^{125}I-cGMP-antibody-complexes is a competing reaction as the antibody binding sites are limited. The antibody complexes were precipitated and the radioactivity was measured with a gamma counter. The amount of cGMP formed in RFL-6 cells is reciprocally proportional to the measured radioactivity and was calculated with the help of a calibration curve.

3.8.1 Transfer-Assay

To analyze the amount of NO produced by human endothelial cells after DEX treatment, EA.hy 926 cells were incubated with DMSO (as control) or DEX in three different concentrations (1, 10 and 100 nM) for 24 or 48 h. Subsequently the transfer assay was performed. RFL-6 cells in 6-well plates were kept in Ham's F12 medium until confluence (about 3 days). 30 min prior to transfer assay they were incubated in Locke's solution (10x Locke's stock solution: 154 mM NaCl, 5.6 mM KCl, 1 mM $MgCl_2$, 10 mM HEPES, 3.6 mM $NaHCO_3$, pH 7.4, autoclaved; 1x Locke's solution had to be freshly prepared with 5.6 mM glucose and 14.7 mg $CaCl_2$) supplemented with IBMX (600 µM, Serva) at 37 °C. Confluent EA.hy 926 cells in 6-well plates were kept in usual growth medium for at least 3 days to develop a very dense layer of endothelial cells with corresponding endothelial functions. Thereafter cells were washed twice with 1x

Locke's solution. Subsequently EA.hy 926 cells were incubated in 1 ml per well of 1x Locke's solution supplemented with 1 mM arginine in presence of 40 U / ml SOD for 30 min.

The solution was extracted and EA.hy 926 cells were covered with transfer solution containing Locke's solution supplemented with 40 U / ml SOD (to quench superoxide that would inactivate NO), 1 mM arginine (as substrate for eNOS), 600 µM IBMX (a phosphodiesterase inhibitor that prevents cGMP degradation) and 10 µM of the calcium ionophore A23187 (to mediate calcium influx and insure maximal eNOS stimulation). Endothelial cells were incubated for exactly 3 min at 37 °C. Meanwhile the supplemented Locke's solution was drawn off the RFL-6 cells. Then the endothelial cells' supernatant containing NO, formed in 3 min of stimulation, was transferred onto the RFL-6 cells. Those were incubated for another 3 min at 37 °C and then the supernatants were taken off. The cells were immediately covered with 500 µl of cooled 50 mM sodium acetate solution, frozen with liquid nitrogen and stored at -80 °C until further processing.

To determine the cGMP baseline in RFL-6 cells and the maximal cGMP formation the cells were covered in Locke's solution containing 600 µM IBMX and incubated for 3 min at 37 °C. For the baseline no further supplement was added. For the maximal cGMP formation the Locke's solution was supplemented with 100 µM of the NO-donor linsidomine (SIN-1). Then they were lysed as described above.

3.8.2 Radioimmunoassay

After thawing samples were transferred into 1.5 ml Eppendorf reaction tubes for 10 min of centrifugation at 13000 rpm and 4 °C. The pellets, consisting of cell debris, were discarded. The supernatants were transferred into fresh reaction tubes.

Essential values needed for the calibration curve to measure cGMP concentrations:

1 - Standard: Consisting of a cGMP dilution series, ranging from 0.2 pmol to 5 pmol per 50 µl of a 50 mM sodium acetate buffer (pH 4)

2 - Blank value: Without antibody, defines minimum of calibration curve

3 - Binding value: Definition of maximum binding capacity of cGMP to antibody

4 - Total value: Represents total of radioactivity, contains 100 µl of ^{125}I-cGMP solution per vial

150 µl of a 50 mM sodium acetate buffer equilibrated at pH 4 were given to each vial except for the total value. Then 50 µl of cell lysate were given to each sample and 50 µl of cGMP solution in the appropriate dilution were added to each standard vial. A 1:10000 anti-cGMP antibody dilution was prepared in 50 mM sodium acetate buffer containing 0.01 % BSA. In an authorized radioactive lab a ^{125}I-cGMP solution of 50 mM sodium acetate buffer equilibrated at pH 4 and an activity of 100 cpm / µl was prepared. Subsequently 100 µl of this solution were given to each vial (for a total activity of 10000 cpm). Then 100 µl of the diluted antibody solution were added to each sample except for the total and the blank value. All vials were blended and centrifuged for a short time at 4000 x g and 4 °C. The reaction occurred at 4 °C over night.

On the next day 50 µl of a 1 % γ-globulin solution were added to each sample except for the total value. cGMP-antibody complexes were precipitated with 2.5 ml of cooled isopropanol (except for total value). All vials were blended and centrifuged at 4 °C and 4000 x g for 45 min. The supernatants were discarded and the pellets were dried for approximately 2 h. Subsequently the radioactivity was measured in a gamma scintillation counter (Cobra Quantum 5200, Perkin Elmer). The cGMP concentration of each sample was calculated with the help of the calibration curve.

Table 3.12: Pipetting scheme for the radioimmunoassay.

	50 mM sodium acetate	Standard / Sample	^{125}I-cGMP 100 cpm / µl	Anti-cGMP antibody
Total	-	-	100 µl	-
Blank value	200 µl	-	100 µl	-
Binding value	200 µl	-	100 µl	100 µl
Standard	150 µl	50 µl	100 µl	100 µl
Sample	150 µl	50 µl	100 µl	100 µl

3.9 *In vivo* Experiments

3.9.1 Animal Treatment

To investigate the *in vivo* effect of DEX, normotensive Wistar Kyoto rats (6 months of age) were orally treated with water-soluble DEX (D2915, Sigma-Aldrich). Based on the average water intake of the rats (60 ml / kg bodyweight / day) a quantity of 0.5 mg DEX / Liter was added to the drinking water to reach an approximate target dose of 0.03 mg / kg bodyweight / day. Animals were treted with DEX for 12 days; untreated rats served as controls. Rats were housed under controlled conditions (24 ± 2 °C, humidity 60 ± 10 %, light:dark 12:12 h, light on at 6:00 am) with free access to food (standard rat chow diet) and water. All experiments were approved by the Landesuntersuchungsamt Rheinland-Pfalz and were performed in accordance with institutional guidelines for health and care of experimental animals.

3.9.2 Dissection of the Aorta

After 12 days of experiment the animals were sacrificed under isoflurane anesthesia and aorta tissue was harvested for analysis by qRT-PCR, thoroughly cleaned of surrounding connective tissue, snap-frozen in liquid nitrogen and stored at -80 °C until further use.

3.9.3 Organ Bath

The thoracic aorta was dissected, thoroughly cleaned of surrounding connective tissue and placed in freshly prepared ice-cold and oxygenated Krebs–Henseleit buffer (118 mM NaCl, 25 mM $NaHCO_3$, 4.8 mM KCl, 1.2 mM $MgSO_4 \cdot 7H_2O$, 1.2 mM KH_2PO_4, 0.026 mM $Na_2EDTA \cdot 2H_2O$, 11.1 mM $Glucose \cdot H_2O$, 2.5 mM $CaCl_2 \cdot 2H_2O$) and then cut into ring segments (about 2 mm in length). Each ring was suspended between two stainless steel hooks in a 10 ml organ bath filled with Krebs–Henseleit buffer. Bathing solution was continuously bubbled with 95 % O_2 and 5 % CO_2 and maintained at 37 °C (pH of 7.3 – 7.5). An optimal baseline tone of 10 mN was applied to all rings. The aorta segments were incubated with the terminal tension for 30 min. The value was then set

to zero and the aorta samples were pre-constricted twice with 600 µl of 2 M KCl. The achieved tension was considered as max tension. To analyze the constriction ability of the aortas, norepinephrine was added from low to high concentrations until 80 % of the max tension was reached. For dilation analyses accumulative concentrations of acetylcholine (ACh) were added into the organ bath to induce a relaxation of the vessel rings. To see if the observed effect was eNOS-dependent, the procedure was repeated after the aorta segments were washed and subsequently incubated with 500 µM L-NAME for 30 min.

3.9.4 Blood Pressure Measurement

Blood pressure was non-invasively measured by determining the tail blood volume with a volume pressure recording (VPR) sensor and an occlusion tail-cuff (CODA System, Kent Scientific, Torrington, CT, USA). The non-invasive blood pressure methodology consists of utilizing a tail-cuff placed on the tail of the animal to occlude the blood flow. Upon deflation the non-invasive blood pressure sensor, placed distal to the occlusion cuff, can be utilized to monitor the blood pressure. The VPR sensor utilizes a specially designed differential pressure transducer to non-invasively measure the blood volume in the tail. Since VPR is a volumetric method to measure the blood flow and blood volume in the tail, there are no measurement artifacts related to ambient light; movement artifact is also greatly reduced. In addition, VPR is not dependent on the animal's skin pigmentation. Dark-skinned animals have no negative effect on VPR measurements. Also very small animals are easily measured by the VPR method. VPR is the most reliable, consistent and accurate method to non-invasively measure the blood pressure in mice as small as 10 g to rats greater than 950 g. Physiological values for rats: HR: 350-450 bpm, SBP: 100-140, DBP: 80-100.

3.10 Statistics

Statistical analyses were performed with ANOVA (analysis of variance) followed by Bonferroni post-test to compare replicate means by row, with the computer software GraphPad Prism 5. $p < 0.05$ was considered being statistically significant.

4 Results

4.1 *In vivo* Analyses of Glucocorticoid Effects on the Vascular System of the Rat

4.1.1 Effect of DEX on Blood Pressure

To investigate the *in vivo* GC effect on blood pressure, normotensive Wistar Kyoto rats (6 months of age) were orally treated with water-soluble DEX. The approximate target dose of 0.03 mg / kg / day DEX was given for 12 days; untreated rats served as controls (3.9.1). During the time of the experiment the animal's blood pressure was non-invasively measured three times, on day 1, day 6 and day 12 (3.9.4). After 12 days a clear tendency was seen. The blood pressure of DEX treated animals increased with the time of the experiment compared to the control animals. However, this effect was not significant with the number of animals analyzed (Figure 4.1, top). The animal's bodyweight was also monitored during the experiment. Whereas control animals did not have noteworthy changes in their bodyweight, DEX treated rats slightly but not significantly lost weight compared to control rats (Figure 4.1, bottom). Since no animal lost more than about 10-15 % of its original bodyweight, this loss was acceptable and the experiment could be continued.

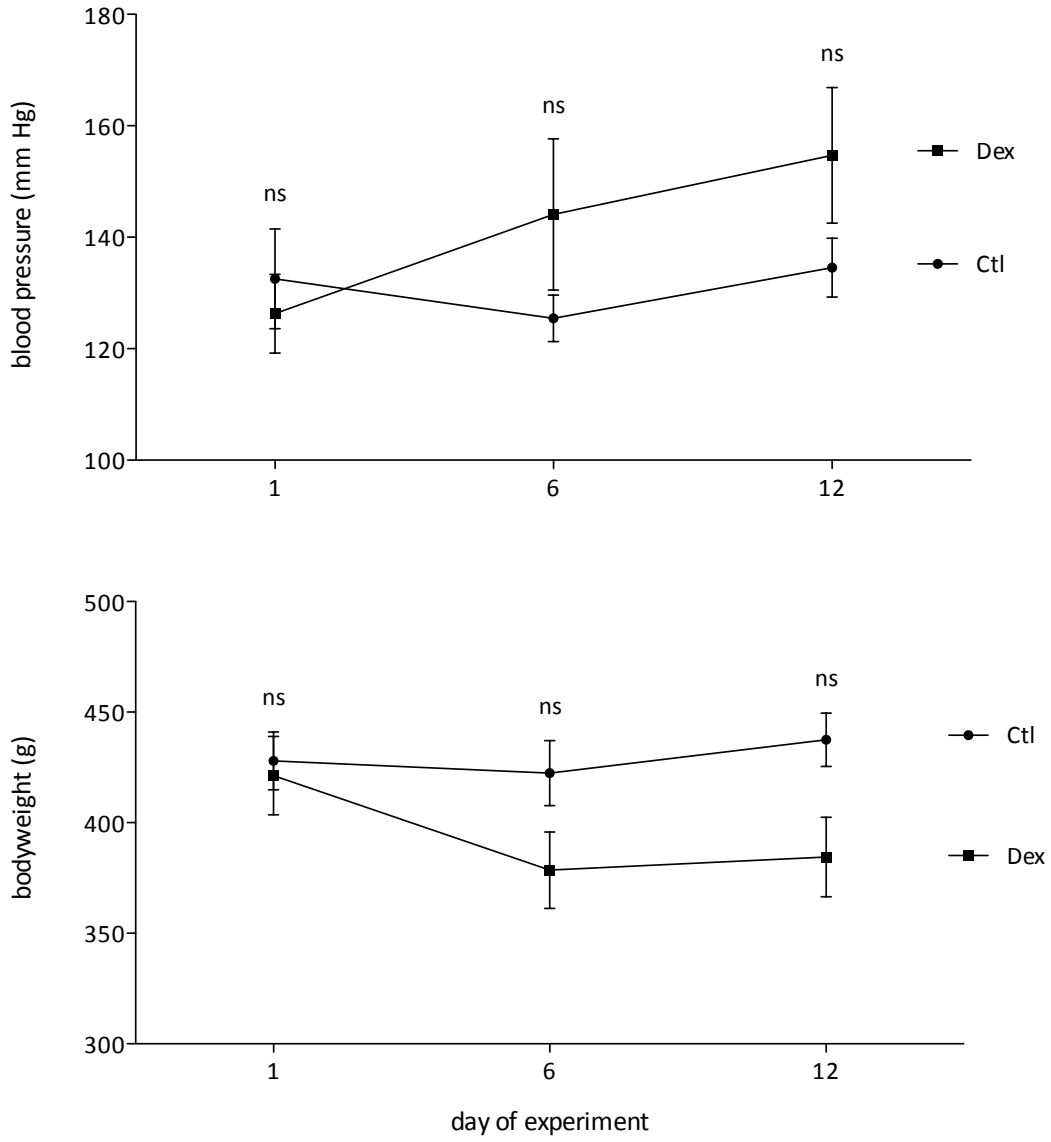

Figure 4.1: Changes in blood pressure and bodyweight of rats after treatment with DEX. Normotensive Wistar Kyoto (WKY) rats were orally treated with water-soluble DEX (0.03 mg / kg / day) for 12 days. During the time of the experiment, on day 1, 6 and 12 the animal's blood pressure was measured non-invasively with the CODA monitor (Kent Scientific). Columns represent mean + SEM, n=12. ns=not significant, between Dex and Ctl.

4.1.2 DEX Altered the Relaxation & Constriction Ability of the Aorta

To investigate the *in vivo* GC effect on endothelial function, normotensive Wistar Kyoto rats (6 months of age) were orally treated with water-soluble DEX. The approximate target dose of 0.03 mg / kg / day DEX was given for 12 days; untreated rats served as controls (3.9.1). To analyze the endothelial function after treatment with DEX, organ bath experiments were performed (3.9.3). Relaxation ability of the analyzed aorta rings was improved in samples taken from DEX treated rats (Figure 4.2, top). When aorta samples were pre-incubated with L-NAME (NOS inhibitor) the maximum relaxation capacity was reduced (Figure 4.2, bottom).

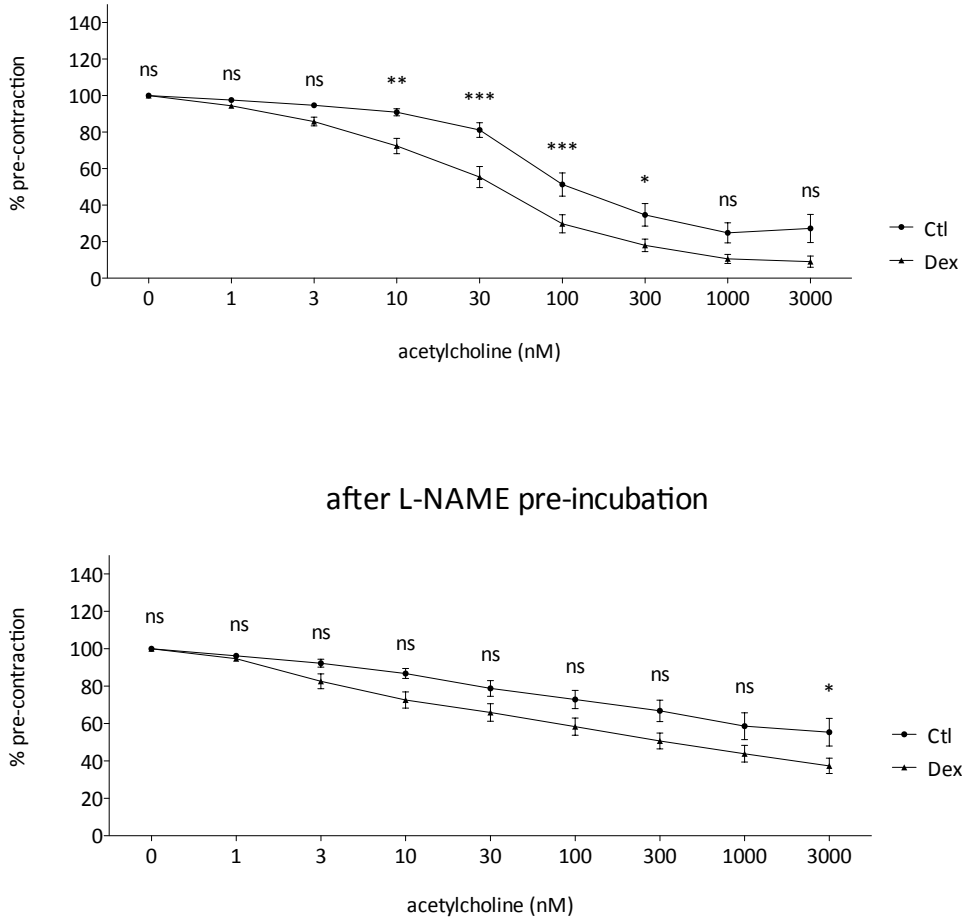

Figure 4.2: Impact of DEX on relaxation ability of rat aorta. Normotensive Wistar Kyoto (WKY) rats were orally treated with water-soluble DEX (0.03 mg / kg / day) for 12 days. On day 13 the animals were sacrificed and the rat's aortas were dissected. For subsequent analysis of the endothelial function, rings (2 mm in length) were cut out of the aorta and fixed in an organ bath gadget for further investigation. Columns represent mean + SEM, n=12. ns=not significant, *p<0.05, **p<0.01, ***p<0.001, between Dex and Ctl.

Not only relaxation but also the aorta's constriction ability was investigated (Figure 4.3). The rings were treated with norepinephrine in increasing concentrations. The vessel's constriction ability was diminished in aortas of DEX treated rats compared to those dissected from control animals (Figure 4.3, top). After pre-incubation of the aorta rings with L-NAME (NOS inhibitor) the response to norepinephrine and therefore the ability to constrict was improved (Figure 4.3, bottom).

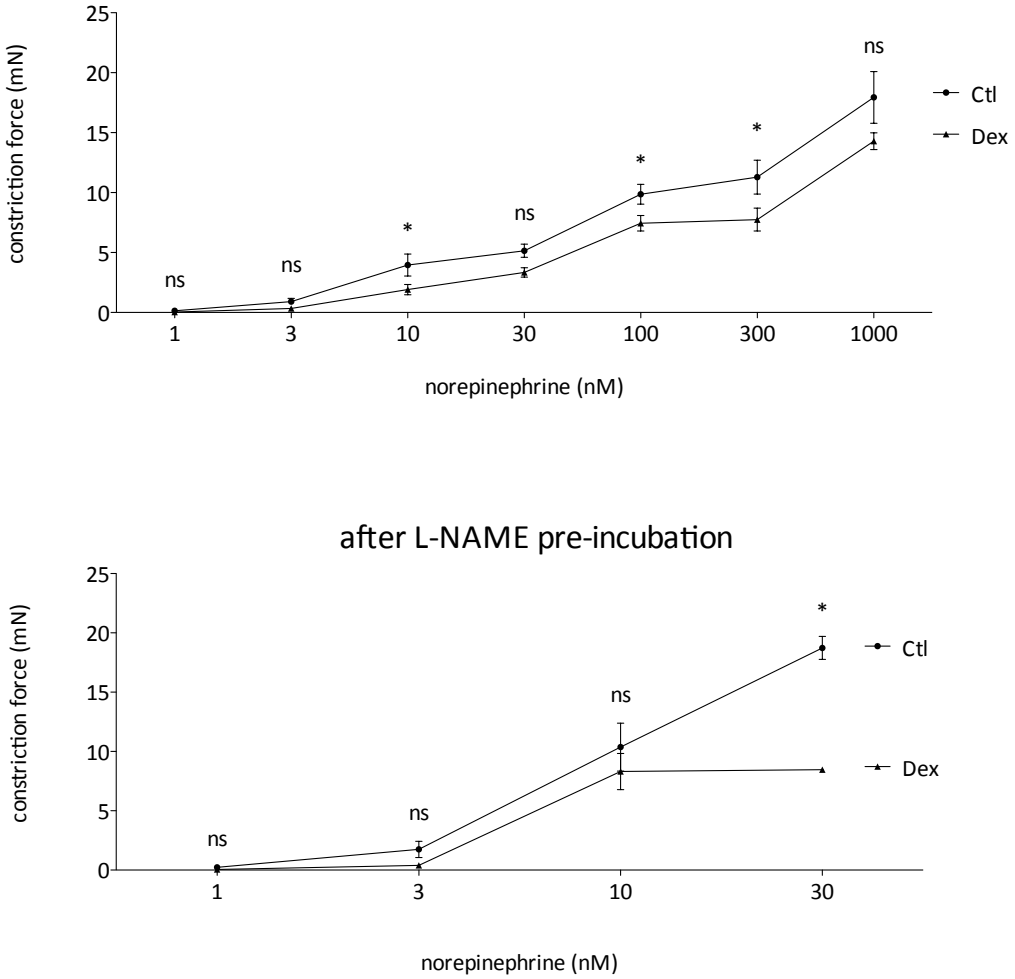

Figure 4.3: Impact of DEX on constriction ability of rat aorta. Normotensive Wistar Kyoto (WKY) rats were orally treated with water-soluble DEX (0.03 mg / kg / day) for 12 days. On day 13 the animals were sacrificed and the rat's aortas were dissected. For subsequent analysis of the endothelial function, rings (2 mm in length) were cut out of the aorta and fixed in an organ bath gadget for further investigation. Columns represent mean + SEM, n=12. ns=not significant, *p<0.05, between Dex and Ctl.

After analysis of the aorta's constriction ability in absence and presence of the NOS inhibitor L-NAME, the difference in force (depending on L-NAME) between those two conditions (for detailed data see Figure 4.3) was calculated (Figure 4.4).

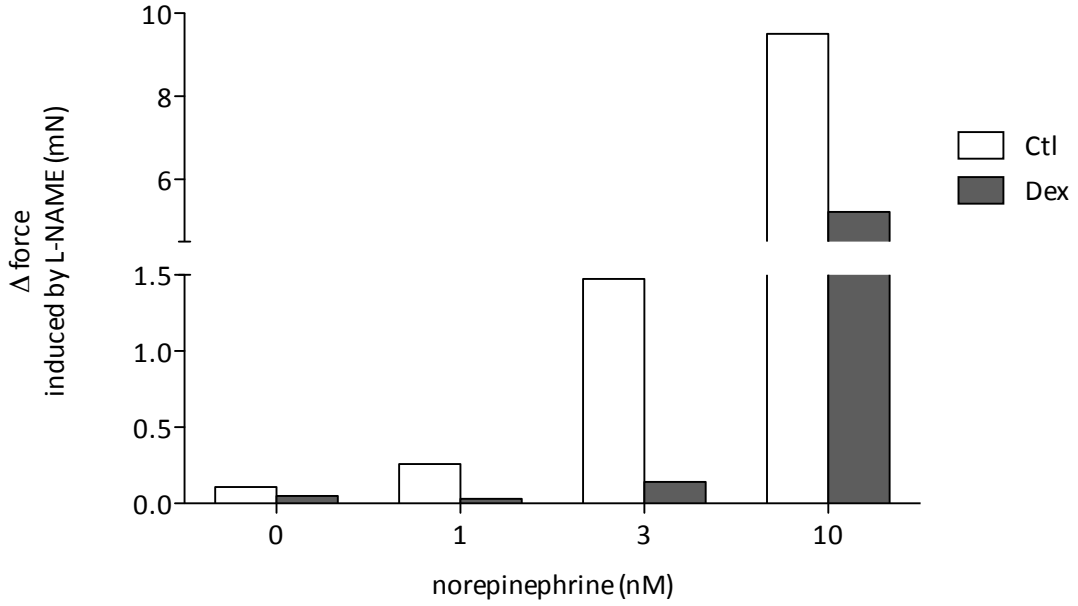

Figure 4.4: L-NAME-induced constriction ability in rat aorta. Normotensive Wistar Kyoto (WKY) rats were orally treated with water-soluble DEX (0.03 mg / kg / day) for 12 days. On day 13 the animals were sacrificed and the rat's aortas were dissected. For subsequent analysis of the endothelial function, rings (2 mm in length) were cut out of the aorta and fixed in an organ bath gadget for further investigation. The graph above shows the delta force depending on L-NAME of the two graphs shown in Figure 4.3.

Indomethacin is a nonselective inhibitor of cyclooxygenase 1 and 2 (COX1 and COX2), enzymes that participate in prostaglandin synthesis from arachidonic acid. Aortas were pre-incubated for 30 min with indomethacin (5×10^{-4} M), contraction/relaxation experiments were performed in the presence of indomethacin to analyze a possible role of prostaglandins. In the presence of indomethacin, no significant differences in vasomotion were found between aortas of DEX treated rats compared to those dissected from control animals (Figure 4.5).

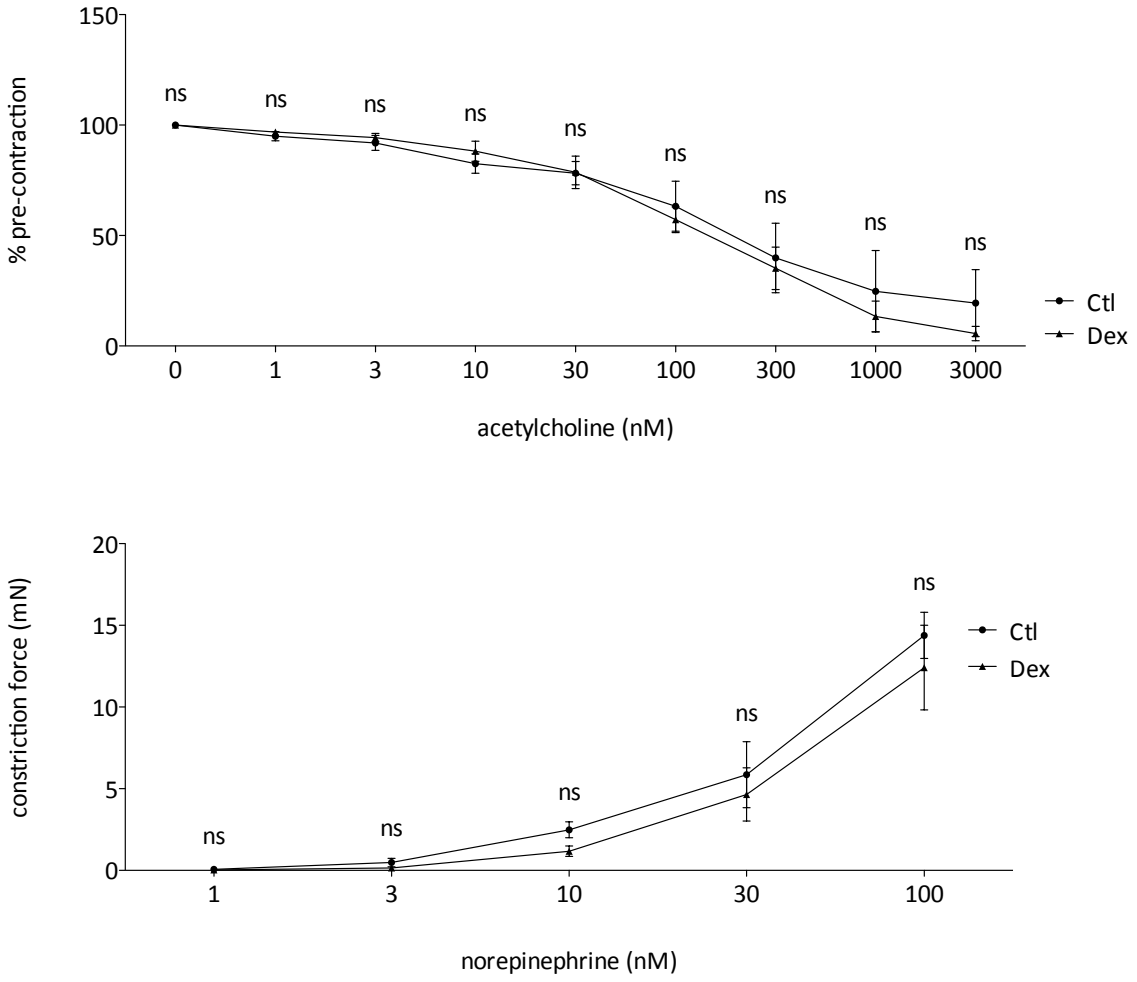

Figure 4.5: Impact of DEX on the aorta's function in rats in presence of indomethacin. Normotensive Wistar Kyoto (WKY) rats were orally treated with water-soluble DEX (0.03 mg / kg / day) for 12 days. On day 13 the animals were sacrificed and the rat's aortas were dissected. For subsequent analysis of the endothelial function, rings (2 mm) were cut out of the aorta and fixed in an organ bath gadget for further investigation. Samples were pre-incubated with indomethacin ($5*10^{-4}$ M) for 30 min prior to measurement of the vessel function. Columns represent mean + SEM, n=4. ns=not significant, between Dex and Ctl.

4.1.3 In Whole Blood the production of ROS Was Increased

In the following experiment the effect of DEX on ROS production in whole blood was analyzed. Normotensive Wistar Kyoto rats (6 months of age) were orally treated with water-soluble DEX. The approximate target dose of 0.03 mg / kg / day DEX was given for 12 days; untreated rats served as controls (3.9.1). To investigate the production of reactive oxygen radicals after treatment with DEX, chemiluminescence measurements were performed (3.6.2). There was a slightly elevated ROS production in DEX treated animals compared to control animals; but this effect was not significant. When blood samples were stimulated with PMA, a PKC activator, the difference between control and DEX is highly significant. An increased production of ROS could be demonstrated for blood samples of DEX treated rats (Figure 4.6).

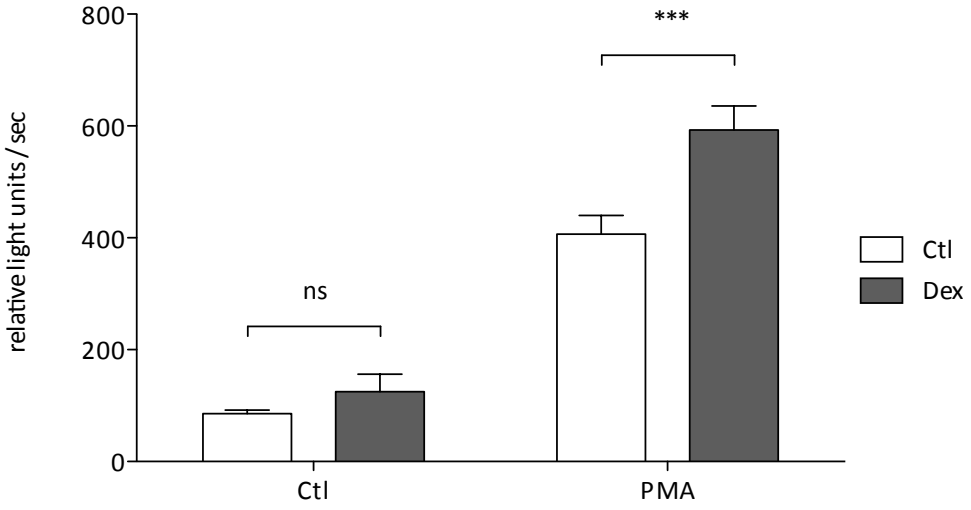

Figure 4.6: Impact of DEX on ROS production in whole blood of rats. Normotensive Wistar Kyoto (WKY) rats were orally treated with water-soluble DEX (0.03 mg / kg / day) for 12 days. On day 13 the animals were sacrificed and the rat's blood was collected out of the heart. For subsequent analysis of ROS production, blood samples were used in a 1:100 dilution (in PBS) and incubated with 100 µM L-012 and 100 nM PMA for 20 min at 37 °C. Columns represent mean + SEM, n=12. ns=not significant, ***p<0.001, compared to corresponding control.

4.1.4 Pro-oxidative Enzymes: Nox1, Nox4 and XDH Were Upregulated by DEX Whereas Nox2 and $p22^{phox}$ Were Not Altered

In the following experiment the *in vivo* GC effect on mRNA expression of pro-oxidative enzymes was investigated. Normotensive Wistar Kyoto rats (6 months of age) were orally treated with an approximate target dose of 0.03 mg / kg / day water-soluble DEX for 12 days; untreated rats served as controls (3.9.1). After dissecton of the aortas (3.9.2) samples were prepared for mRNA expression analysis. Total RNA was isolated (3.3.1) and the mRNA expression levels of the following genes were analyzed via quantitative RT-PCR (3.3.5): Nox1, Nox2, Nox4, $p22^{phox}$ and XDH. A significant increase in mRNA expression could be observed for the NADPH oxidase isoforms Nox1 and Nox4 as well as XDH, whereas no change could be detected for Nox2 and $p22^{phox}$ compared to control (Figure 4.7).

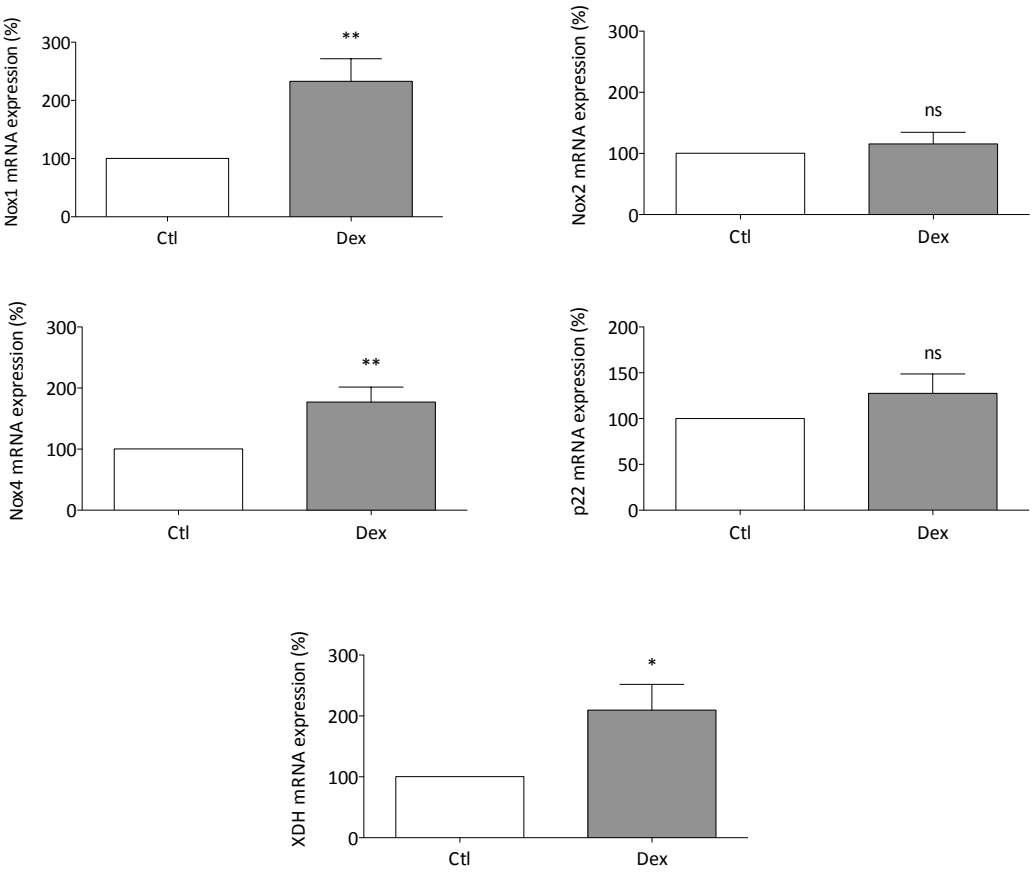

Figure 4.7: mRNA expression of pro-oxidative enzymes in rat aorta after treatment of animals with DEX. Normotensive Wistar Kyoto (WKY) rats were orally treated with water-soluble DEX (0.03 mg / kg / day) for 12 days. On day 13 the animals were sacrificed and the rat's aortas were dissected. For subsequent analysis of the mRNA expression of the enzymes shown above, total RNA was isolated and analyzed by qRT-PCR. The housekeeping gene Pol IIa was used as reference gene for normalization. Columns represent mean + SEM, n=12. ns=not significant, *p<0.05, **p<0.01, compared to control (Ctl).

4.1.5 Anti-Oxidative Enzymes: GPx1 Was Affected by DEX on mRNA Expression Level

To analyze the effects of GCs on anti-oxidative enzymes, normotensive Wistar Kyoto rats (6 months of age) were orally treated with an approximate target dose of 0.03 mg / kg / day water-soluble DEX for 12 days; untreated rats served as controls (3.9.1). After dissecton of the aortas (3.9.2) samples were prepared for mRNA expression analysis. Total RNA was isolated (3.3.1) and the mRNA expression levels of the following genes were analyzed by quantitative RT-PCR (3.3.5): Superoxide dismutases 1-3 (SOD1-3), catalase (Cat), glutathione peroxidase 1 (GPx1), thioredoxin 1 and 2 (TXN1+2). Out of the investigated genes GPx1 was the only one being significantly upregulated after DEX treatment. For the other genes no significant effect could be observed (Figure 4.8).

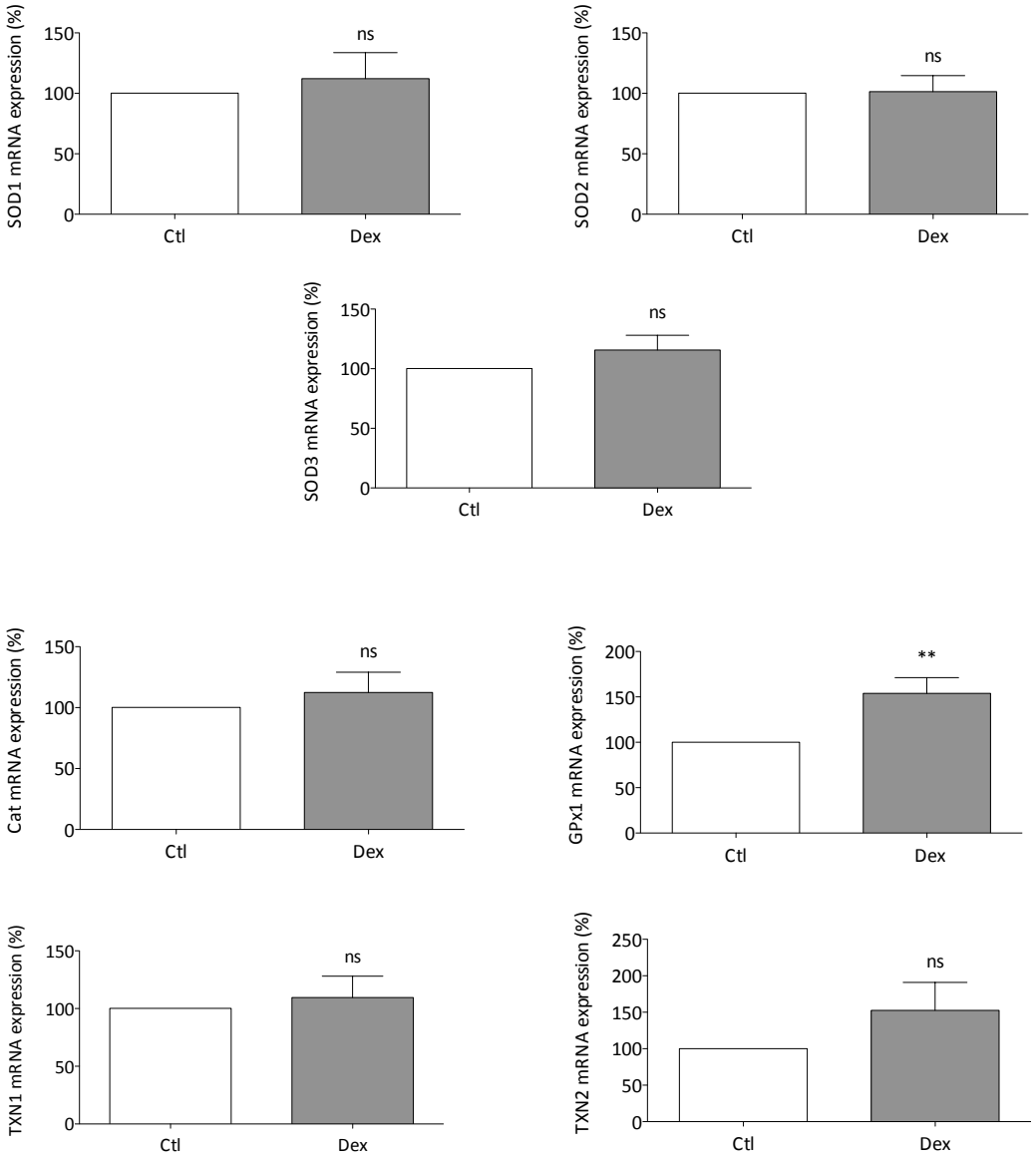

Figure 4.8: mRNA expression of anti-oxidative enzymes in rat aorta after treatment of animals with DEX. Normotensive Wistar Kyoto (WKY) rats were orally treated with water-soluble DEX (0.03 mg / kg / day) for 12 days. On day 13 the animals were sacrificed and the rat's aortas were dissected. For subsequent analysis of the mRNA expression of the enzymes shown above, total RNA was isolated and analyzed by qRT-PCR. The housekeeping gene Pol IIa was used as reference gene for normalization. Columns represent mean + SEM, n=12. ns=not significant, **p<0.01, compared to control (Ctl).

4.1.6 Enzymes Involved in Vascular Inflammation Did Not Consistently Response To DEX Treatment

To analyze *in vivo* GC effects on the expression of enzymes and factors involved in vascular inflammation, normotensive Wistar Kyoto rats (6 months of age) were orally treated with an approximate target dose of 0.03 mg / kg / day water-soluble DEX for 12 days; untreated rats served as controls (3.9.1). After dissecton of the aortas (3.9.2) samples were prepared for mRNA expression analysis. Total RNA was isolated (3.3.1) and the mRNA expression levels of the following genes were analyzed via quantitative RT-PCR (3.3.5): IL-6, ICAM-1 and NF-κB. Out of the investigated genes NF-κB was the only one being significantly upregulated after DEX treatment. For the other genes no significant DEX effect could be observed (Figure 4.9).

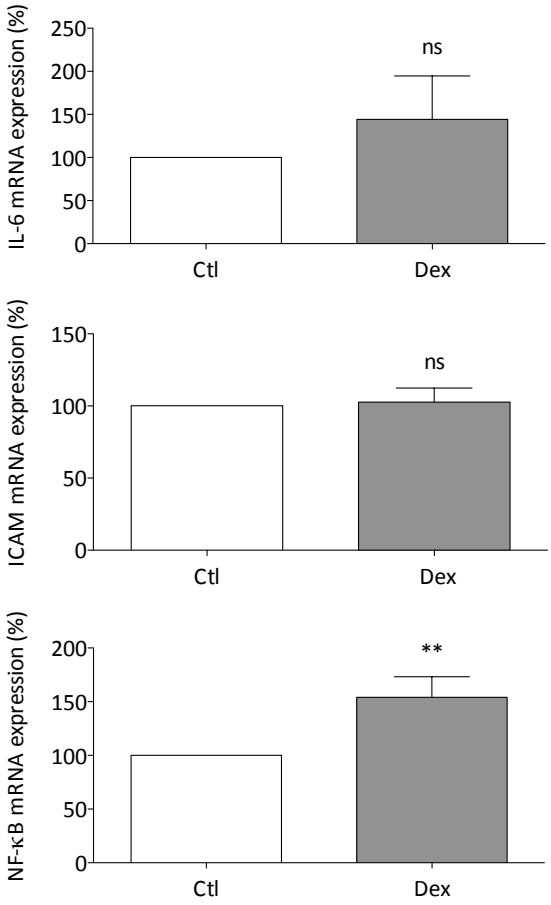

Figure 4.9: mRNA expression of different genes involved in vascular inflammation in rat aorta after treatment of animals with DEX. Normotensive Wistar Kyoto (WKY) rats were orally treated with water-soluble DEX (0.03 mg / kg / day) for 12 days. On day 13 the animals were sacrificed and the rat's aortas were dissected. For subsequent analysis of the mRNA expression of the enzymes IL-6, ICAM-1 and NF-κB, total RNA was isolated and analyzed by qRT-PCR. The housekeeping gene Pol IIa was used as reference gene for normalization. Columns represent mean + SEM, n=12. ns=not significant, **p<0.01, compared to control (Ctl).

4.1.7 DEX Treatment Led to an Increase in COX1 mRNA Expression But Did Not Affect COX2 mRNA Expression

In the following experiment the *in vivo* GC effect on mRNA expression of cyclooxygenases (COX) was investigated. Normotensive Wistar Kyoto rats (6 months of age) were orally treated with an approximate target dose of 0.03 mg / kg / day water-soluble DEX for 12 days; untreated rats served as controls (3.9.1). After dissecton of the aortas (3.9.2) samples were prepared for mRNA expression analysis. Total RNA was isolated (3.3.1) and the mRNA expression levels of both isoforms COX1 and COX2 were analyzed via quantitative RT-PCR (3.3.5). The COX1 expression level was significantly upregulated by DEX but the isoform COX2 was not altered by the same treatment (Figure 4.10).

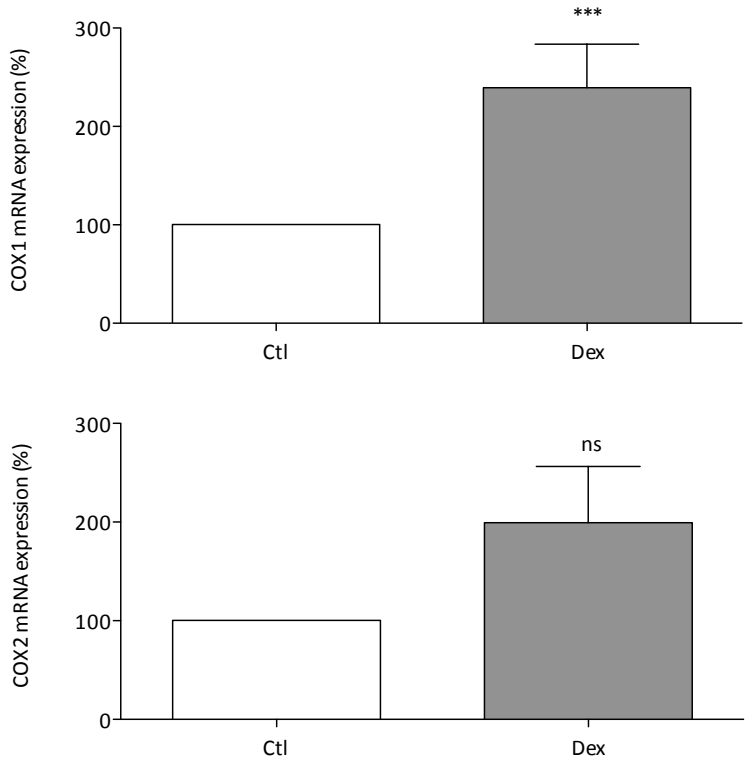

Figure 4.10: mRNA expression of COX1 and COX2 in rat aorta after treatment with DEX. Normotensive Wistar Kyoto (WKY) rats were orally treated with water-soluble DEX (0.03 mg / kg / day) for 12 days. On day 13 the animals were sacrificed and the rat's aortas were dissected. For subsequent analysis of the COX1 and COX2 mRNA expression, total RNA was isolated and investigated via qRT-PCR. The housekeeping gene Pol IIa was used as reference gene for normalization. Columns represent mean + SEM, n=12. ns=not significant, ***p<0.001, compared to control.

4.1.8 Biopterin, BH_2 and BH_4 Level in Rat Aorta Were Not Altered After DEX Treatment

Tetrahydrobiopterin (BH_4) is an essential cofactor required for the activity of eNOS. Suboptimal concentrations of BH_4 in the endothelium reduce the biosynthesis of NO, thus contributing to the pathogenesis of vascular endothelial dysfunction. To analyze how GCs affect BH_4 availability and thereby eNOS functionality the following experiment was conducted. Normotensive Wistar Kyoto rats (6 months of age) were orally treated with an approximate target dose of 0.03 mg / kg / day water-soluble DEX for 12 days; untreated rats served as controls (3.9.1). After dissection of the aortas (3.9.2) samples were prepared for HPLC analyses (3.7). In aorta samples of DEX treated rats a slightly lowered concentration of BH_4 and BH_2 as well as total biopterin could be observed but none of those changes was statistically significant (Figure 4.11).

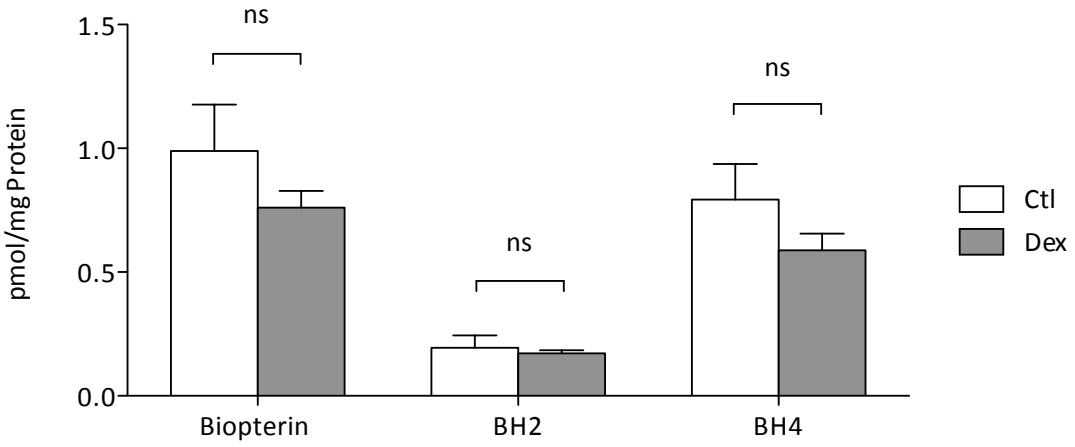

Figure 4.11: BH_4 availability in rat aorta after treatment of animals with DEX. Normotensive Wistar Kyoto (WKY) rats were orally treated with water-soluble DEX (0.03 mg / kg / day) for 12 days. On day 13 the animals were sacrificed and the rat's aortas were dissected. For subsequent analysis of the biopterin, BH_2 and BH_4 levels, aorta samples were prepared and analyzed by HPLC. Columns represent mean + SEM, n=9. ns=not significant, compared to corresponding control (Ctl).

4.1.9 In Rat Aorta eNOS mRNA Expression Is Upregulated After DEX Treatment Whereas GCH1 & DHFR Are not Altered

To gain insight into eNOS functionality, effects of DEX on eNOS and the enzymes GCH1 and DHFR was investigated. Normotensive Wistar Kyoto rats (6 months of age) were orally treated with an approximate target dose of 0.03 mg / kg / day water-soluble DEX for 12 days; untreated rats served as controls (3.9.1). After dissecton of the aortas (3.9.2) samples were prepared for mRNA expression analysis. Total RNA was isolated (3.3.1) and the mRNA expression levels of eNOS, GCH1 as well as DHFR were analyzed via quantitative RT-PCR (3.3.5). Neither GCH1 nor DHFR were significantly affected by DEX. However, for eNOS, a significantly increased mRNA expression could be demonstrated (Figure 4.12).

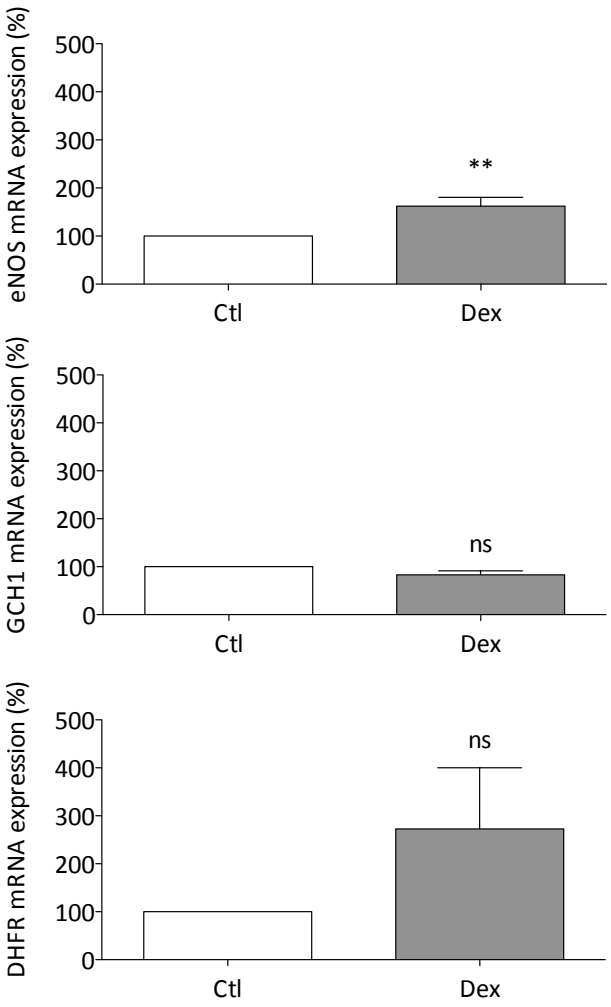

Figure 4.12: mRNA expression of eNOS, GCH1 and DHFR in rat aorta after treatment with DEX. Normotensive Wistar Kyoto (WKY) rats were orally treated with water-soluble DEX (0.03 mg / kg / day) for 12 days. On day 13 the animals were sacrificed and the rat's aortas were dissected. For subsequent analysis of the mRNA expression of the enzymes shown above, total RNA was isolated and analyzed by qRT-PCR. The housekeeping gene Pol IIa was used as reference gene for normalization. Columns represent mean + SEM, n=12. ns=not significant, **p<0.01, compared to control (Ctl).

4.2 *In vitro* Analyses of Glucocorticoid Effects in Rat Aortic Smooth Muscle Cells (A7r5)

4.2.1 Measurement of ROS With Two Different Methods Did Not Reveal Consistent Results

To investigate the effect of GC treatment on production of reactive oxygen species (ROS) A7r5 cells were incubated with 10 nM DEX for 48 h. Untreated cells served as a control and were incubated with DMSO as this was the solvent used for DEX. Subsequently cells were washed with pre-warmed HBSS and incubated with H_2DCFDA for 30 min at 37 °C (3.6.1). A slight but significant increase in ROS level after DEX treatment could be observed with this method (Figure 4.13).

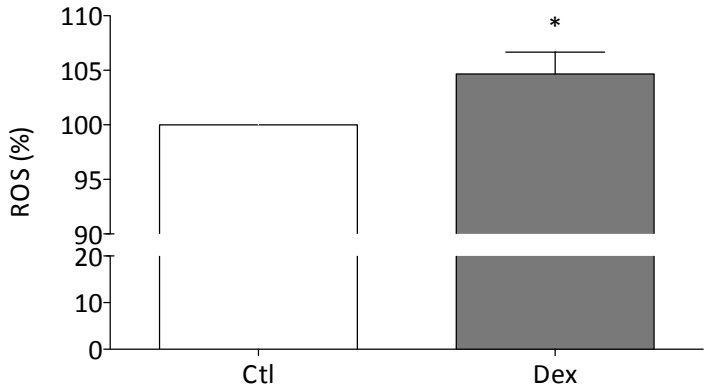

Figure 4.13: DEX effect on ROS production in rat aortic smooth muscle cells. A7r5 cells were either not treated (DMSO as control) or incubated with DEX (10 nM) for 48 h. For analysis of ROS production via fluorescence, samples were incubated with H_2DCFDA (2.5 µM) in HBSS for 30 min at 37 °C. Columns represent mean + SEM, n=36. *p<0.05, compared to control (Ctl).

The same experiment was done again and after cells were washed with pre-warmed HBSS, they were incubated with L-012 for 20 min at 37 °C. ROS development was measured by recording of chemiluminescence signals (3.6.2). In contrast to ROS determination via fluorescence measurement (3.6.1), an increase in ROS production after DEX treatment could not be observed with this method (Figure 4.14).

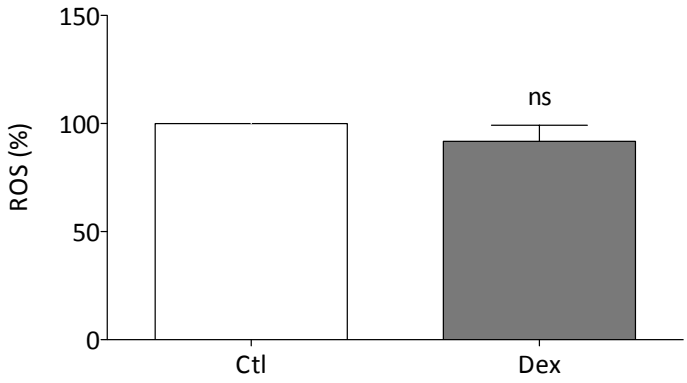

Figure 4.14: DEX effect on ROS production in rat aortic smooth muscle cells. A7r5 cells were either not treated (DMSO as control) or incubated with DEX (10 nM) for 48 h. For analysis of ROS production via luminescence, samples were incubated with L-012 (100 µM) in HBSS for 20 min at 37 °C. Columns represent mean + SEM, n=36. ns=not significant, compared to control (Ctl).

4.2.2 Nox1 mRNA Expression Was Increased After DEX Treatment Dependent on Time and Concentration

The NADPH oxidases are one of the most important ROS-producing enzyme systems in the vasculature. To analyze if DEX has any influence on the mRNA expression level of the isoform Nox1, A7r5 cells were incubated with 1, 10 or 100 nM DEX for time periods from 6 h up to 7 days. Untreated cells served as a control and were incubated with DMSO as this was the solvent used for DEX. Subsequently, total RNA was isolated (3.3.1) and the mRNA expression level of the Nox1 gene was analyzed via quantitative RT-PCR (3.3.5). Compared to control cells the expression analysis showed a time- and concentration-dependent increase of Nox1 mRNA after DEX incubation (Figure 4.15).

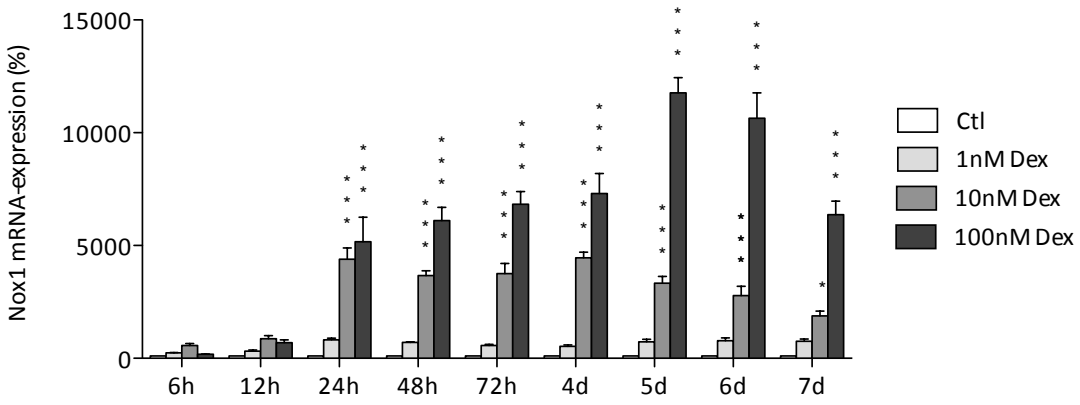

Figure 4.15: Time- and concentration-dependent effect of DEX on Nox1 mRNA expression in rat aortic smooth muscle cells. A7r5 cells were either not treated (DMSO as control) or incubated with DEX (1, 10 or 100 nM) for different periods of time (6 h up to 7 days). For subsequent analysis of the Nox1 mRNA expression, total RNA was isolated and analyzed by qRT-PCR. The housekeeping gene Pol IIa was used as reference gene for normalization. Columns represent mean + SEM, n=30. *p<0.05, ***p<0.001, compared to corresponding control (Ctl).

4.2.3 Nox4 mRNA Expression Was Decreased After DEX Treatment Dependent on Time and Concentration

Since not only Nox1 but also Nox4 is a crucial enzyme in smooth muscle cells it was important to also analyze if DEX has any influence on the mRNA expression level of this isoform. A7r5 cells were incubated with 1, 10 and 100 nM DEX for time periods from 6 h up to 7 days. Untreated cells served as a control and were incubated with DMSO as this was the solvent used for DEX. Subsequently, total RNA was isolated (3.3.1) and the mRNA expression level of the Nox4 gene was analyzed via quantitative RT-PCR (3.3.5). In contrast to the DEX effect on Nox1, the expression analysis showed a time- and concentration-dependent decrease of Nox4 mRNA compared to control cells. The mRNA was significantly lowered in cells treated with 100 nM DEX for 48 h and 4 days. Highly significant was the effect on cells treated with 10 and 100 nM DEX for 5 days. For other time-points and concentrations no significant effect could be demonstrated (Figure 4.16).

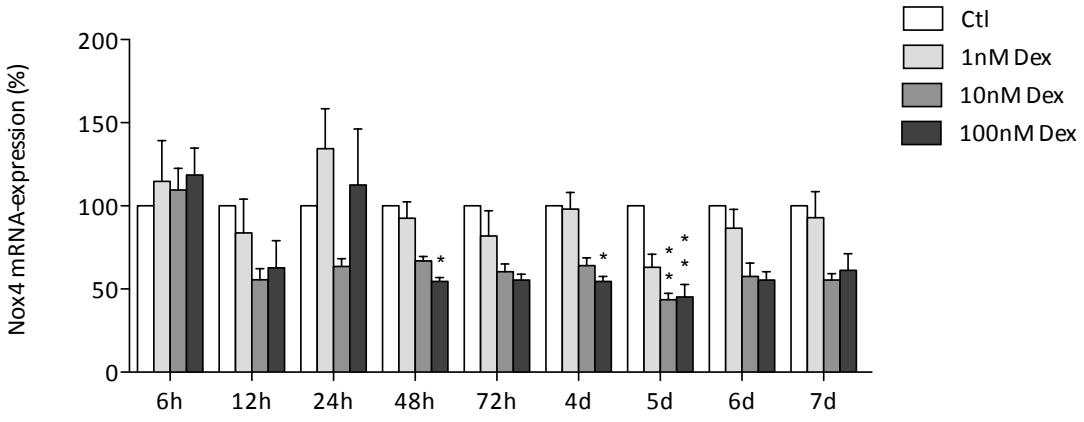

Figure 4.16: Time- and concentration-dependent effect of DEX on Nox4 mRNA expression in rat aortic smooth muscle cells. A7r5 cells were either not treated (DMSO as control) or incubated with DEX (1, 10 or 100 nM) for different periods of time (6 h up to 7 days). For subsequent analysis of the Nox4 mRNA expression, total RNA was isolated and analyzed via qRT-PCR. The housekeeping gene Pol IIa was used as reference gene for normalization. Columns represent mean + SEM, n=30. *p<0.05, **p<0.01, compared to corresponding control (Ctl).

4.2.4 DEX Did Not Alter p22^{phox} mRNA Expression

p22^{phox} is the α-subunit of the cytochrome b558-reductase and crucial for the activation of both Nox1 and Nox4. As DEX showed a significant increase in Nox1 mRNA but in contrast to this, a significant decrease in Nox4 mRNA, it was important to see whether there are any changes in the p22^{phox} mRNA expression level after DEX treatment. Therefore, A7r5 cells were incubated with 1, 10 and 100 nM DEX for time periods from 6 h up to 7 days. Untreated cells served as a control and were incubated with DMSO as this was the solvent used for DEX. Subsequently, total RNA was isolated (3.3.1) and the mRNA expression level of the p22^{phox} gene was analyzed via quantitative RT-PCR (3.3.5). Compared to control cells the expression analysis showed a significant increase in p22^{phox} mRNA after 24h-treatment with 100 nM. For other time-points and concentrations no significant effect could be demonstrated (Figure 4.17).

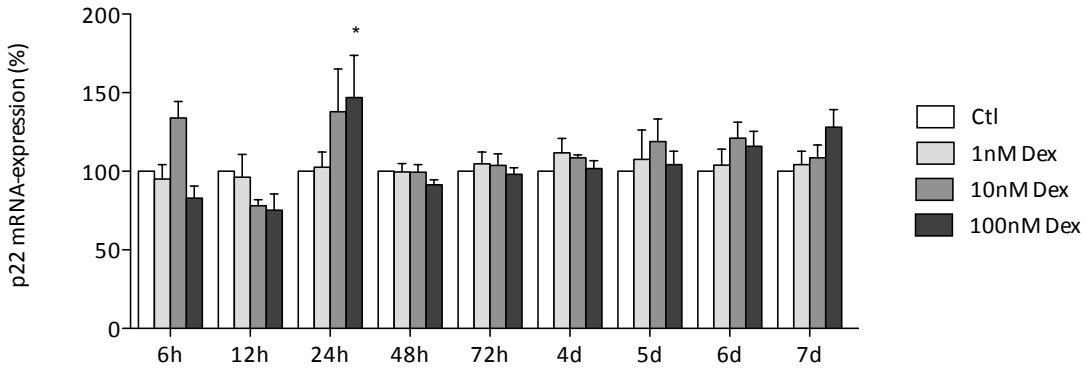

Figure 4.17: Effect of DEX on p22^{phox} mRNA expression in rat aortic smooth muscle cells. A7r5 cells were either treated with DMSO (as control) or incubated with DEX (1, 10 or 100 nM) for different periods of time (6 h up to 7 days). For subsequent analysis of the p22^{phox} mRNA expression, total RNA was isolated and analyzed via qRT-PCR. The housekeeping gene Pol IIa was used as reference gene for normalization. Columns represent mean + SEM, n=30. *p<0.05, compared to corresponding control (Ctl).

4.2.5 The Upregulation of Nox1 mRNA Expression by DEX Was Glucocorticoid Receptor-Dependent

Since incubation of A7r5 cells with DEX demonstrated a significant time- and concentration-dependent increase in Nox1 mRNA expression, the next step was to analyze whether this effect was dependent on the glucocorticoid receptor. Therefore, A7r5 cells were treated either with 10 nM DEX, with 100 nM of the glucocorticoid antagonist mifepristone (RU486) or with both substances in combination for 24 h. Subsequently, total RNA was isolated (3.3.1) and the mRNA expression level of the Nox1 gene was analyzed via quantitative RT-PCR (3.3.5). Compared to control cells the expression analysis showed a significant increase in Nox1 mRNA after 24h-treatment, as expected based on results from the previous experiment. Treatment with RU486 alone had no effect on the basal Nox1 mRNA expression, but completely blocked DEX-induced Nox1 upregulation (Figure 4.18).

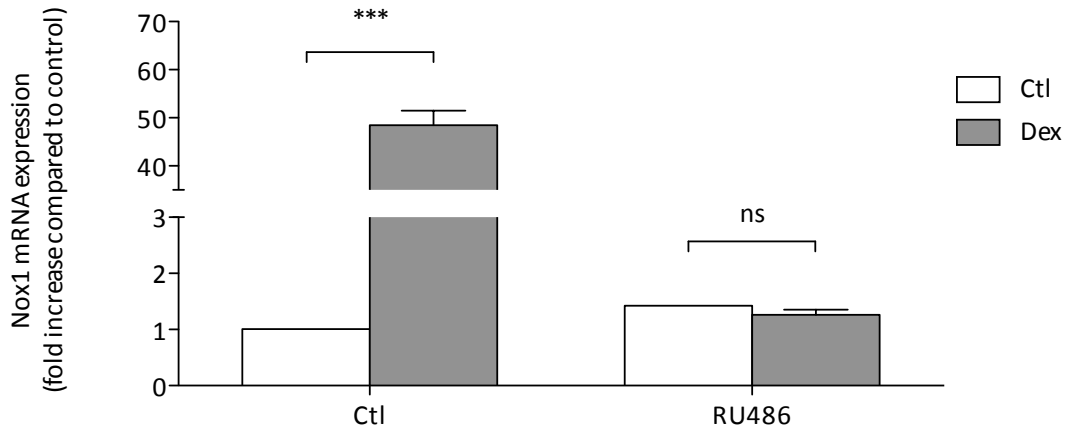

Figure 4.18: Glucocorticoid receptor-dependency of DEX effect on Nox1 mRNA expression. A7r5 cells were either not treated (DMSO as control), incubated with DEX (10 nM), with the GR antagonist mifepristone (RU486, 100 nM) or with a combination of both substances in given concentrations for 24 h. For subsequent analysis of the Nox1 mRNA expression, total RNA was isolated and investigated via qRT-PCR. The housekeeping gene Pol IIa was used as reference gene for normalization. Columns represent mean + SEM, n=12. ns=not significant, ***p<0.001, compared to control (Ctl).

4.2.6 The Downregulation of Nox4 mRNA Expression by DEX Was Glucocorticoid Receptor-Dependent

Since incubation of A7r5 cells with DEX showed a significant time- and concentration-dependent decrease in Nox4 mRNA expression, the next step was to analyze whether this effect was dependent on the glucocorticoid receptor (GR). Therefore, A7r5 cells were treated either with 10 nM DEX, with 100 nM of the GR antagonist RU486 or with both substances in combination for 24 h. Subsequently, total RNA was isolated (3.3.1) and the mRNA expression level of the Nox4 gene was analyzed via quantitative RT-PCR (3.3.5). Compared to control cells the expression analysis showed a significant decrease in Nox4 mRNA after 24h-treatment as expected. Treatment with RU486 had no effect on the basal Nox4 mRNA expression, but prevented the Nox4 downregulation by DEX (Figure 4.19).

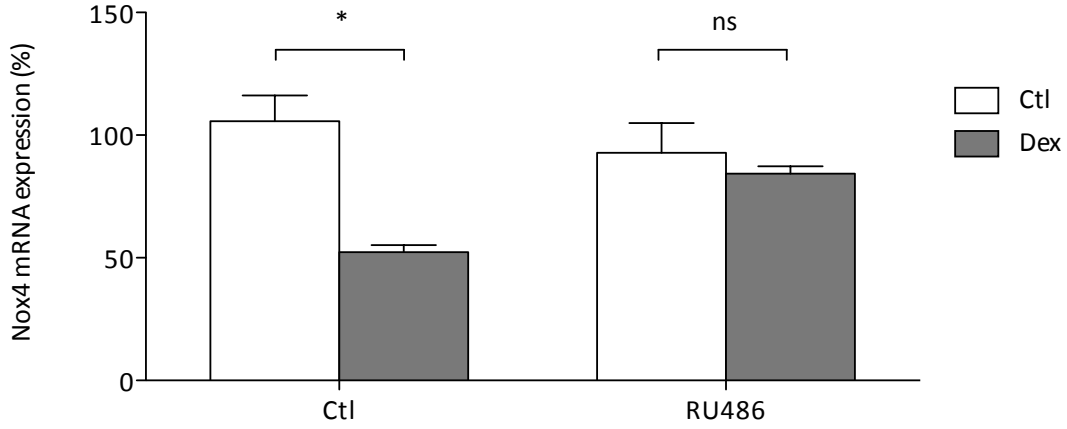

Figure 4.19: Glucocorticoid receptor-dependency of DEX effect on Nox4 mRNA expression. A7r5 cells were either not treated (DMSO as control), incubated with DEX (10 nM) or with the GR antagonist mifepristone (RU486, 100 nM) or with a combination of both substances for 24 h. For subsequent analysis of the Nox4 mRNA expression, total RNA was isolated and analyzed via qRT-PCR. The housekeeping gene Pol IIa was used as reference gene for normalization. Columns represent mean + SEM, n=12. ns=not significant, *p<0.05, compared to control (Ctl).

4.2.7 DEX Enhanced Nox1 mRNA Stability

To analyze whether DEX has an effect on Nox1 RNA decay, A7r5 cells were treated with 10 nM DEX for 24 h. Subsequently, some cells were additionally incubated with the transcription inhibitor DRB for 6 or 24 h. Thereafter, total RNA was isolated (3.3.1) and the mRNA expression level of the Nox1 gene was analyzed via quantitative RT-PCR (3.3.5). In cells treated with DEX the mRNA stability was significantly increased compared to control cells (Figure 4.20).

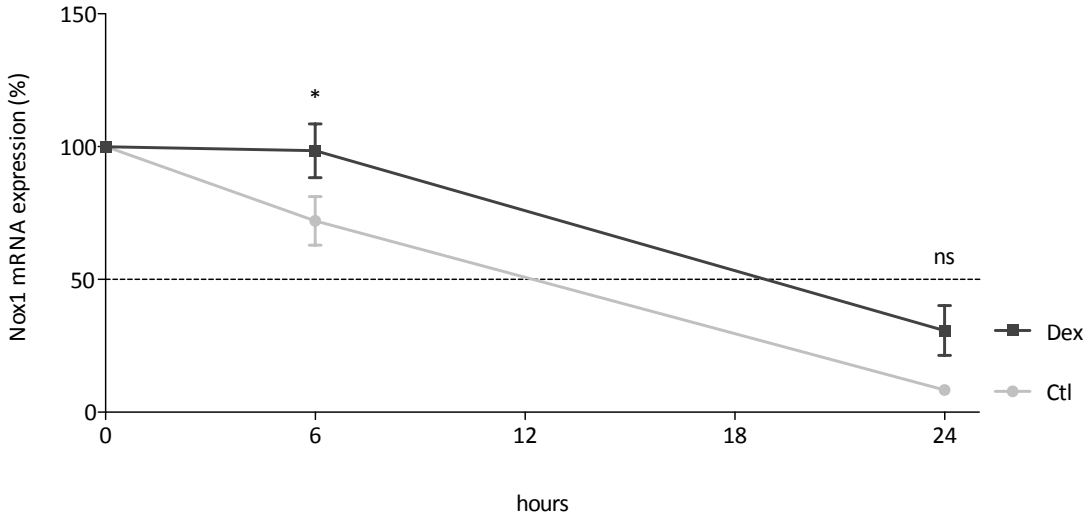

Figure 4.20: Effect of DEX on half-life of Nox1 mRNA. A7r5 cells were either not treated (DMSO as control) or incubated with DEX (10 nM) for 24 h. Some cells was incubated further with the transcription inhibitor DRB (60 µM) for 6 h or 24 h, respectively. For subsequent analysis of the Nox1 mRNA expression, total RNA was isolated and analyzed via qRT-PCR. The housekeeping gene Pol IIa was used as reference gene for normalization. Columns represent mean ± SEM, n=24. ns=not significant, *p<0.05, compared to control (Ctl).

4.2.8 The Effect of DEX on Nox1 mRNA Expression Was Transcription-Dependent

To analyze whether the observed DEX effect on Nox1 is a transcriptional event, A7r5 cells were first pre-incubated with the transcription inhibitor DRB (60 µM) for 30 min and subsequently treated additionally with 10 nM DEX for another 6 or 24 h. Afterwards total RNA was isolated (3.3.1) and the mRNA expression level of the Nox1 gene was analyzed via quantitative RT-PCR (3.3.5). The upregulation of Nox1 mRNA after 6 h of DEX incubation could be blocked with DRB (Figure 4.21, top). The upregulation of Nox1 after 24 h DEX (26-fold), however, was only partially blocked by DRB (4-fold induction by DEX) (Figure 4.21, bottom).

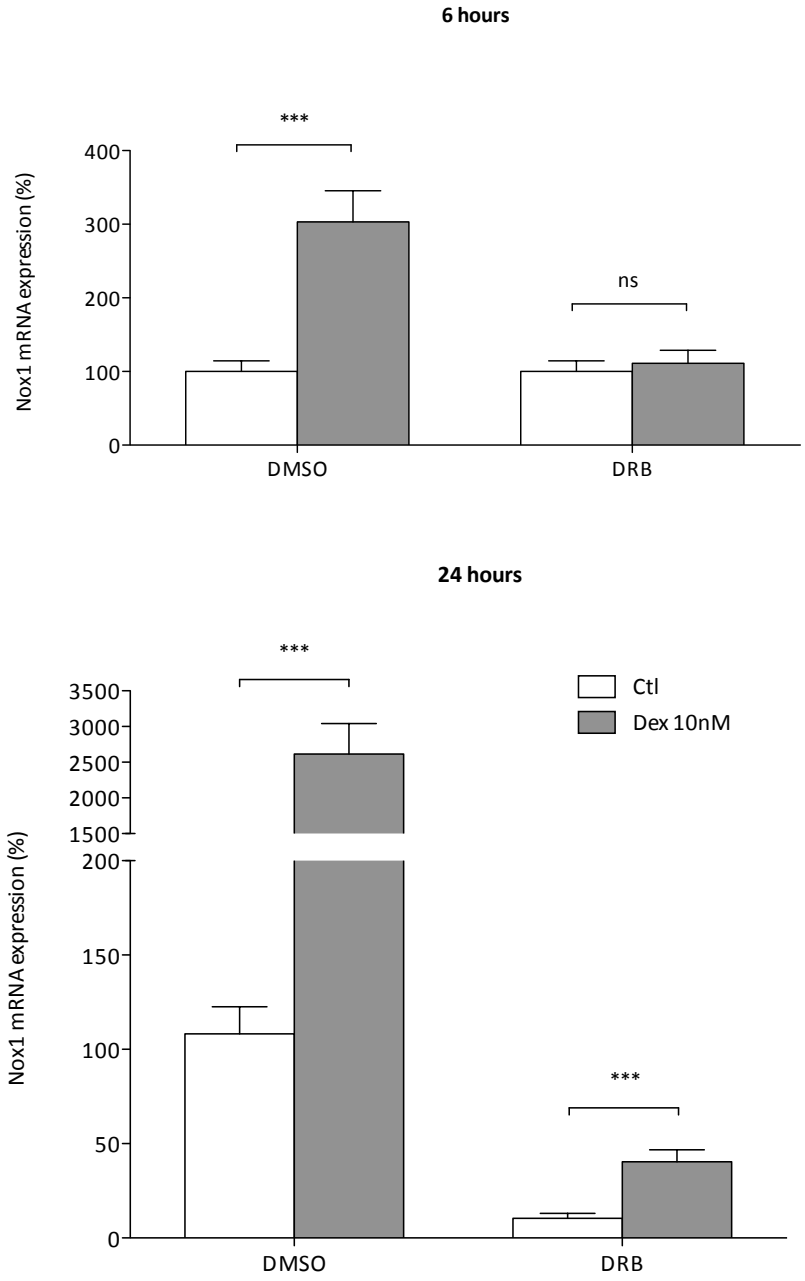

Figure 4.21: Transcription dependency of DEX effect on Nox1. A7r5 cells were pre-incubated with either DMSO or the transcription inhibitor DRB (60 µM) for 30 min, followed by an additional incubation with DMSO as control or DEX (10 nM) for 6 h or 24 h, respectively. For subsequent analysis of the Nox1 mRNA expression, total RNA was isolated and analyzed via qRT-PCR. The housekeeping gene Pol IIa was used as reference gene for normalization. Columns represent mean + SEM, n=9. ns=not significant, ***p<0.001, compared to control (Ctl).

4.2.9 DEX Decreased the Activity of an Exogenous Nox1 Promoter

To analyze the effect of DEX on the Nox1 promoter activity, A7r5 cells were transiently transfected with the pGl3_huNox1_6000 plasmid (3.2.5). On the next day cells were treated with 10 nM DEX or DMSO as a control (as this is the solvent used for DEX) for 24 h. Subsequently, cell extracts were isolated (3.5.2) and samples were prepared for analysis via luciferase assay (3.5.3). DEX treatment led to a significant decrease of Nox1 promoter activity (Figure 4.22).

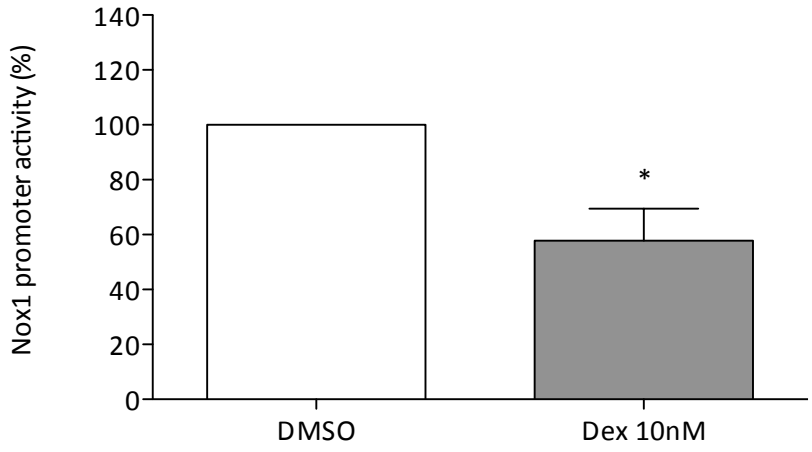

Figure 4.22: Effect of DEX on Nox1 promoter activity in rat aortic smooth muscle cells. A7r5 cells were transfected with a Nox1 promoter construct (cloned into a pGl3_basic vector) an treated with either DMSO as control or DEX (10 nM) for 24 h. For subsequent analysis of Nox1 promoter activity, samples were prepared and analyzed via luciferase assay. Columns represent mean + SEM, n=24. *p<0.05, compared to DMSO control.

4.2.10 Pro-oxidative Enzymes: DEX Led to an Increase in XDH and Nox1 mRNA Expression But to a Decrease in Nox4 mRNA Expression

In the following experiment A7r5 cells were incubated with 10 nM DEX for 24 h to analyze the effect of DEX on pro-oxidative enzymes. Control cells were incubated with DMSO as this is the solvent used for DEX. Subsequently, total RNA was isolated (3.3.1) and the mRNA expression levels of the following genes were analyzed via quantitative RT-PCR (3.3.5): Nox1, Nox4, xanthine dehydrogenase (XDH). In cells treated with DEX the mRNA expression level of XDH and Nox1 was significantly upregulated, whereas Nox4 was downregulated compared to control (Figure 4.23).

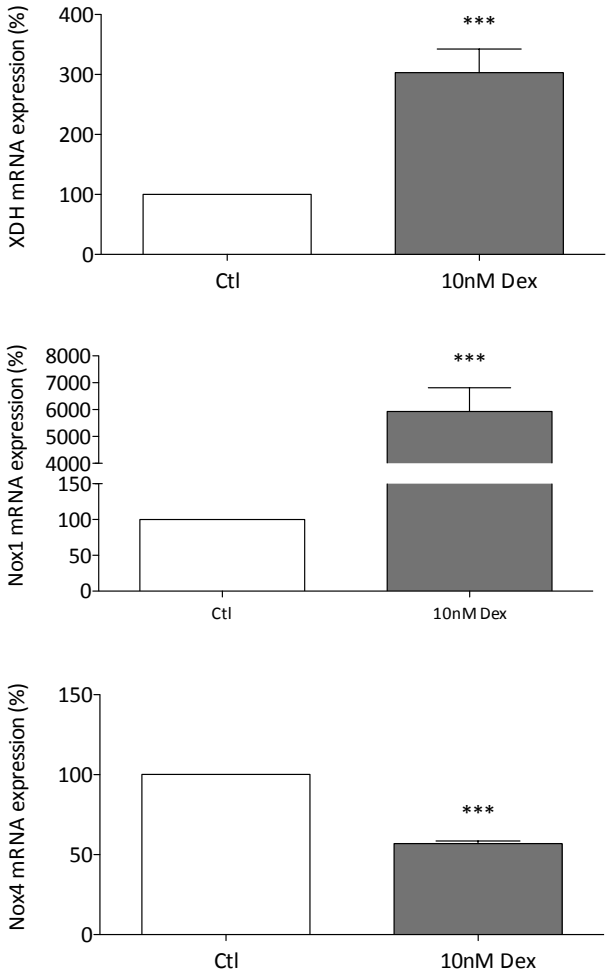

Figure 4.23: Effect of DEX on pro-oxidative enzymes in rat aortic smooth muscle cells. A7r5 cells were either treated with DMSO (as control) or incubated with DEX (10 nM) for 24 h. For subsequent mRNA expression analysis, total RNA was isolated and analyzed via qRT-PCR. The housekeeping gene Pol IIa was used as reference gene for normalization. Columns represent mean + SEM, n=21-36. ***p<0.001, compared to control.

4.2.11 Effect of DEX on Anti-Oxidative Enzymes

To study the potential effect of DEX on anti-oxidative enzymes, A7r5 cells were incubated with 10 nM DEX for 24 h. Control cells were incubated with DMSO as this was the solvent used for DEX. Subsequently, total RNA was isolated (3.3.1) and the mRNA expression levels of the following genes were analyzed via quantitative RT-PCR (3.3.5): SOD1-3, GPx1, Cat, TXN1 and TXN2. Out of the three SOD isoforms only SOD2 was slightly upregulated by DEX. A significantly decreased expression was observed for both enzymes Cat and GPx1, whereas neither of both TXN isoforms was affected by DEX (Figure 4.24).

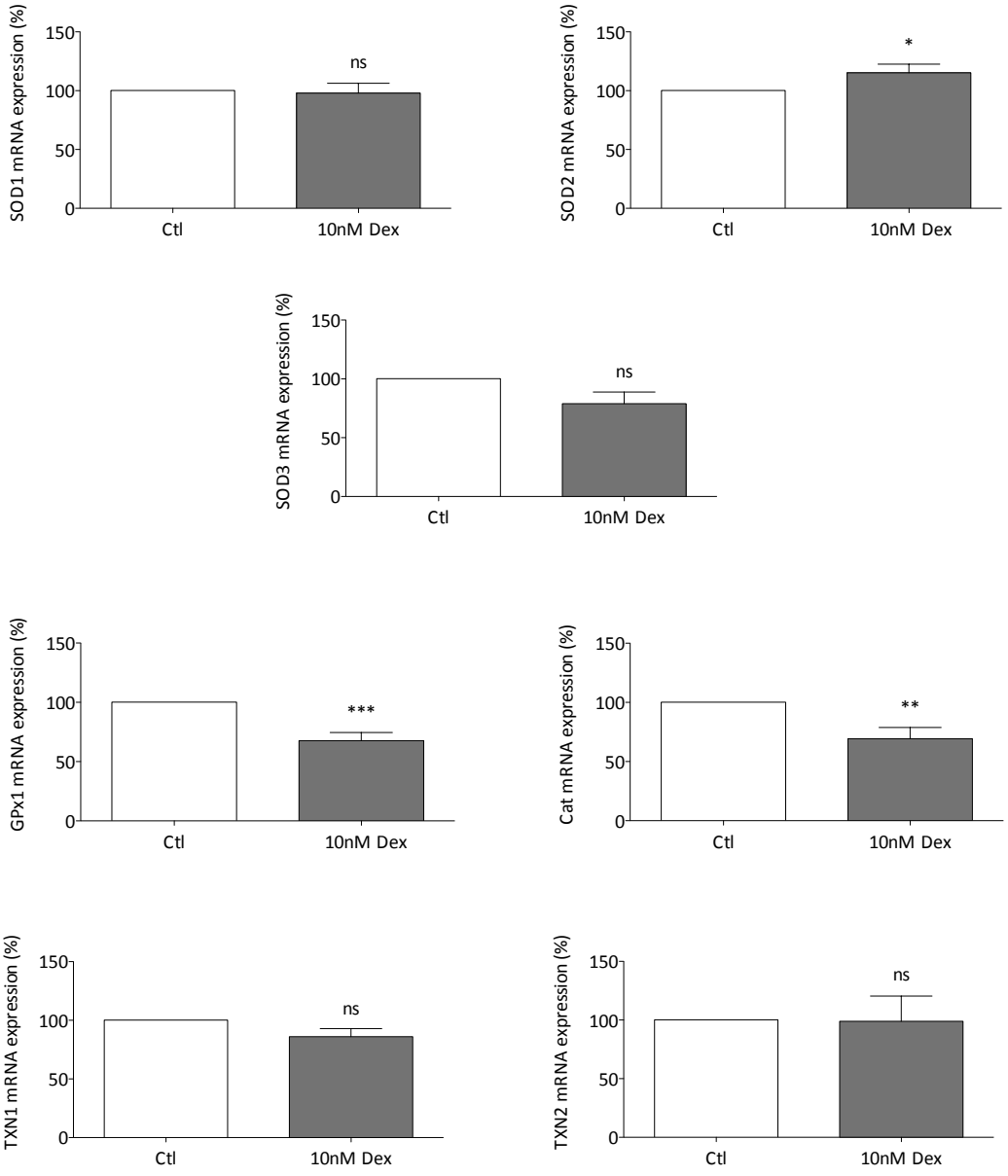

Figure 4.24: Effect of DEX on anti-oxidative enzymes in rat aortic smooth muscle cells. A7r5 cells were either treated with DMSO (as control) or incubated with DEX (10 nM) for 24 h. For subsequent analysis of the mRNA expression, total RNA was isolated and analyzed via qRT-PCR. The housekeeping gene Pol IIa was used as reference gene for normalization. Columns represent mean + SEM, n=21-36. ns=not significant, *p<0.05, **p<0.01, ***p<0.001, compared to control (Ctl).

4.3 Analyses of Glucocorticoid Effects in Human Endothelial Cells (EA.hy 926)

4.3.1 Effect of DEX on ROS production

EA.hy 926 cells were either treated with DMSO (as control) or incubated with DEX (1, 10 or 100 nM) for 24 h. For subsequent analysis of the ROS production, fluorescence measurement in a plate reader was performed (3.6.1). A total of 8 experiments were carried out. It was not possible to draw a clear conclusion from this set of experiments. In most experiments, DEX tended to increase ROS levels (represented by the red lines). There was a tendency in some experiments that L-NAME reduced DEX-induced ROS production (represented by the grey lines). Unfortunately, the results of the experiments were not always consistent (Figure 4.25).

Figure 4.25: Effect of DEX on ROS production in EA.hy 926 cells. EA.hy 926 cells were either treated with DMSO (as control) or incubated with DEX (1, 10 or 100 nM) for 24 h. Subsequently cells were incubated with H_2DCFDA (2.5 µM) in HBSS for 30 min at 37 °C, in presence or absence of the NOS inhibitor L-NAME (500 µM). ROS were detected by fluorescence measurement in a plate reader. Graphs show all 8 experiments carried out. Red lines: measurement without L-NAME, grey lines: measurement in the presence of L-NAME. Columns represent mean ± SEM, n=12. (see next page)

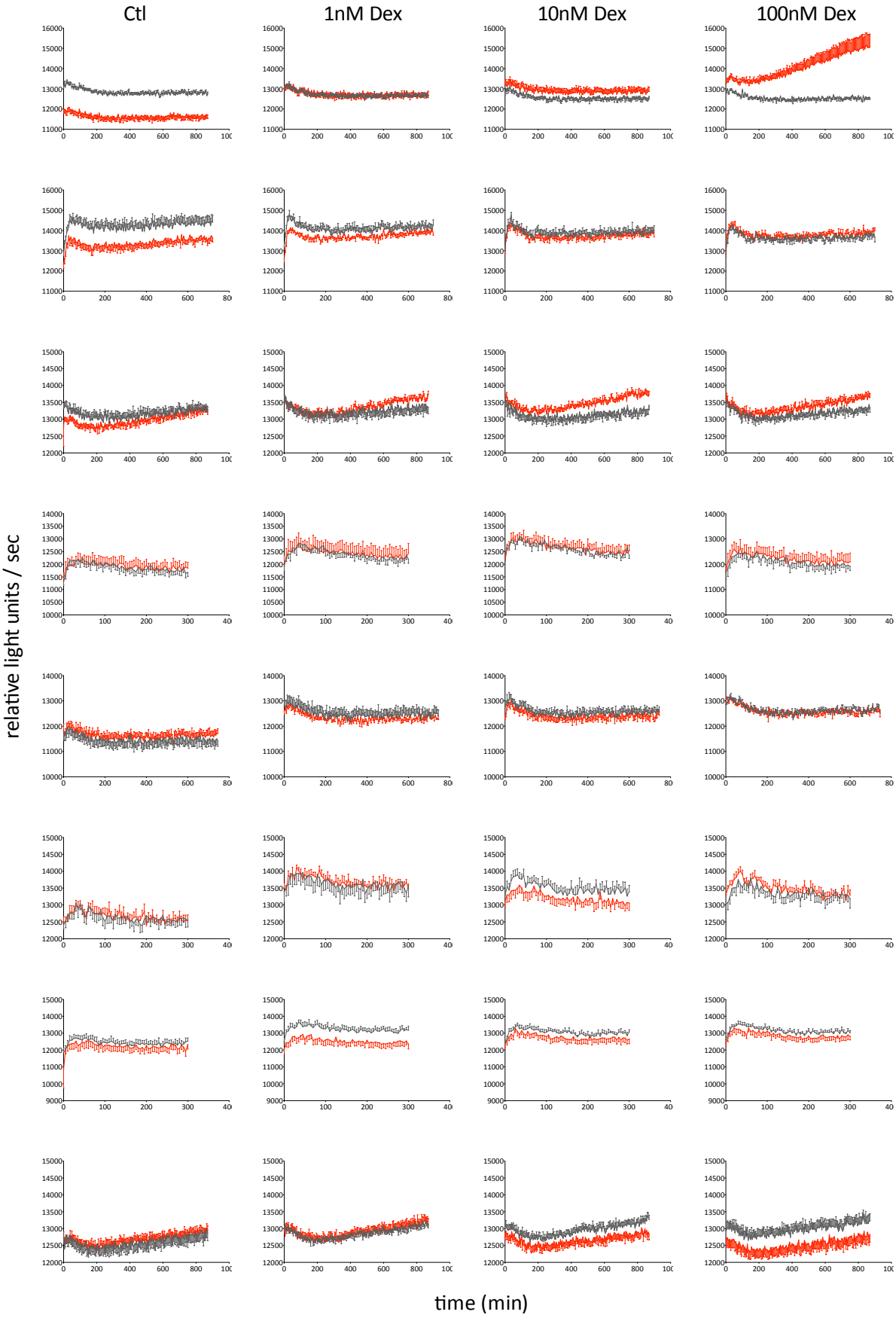
Ctl
1nM Dex
10nM Dex
100nM Dex
relative light units / sec
time (min)

Using just one single technique for detecting intracellular ROS is not reliable enough to judge the oxidative stress status. Therefore, additional experiments were performed using Fluorescence-Activated Cell Sorting (FACS) for ROS measurement (3.6.3). The graph below shows one representative experiment. A concentration-dependent ROS generation after DEX treatment (represented by the red columns) was observed. When measured in the presence of L-NAME (represented by the grey columns), ROS levels were inversely correlated with DEX concentrations (Figure 4.26).

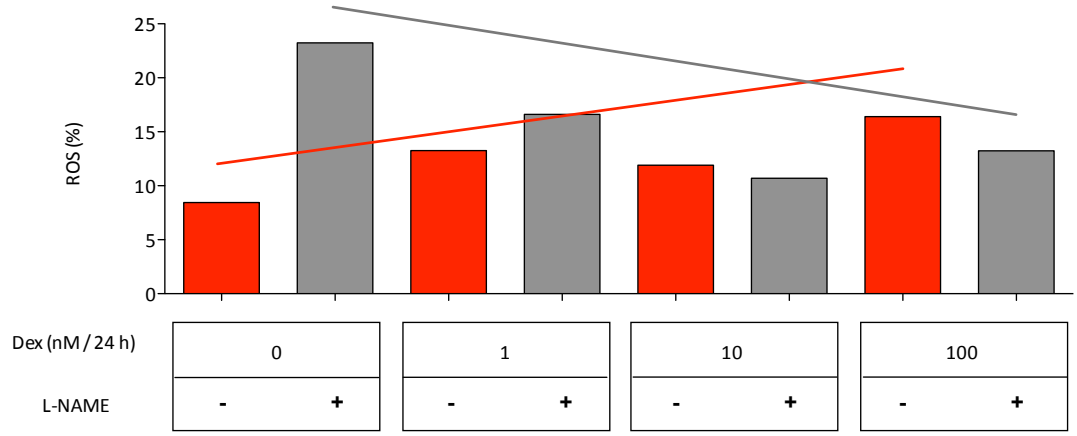

Figure 4.26: Effect of DEX effect on ROS production in EA.hy 926 cells - FACS measurement. EA.hy 926 cells were either treated with DMSO (as control) or incubated with DEX (1, 10 or 100 nM) for 24 h. Subsequently cells were incubated with H_2DCFDA (2.5 µM) in HBSS for 30 min at 37 °C, with or without the NOS inhibitor L-NAME (500 µM). The following determination of ROS was performed with Fluorescence-Activated Cell Sorting (FACS). The graph above shows representative results of one experiment with n=1. Red: without L-NAME, grey: with L-NAME. Integrated lines demonstrate tendency of ROS development with increasing DEX concentration in absence or presence of L-NAME.

4.3.2 Effect of DEX on Pro-oxidative Enzymes

In the following experiment the effect of GCs on mRNA expression of pro-oxidative enzymes was investigated. EA.hy 926 cells were incubated with 1, 10 and 100 nM DEX for 24 h. Control cells were incubated with DMSO as this was the solvent used for DEX. Subsequently, total RNA was isolated (3.3.1) and the mRNA expression levels of XDH and also Nox4 were analyzed via quantitative RT-PCR (3.3.5). The XDH expression was not significantly changed after DEX treatment. The enzyme Nox4 showed a significant downregulation of the mRNA expression level after incubation of cells with 100 nM DEX (Figure 4.27).

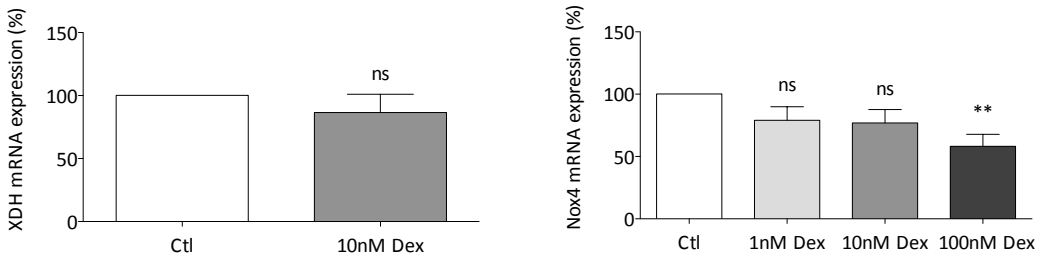

Figure 4.27: Effect of DEX on pro-oxidative enzymes in human endothelial cells. EA.hy 926 cells were either treated with DMSO (as control, Ctl) or incubated with with DEX (1, 10 or 100 nM) for 24 h. For subsequent analysis of the mRNA expression, total RNA was isolated and analyzed via qRT-PCR. The housekeeping gene TBP was used as reference gene for normalization. Columns represent mean + SEM, n=18-36. ns=not significant, **p<0.01, compared to Ctl.

4.3.3 Anti-Oxidative Enzymes: TXN2 Was the Only Investigated Enzyme That Was Regulated by DEX Treatment

After investigating the effect of GCs on mRNA expression of pro-oxidative enzymes it was also important to analyze whether there were changes in anti-oxidative enzymes as well. Therefore, EA.hy 926 cells were incubated with 1, 10 and 100 nM DEX for 24 h. Control cells were incubated with DMSO as this was the solvent used for DEX. Subsequently, total RNA was isolated (3.3.1) and the mRNA expression level of the following genes was analyzed via quantitative RT-PCR (3.3.5): Cat, SOD1, GPx1 and TXN2. Whereas for the enzymes Cat, SOD1 and GPx1 no significant change in mRNA expression could be revealed, TXN2 showed a concentration-dependent and significant down-regulation (Figure 4.28). Although not displayed in the graph below, also TXN1 was investigated after incubation with 10 nM DEX, indicating no change in mRNA expression.

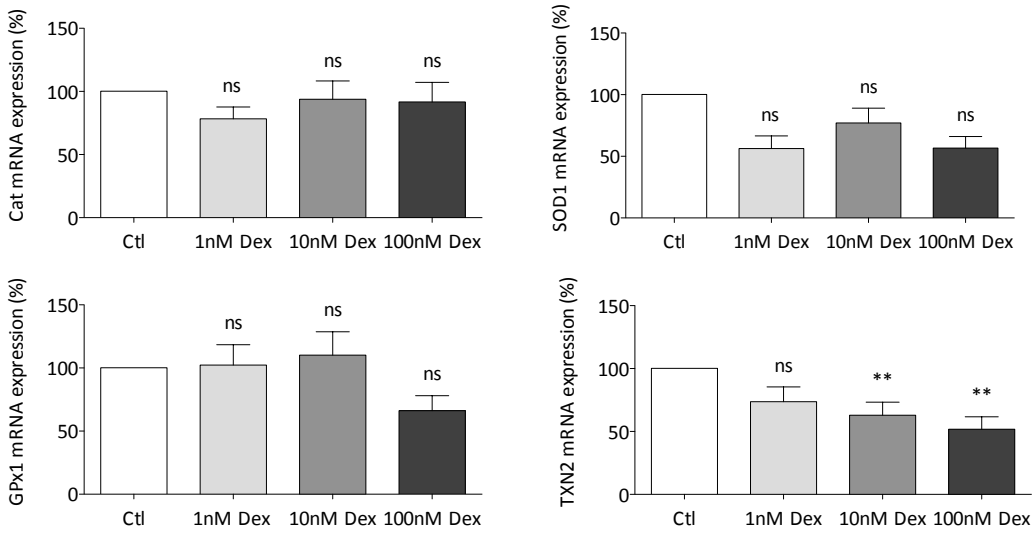

Figure 4.28: Effect of DEX on anti-oxidative enzymes in human endothelial cells. EA.hy 926 cells were either treated with DMSO (as control, Ctl) or incubated with with DEX (1, 10 or 100 nM) for 24 h. For subsequent analysis of the mRNA expression, total RNA was isolated and analyzed via qRT-PCR. The housekeeping gene TBP was used as reference gene for normalization. Columns represent mean + SEM, n=18-36. ns=not significant, **p<0.01, compared to Ctl.

4.3.4 DEX Led to a Time- and Concentration-Dependent Decrease in eNOS mRNA Expression

For the functionality of eNOS it is important to determine whether NO is produced or oxygen radicals. To analyze whether DEX has any effect on the eNOS mRNA expression, EA.hy 926 cells were incubated with 1, 10 and 100 nM DEX for time periods from 24 h up to 72 h. Control cells were incubated with DMSO as this is the solvent used for DEX. Subsequently, total RNA was isolated (3.3.1) and the mRNA expression level of the eNOS gene was analyzed via quantitative RT-PCR (3.3.5). Compared to corresponding controls, cells treated for 24 h with 1 nM DEX showed an elevated mRNA expression level. After 72 h DEX treatment, a concentration-dependent decrease of eNOS mRNA could be observed (Figure 4.29).

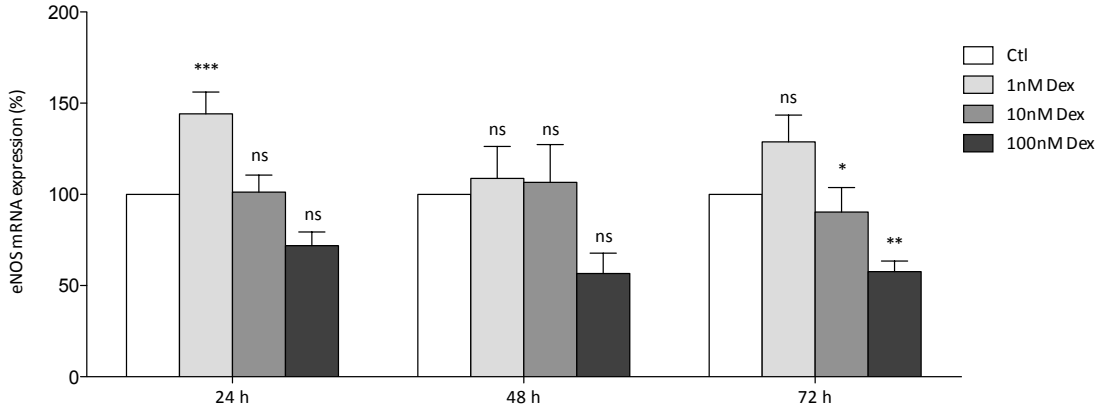

Figure 4.29: Time- and concentration-dependent effect of DEX on eNOS mRNA expression. EA.hy 926 cells were either treated with DMSO (as control) or incubated with DEX (1, 10 or 100 nM) for 24, 48 or 72 h. For subsequent analysis of the eNOS mRNA expression, total RNA was isolated and analyzed via qRT-PCR. The housekeeping gene TBP was used as reference gene for normalization. Columns represent mean + SEM, n=12-24. ns=not significant, *p<0.05, **p<0.01, compared to corresponding control (Ctl).

4.3.5 The Effect of DEX on eNOS Protein Expression

To study eNOS protein expression, EA.hy 926 cells were incubated with 1, 10 and 100 nM DEX for time periods from 24 h up to 72 h. Control cells were incubated with DMSO as this is the solvent used for DEX. Subsequently, total protein was isolated (3.4.1) and the eNOS protein expression level was analyzed via Western blotting (3.4.5). There was a tendency of eNOS downregulation but this effect was only significant after 72 h incubation with the highest DEX concentration of 100 nM (Figure 4.30).

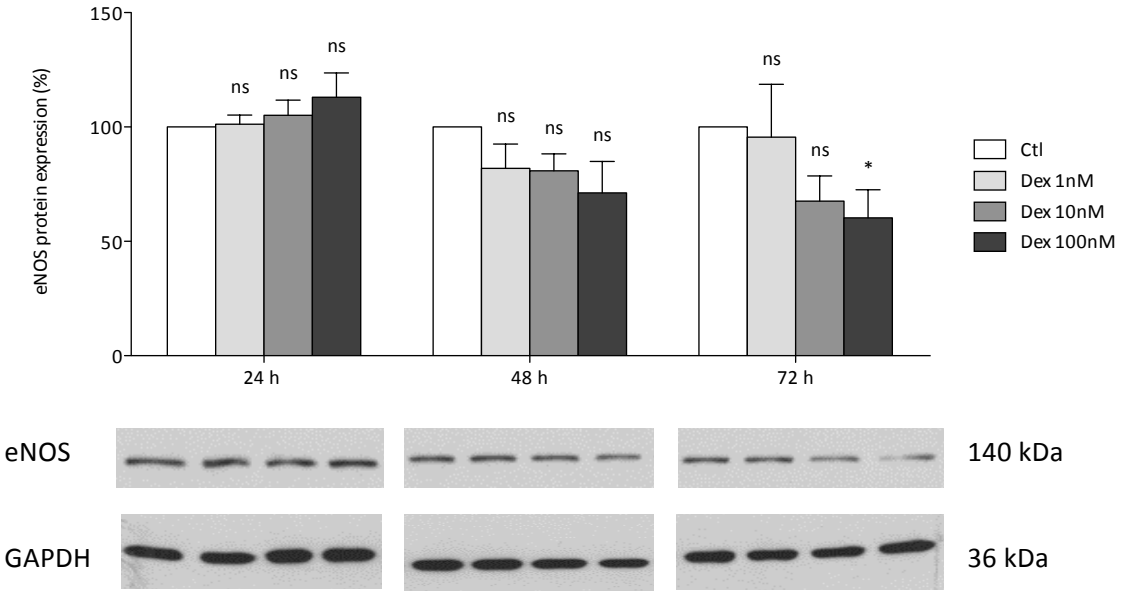

Figure 4.30: Effect of DEX on eNOS protein expression. EA.hy 926 cells were either treated with DMSO (as control) or incubated with DEX (1, 10 or 100 nM) for 24, 48 or 72 h. For subsequent analysis of the eNOS protein expression, total protein was isolated and analyzed via Western blot. The housekeeping gene GAPDH was used as reference gene for normalization. A representative blot is shown. Columns represent mean + SEM, n=4. ns=not significant, compared to the corresponding control (Ctl).

4.3.6 The Effect of DEX on eNOS mRNA Expression is Glucocorticoid Receptor-Dependent

The next step was to analyze whether the observed effect on eNOS mRNA expression in EA.hy 926 cells was dependent on the glucocorticoid receptor (GR). EA.hy 926 cells were treated either with 1 nM DEX or with 100 nM of the GR antagonist mifepristone (RU486) or with both substances in combination for 24 h. Subsequently, total RNA was isolated (3.3.1) and the mRNA expression level of the eNOS gene was analyzed via quantitative RT-PCR (3.3.5). Treatment with mifepristone alone had no effect on the eNOS mRNA expression. The effect of DEX treatment on eNOS expression was blocked by RU486 (Figure 4.31).

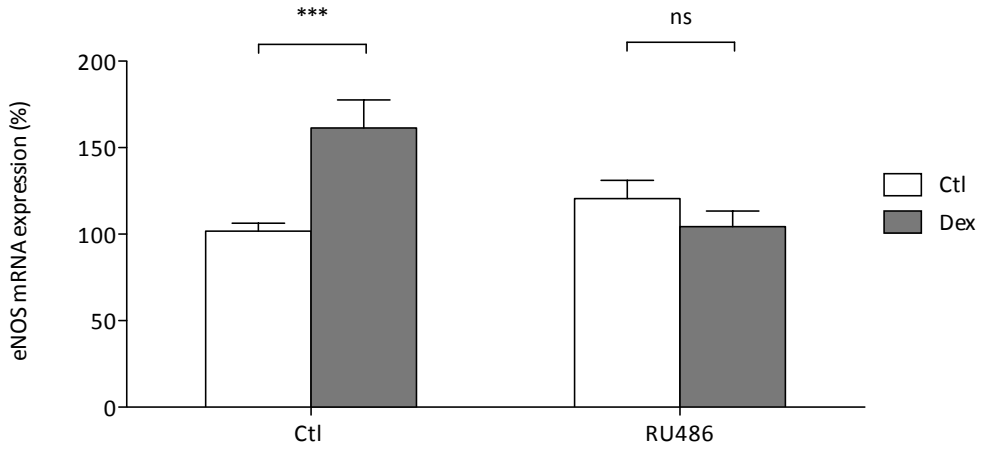

Figure 4.31: Glucocorticoid receptor-dependency of DEX effect on eNOS mRNA expression. EA.hy 926 cells were either treated with DMSO (as control), incubated with DEX (1 nM) or with the GR antagonist mifepristone (RU486, 100 nM) or with both substances in combination for 24 h. For subsequent analysis of the eNOS mRNA expression, total RNA was isolated and analyzed via qRT-PCR. The housekeeping gene TBP was used as reference gene for normalization. Columns represent mean + SEM, n=24. ns=not significant, ***p<0.001, compared to control (Ctl).

4.3.7 The eNOS Phosphorylation Status on Serine^{1177} Is Diminished by DEX

eNOS activity can be regulated by phosphorylation via different protein kinases and phosphorylation on serine^{1177} leads to a Ca^{2+}-independent stimulation of NO production. To analyze whether DEX has any influence on the eNOS phosphorylation status on serine^{1177}, EA.hy 926 cells were incubated with 1, 10 and 100 nM DEX for time periods from 24 h up to 72 h. Control cells were incubated with DMSO as this is the solvent used for DEX. Subsequently, total protein was isolated (3.4.1) and the protein expression level of eNOS phosphorylated on serine^{1177} was analyzed via Western blotting (3.4.5). Compared to the corresponding control cells, DEX time- and concentration-dependently decreased of eNOS serine^{1177} phosphorylation (Figure 4.32).

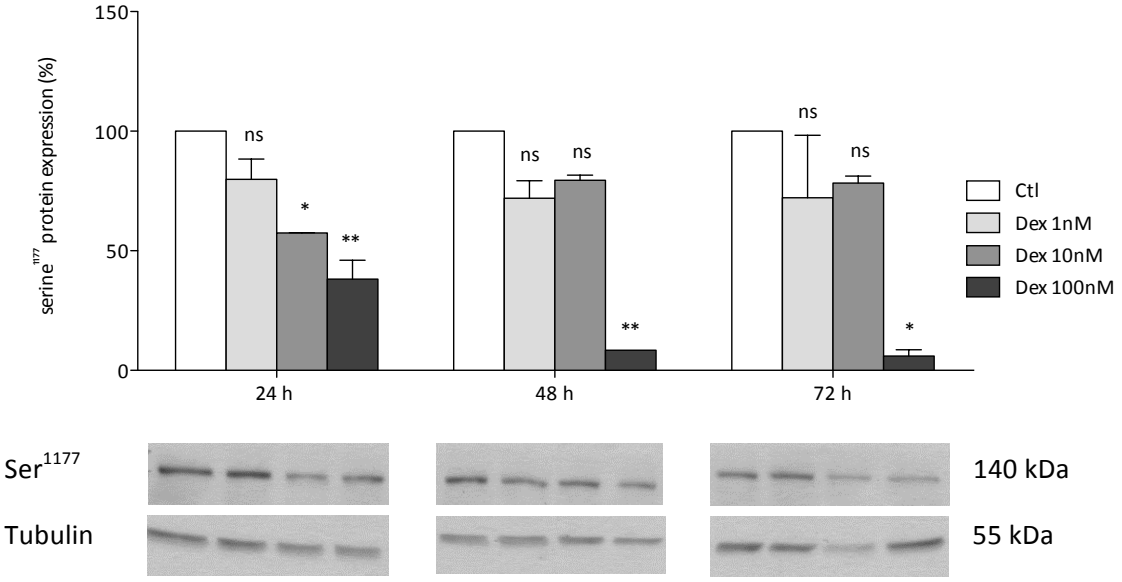

Figure 4.32: Status of eNOS phosphorylation on serine^{1177}. EA.hy 926 cells were either treated with DMSO (as control) or incubated with DEX (1, 10 or 100 nM) for 24, 48 or 72 h. For subsequent analysis of the serine^{1177} phosphorylation, total protein was isolated and analyzed via Western blot. The housekeeping gene GAPDH was used as reference gene for normalization. A representative blot is shown. Columns represent mean + SEM, n=2-3. ns=not significant, *p<0.05, **p<0.01, compared to corresponding control (Ctl).

4.3.8 Total Biopterin, BH_4 and BH_2 Levels Were Decreased by DEX in a Time- and Concentration-Dependent Manner

As a crucial cofactor for eNOS functionality and coupling, BH_4 plays an important role. To analyze whether GCs affect BH_4 availability and thereby eNOS functionality the following experiment was conducted. EA.hy 926 cells were treated with 1, 10 and 100 nM DEX for time periods from 24 up to 72 h. Control cells were incubated with DMSO as this was the solvent used for DEX. Subsequently, samples were prepared for HPLC analyses (3.7). A significant time- and concentration-dependent decrease could be observed for total biopterin and BH_4 after DEX incubation. BH_2 showed a comparable tendency but this was not significant (Figure 4.34). Since it was postulated that for eNOS functionality BH_4 / BH_2 ratio may be even more important than the absolute BH_4 concentration, BH_4 / BH_2 ratio was calculated (Figure 4.35). With increasing time and concentration of DEX treatment, the BH_4 / BH_2 ratio declined.

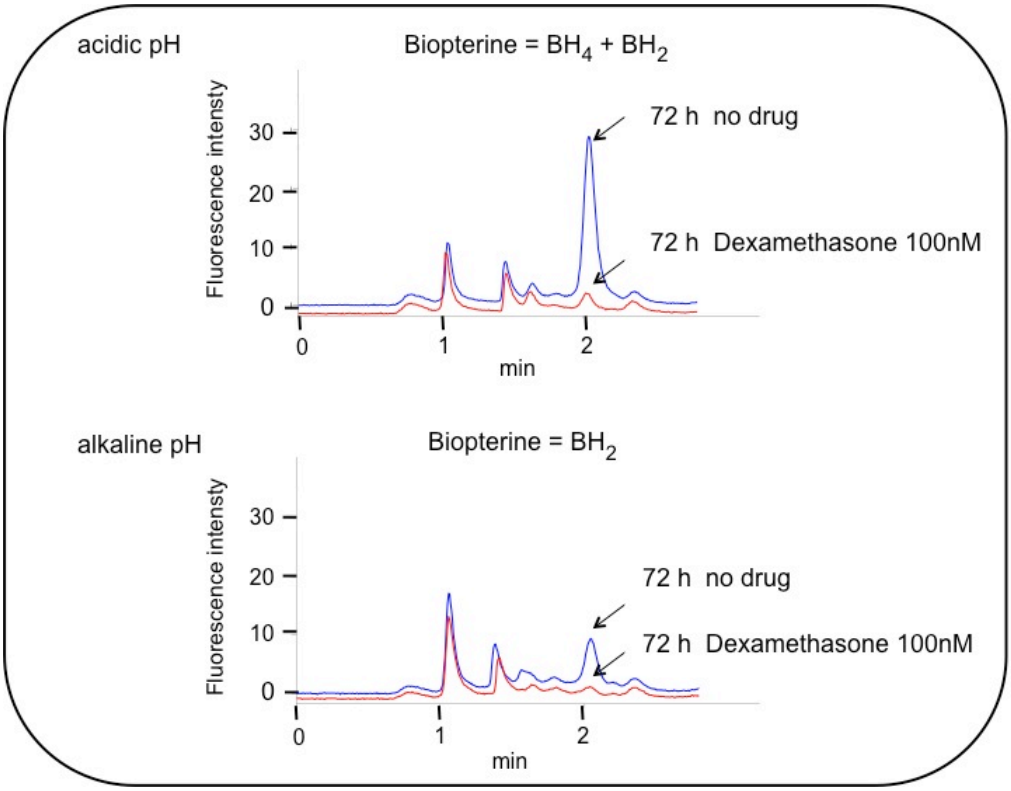

Figure 4.33: Representative chromatogram of HPLC measurement in EA.hy 926 cells.

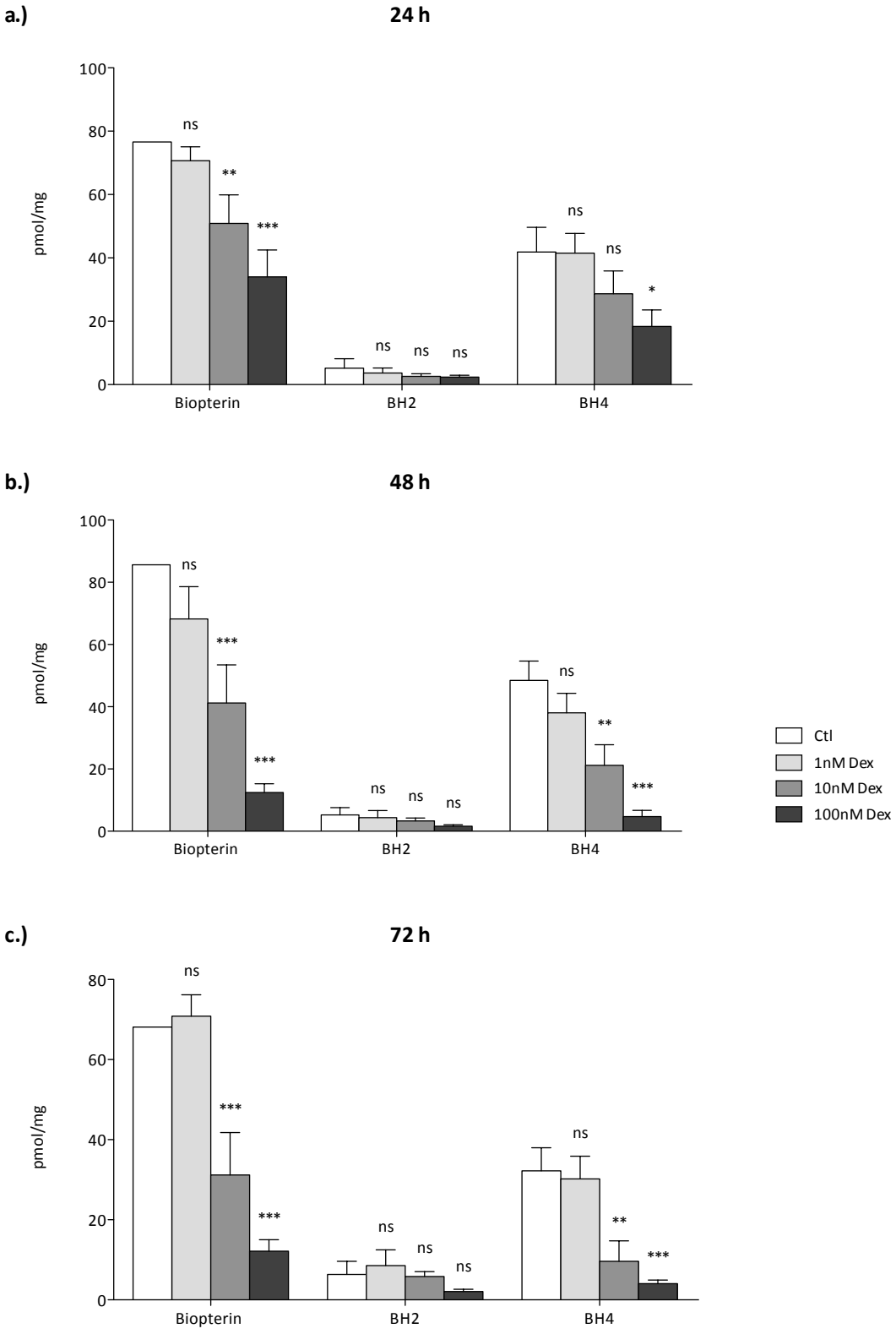

Figure 4.34: Effect of DEX on BH_4 availability. EA.hy 926 cells were either treated with DMSO (as control) or incubated with DEX (1, 10 or 100 nM) for 24, 48 or 72 h. For subsequent analyses of the biopterin, BH_2 and BH_4 levels, samples were prepared and analyzed via HPLC. Columns represent mean + SEM, n=9. ns=not significant, *p<0.05, **p<0.01, compared to corresponding control (Ctl).

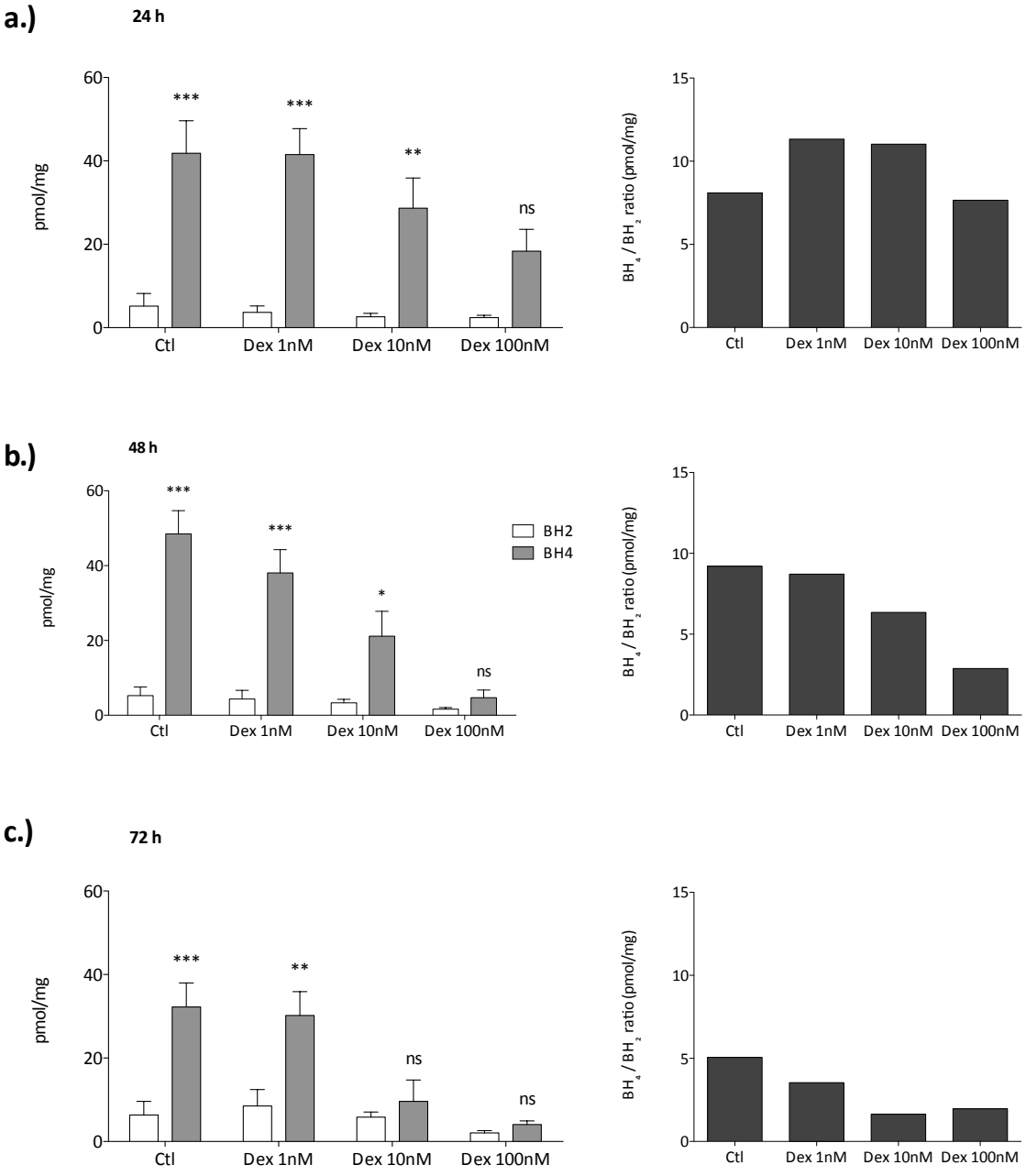

Figure 4.35: Effect of DEX on BH_4 / BH_2 ratio. EA.hy 926 cells were either treated with DMSO (as control) or incubated with DEX (1, 10 or 100 nM) for 24, 48 or 72 h. For subsequent analysis of BH_2 and BH_4 level, samples were prepared and investigated via HPLC, and BH_4 / BH_2 ratio was calculated. Columns represent mean + SEM, n=9. ns=not significant, *p<0.05, **p<0.01, ***p<0.001, compared to corresponding BH_2 value.

4.3.9 The GCH1 Promoter Activity Was Concentration-Dependently Increased by DEX

To analyze the influence of DEX on the GCH1 promoter activity, EA.hy 926 cells were transiently transfected with the pLightSwitch_GCH1-Prom plasmid (3.2.5). On the next day cells were treated for 24 h with 1, 10 and 100 nM DEX or DMSO as a control, as this was the solvent used for DEX. Subsequently cell extracts were isolated (3.5.2) and samples prepared for analysis via luciferase assay (3.5.3). DEX treatment resulted in a significant increase of GCH1 promoter activity (Figure 4.36).

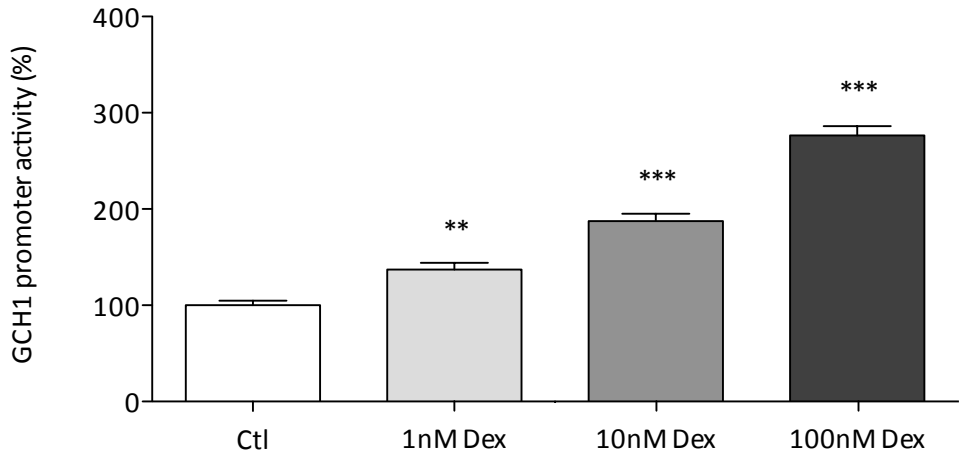

Figure 4.36: Effect of DEX on GCH1 promoter activity. EA.hy 926 cells were transfected with a GCH1 promoter construct (cloned into the pLightSwitch vector) an treated with either DMSO as control or DEX (10 nM) for 24 h. For subsequent analysis of the GCH1 promoter activity, samples were prepared and analyzed via renilla-luciferase assay. Columns represent mean + SEM, n=24. *p<0.05, compared to control (Ctl).

4.3.10 DEX Led to a Time- and Concentration-Dependent Decrease in GCH1 mRNA Expression

As rate limiting enzyme of the *de novo* pathway in the production of BH_4, GCH1 has a crucial function. To analyze whether DEX has any influence on the GCH1 mRNA expression, EA.hy 926 cells were incubated with 1, 10 and 100 nM DEX for time periods from 24 h up to 72 h. Control cells were incubated with DMSO as this was the solvent used for DEX. Subsequently, total RNA was isolated (3.3.1) and the mRNA expression level of the GCH1 gene was analyzed via quantitative RT-PCR (3.3.5). Compared to the corresponding control cells, the expression analysis showed a highly significant time- and concentration-dependent decrease of GCH1 mRNA after DEX incubation for 48 h. For the other time-points the tendency was comparable but not all observed effects were significant (Figure 4.37).

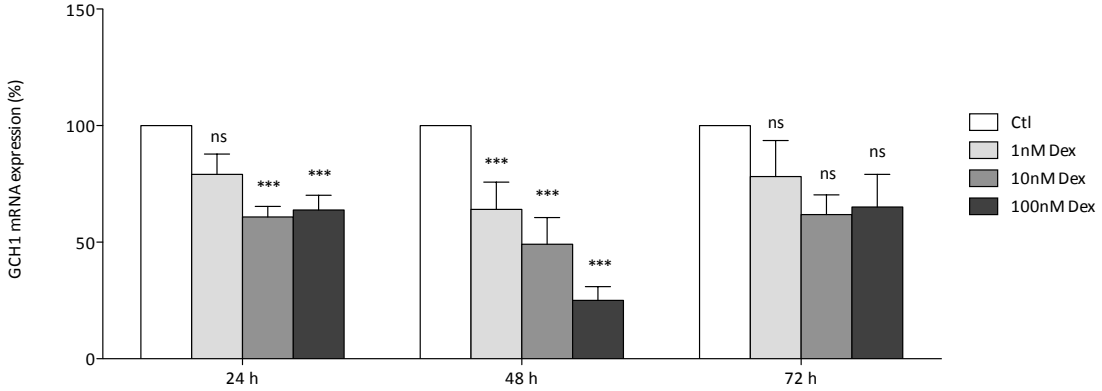

Figure 4.37: Time- and concentration-dependent effect of DEX on GCH1 mRNA expression. EA.hy 926 cells were either treated with DMSO (as control) or incubated with DEX (1, 10 or 100 nM) for 24, 48 or 72 h. For subsequent analysis of the GCH1 mRNA expression, total RNA was isolated and analyzed via qRT-PCR. The housekeeping gene TBP was used as reference gene for normalization. Columns represent mean + SEM, n=12-24. ns=not significant, ***p<0.001, compared to control (Ctl).

4.3.11 The GCH1 Protein Expression Was Decreased After DEX Treatment

To analyze a possible alteration in the protein level of GCH1, EA.hy 926 cells were incubated with 1, 10 and 100 nM DEX for time periods from 24 h up to 72 h. Control cells were incubated with DMSO as this is the solvent used for DEX. Subsequently, total protein was isolated (3.4.1) and the eNOS protein expression level was analyzed via Western blotting (3.4.5). A time- and concentration-dependent downregulation of GCH1 protein expression could be detected after treatment with DEX for 72 h. For the other time-points tendency was comparable but not all observed effects were significant (Figure 4.38).

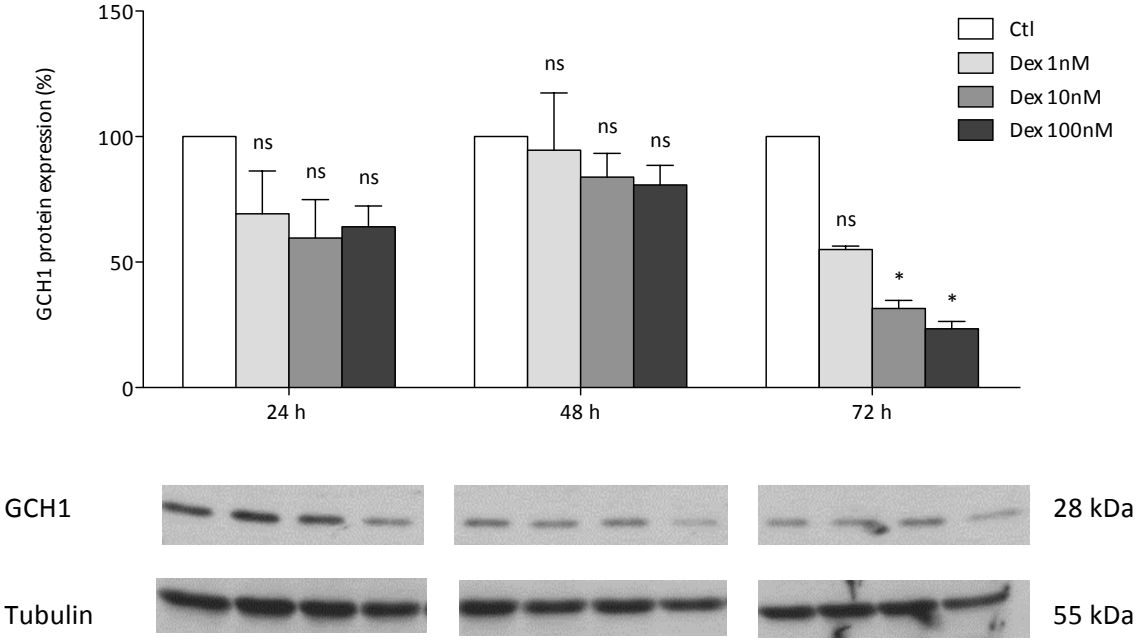

Figure 4.38: Time- and concentration-dependent effect of DEX on GCH1 protein expression. EA.hy 926 cells were either treated with DMSO (as control) or incubated with DEX (1, 10 or 100 nM) for 24, 48 or 72 h. For subsequent analysis of the GCH1 protein expression, total protein was isolated and analyzed via Western blot. The housekeeping gene GAPDH was used as reference gene for normalization. A representative blot is shown. Columns represent mean + SEM, n=3. ns=not significant, *p<0.05, compared to control (Ctl).

4.3.12 The Downregulation of GCH1 mRNA Expression by DEX Is Glucocorticoid Receptor-Dependent

With the following experiment it should be analyzed whether the observed effect of DEX on GCH1 mRNA expression in EA.hy 926 cells was dependent on the glucocorticoid receptor (GR). EA.hy 926 cells were treated either with 10 nM DEX or with 100 nM of the GR antagonist RU486, or with both substances in combination for 24 h. Subsequently, total RNA was isolated (3.3.1) and the mRNA expression level of the GCH1 gene was analyzed via quantitative RT-PCR (3.3.5). Treatment with RU486 alone had no effect on the GCH1 mRNA expression. The effect of DEX treatment on GCH1 expression was abolished by RU486 (Figure 4.39).

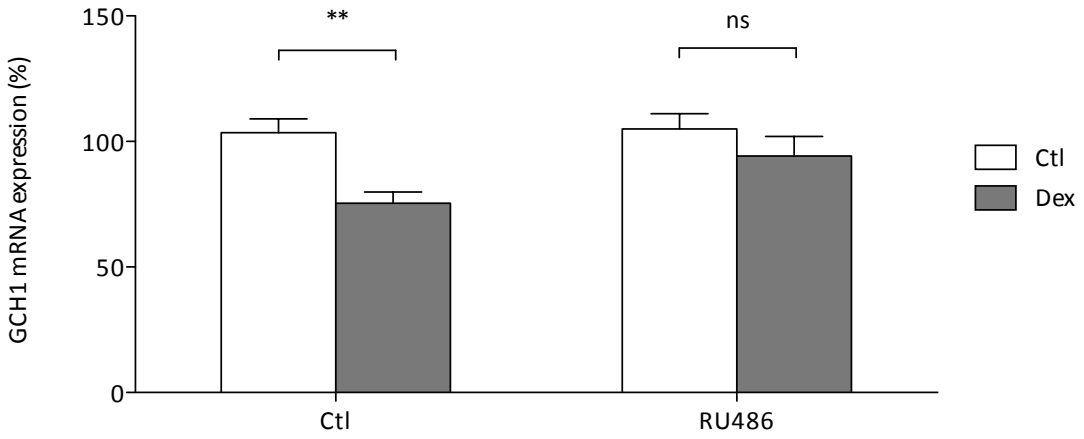

Figure 4.39: Glucocorticoid receptor-dependent effect of DEX on GCH1 mRNA expression. EA.hy 926 cells were either treated with DMSO (as control), incubated with DEX (10 nM) or with the GR antagonist mifepristone (RU486, 100 nM) or with both substances in combination for 24 h. For subsequent analysis of GCH1 mRNA expression, total RNA was isolated and analyzed via qRT-PCR. The housekeeping gene TBP was used as reference gene for normalization. Columns represent mean + SEM, n=24. ns=not significant, **p<0.01, compared to control (Ctl).

4.3.13 DEX Led to a Time- and Concentration-Dependent Decrease in DHFR mRNA Expression

To analyze whether DEX has any effect on DHFR mRNA expression level, EA.hy 926 cells were incubated with 1, 10 and 100 nM DEX for time periods from 24 up to 72 h. Control cells were incubated with DMSO as this was the solvent used for DEX. Subsequently, total RNA was isolated (3.3.1) and the mRNA expression level of the DHFR gene was analyzed via quantitative RT-PCR (3.3.5). Compared to corresponding control cells, a highly significant time- and concentration-dependent effect of DEX on the mRNA expression of DHFR could be detected (Figure 4.40).

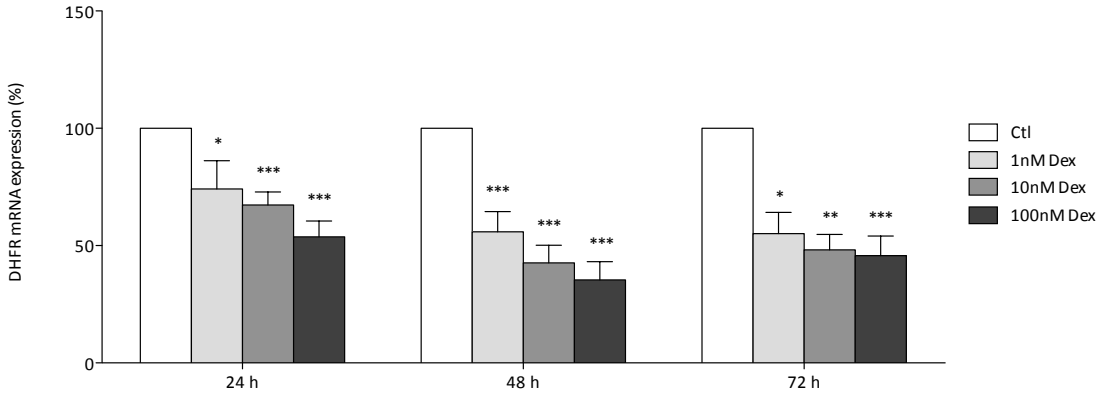

Figure 4.40: Time- and concentration-dependent effect of DEX on DHFR mRNA expression. EA.hy 926 cells were either treated with DMSO (as control) or incubated with DEX (1, 10 or 100 nM) for 24, 48 or 72 h. For subsequent analysis of DHFR mRNA expression, total RNA was isolated and analyzed via qRT-PCR. The housekeeping gene TBP was used as reference gene for normalization. Columns represent mean + SEM, n=12-24. *p<0.05, **p<0.01, ***p<0.001, compared to control (Ctl).

4.3.14 The DHFR Protein Expression Was Decreased After DEX Treatment

After investigation of the DEX effect on DHFR mRNA expression it was also important to analyze whether this also affects the enzyme on protein level. EA.hy 926 cells were incubated with 1, 10 and 100 nM DEX for time periods from 24 up to 72 h. Control cells were incubated with DMSO as this was the solvent used for DEX. Subsequently, total protein was isolated (3.4.1) and the DHFR protein expression level was analyzed via Western blotting (3.4.5). A time- and concentration-dependent decrease of DHFR protein expression could be observed in cells treated with DEX (Figure 4.41).

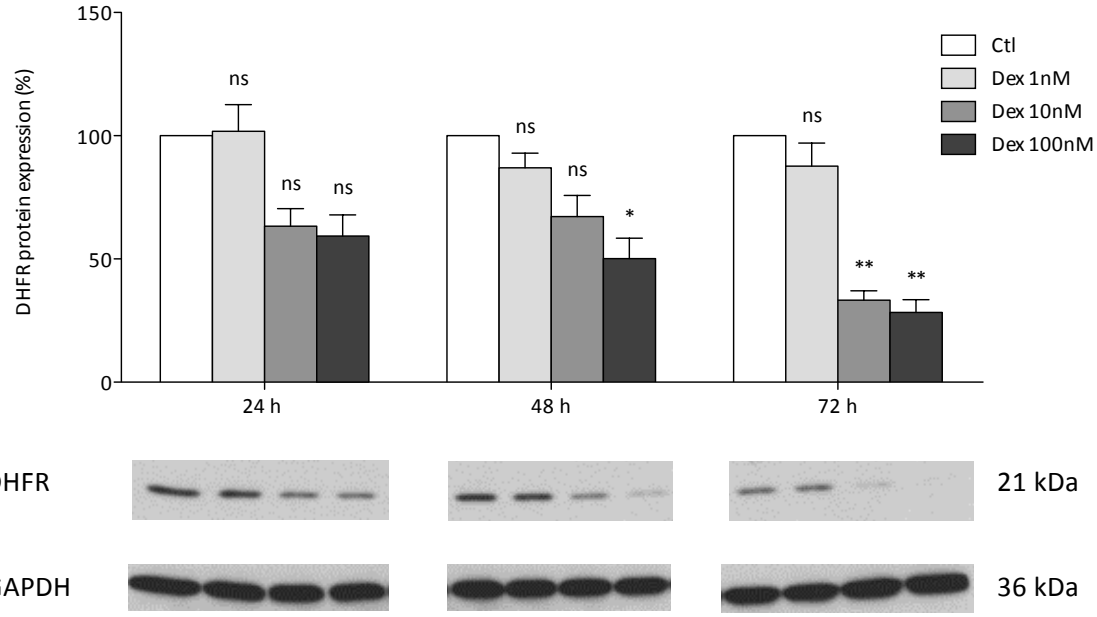

Figure 4.41: Time- and concenctration-dependent effect of DEX on DHFR protein expression. EA.hy 926 cells were either treated with DMSO (as control) or incubated with DEX (1, 10 or 100 nM) for 24, 48 or 72 h. For subsequent analysis of DHFR protein expression, total protein was isolated and analyzed via Western blot. The housekeeping gene GAPDH was used as reference gene for normalization. A representative blot is shown. Columns represent mean + SEM, n=6. ns=not significant, *p<0.05, **p<0.01, compared to control (Ctl).

4.3.15 The Downregulation of DHFR mRNA Expression by DEX Is Glucocorticoid Receptor-Dependent

For eNOS and GCH1 a GR dependency could be demonstrated. In the next step it was important to see whether this was also true for the observed effect of DEX on DHFR mRNA expression in human endothelial cells. EA.hy 926 cells were treated either with 10 nM DEX or with 100 nM of the GR antagonist RU486, or with both substances in combination for 24 h. Subsequently, total RNA was isolated (3.3.1) and the mRNA expression level of the DHFR gene was analyzed via quantitative RT-PCR (3.3.5). Treatment with RU486 alone had no effect on DHFR mRNA expression. The effect of DEX treatment on DHFR expression was prevented by RU486 (Figure 4.42).

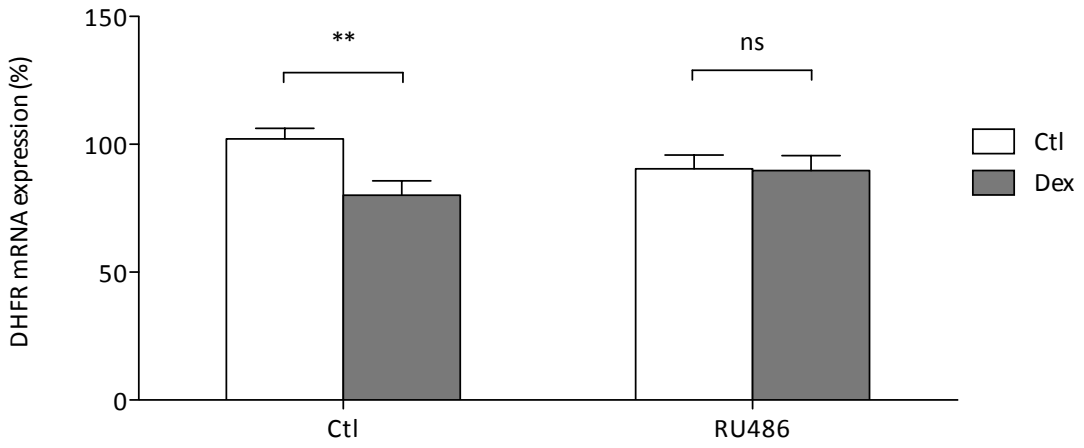

Figure 4.42: Glucocorticoid receptor-dependent effect of DEX on DHFR mRNA expression. EA.hy 926 cells were either treated with DMSO (as control), incubated with DEX (10 nM) or with the GR antagonist mifepristone (RU486, 100 nM), or with both substances in combination for 24 h. For subsequent analysis of DHFR mRNA expression, total RNA was isolated and analyzed via qRT-PCR. The housekeeping gene TBP was used as reference gene for normalization. Columns represent mean + SEM, n=24. ns=not significant, **p<0.01, compared to control (Ctl).

4.3.16 DEX Treatment Diminished NO Production in EA.hy 926 Cells

The following experiment was performed to investigate the effect of DEX on the production of NO, i.e. eNOS functionality. This was done by the indirect method of measuring cGMP in RFL-6 reporter cells after incubation of endothelial cells with DEX (3.8.1). cGMP concentrations in reporter cells, as measured by a radioimmunoassay (3.8.2), can be used as a determinant of the amount of functional NO from endothelial cells. As seen below, a highly significant time- and concentration-dependent decrease in NO production could be observed after treatment with the glucocorticoid DEX (Figure 4.43).

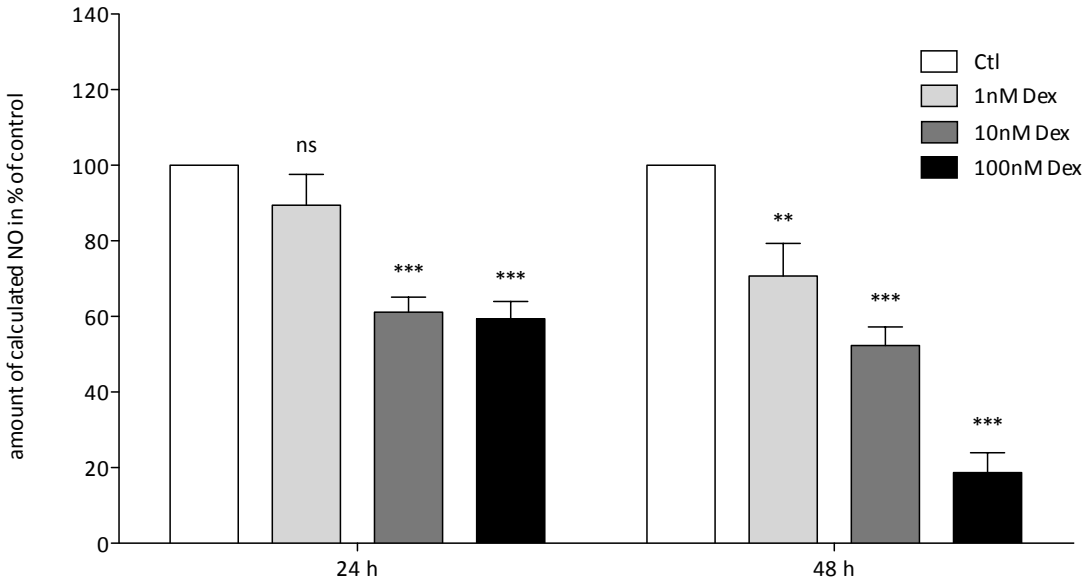

Figure 4.43: Effect of DEX on NO production in EA.hy 926 cells. Cells were either treated with DMSO (as control) or incubated with DEX (1, 10 or 100 nM) for 24 and 48 h. NO production was indirectly measured via RFL-6 reporter cell assay. Columns represent mean + SEM, n=3. ns=not significant, **p<0.01, ***p<0.001, compared to control (Ctl).

5 Discussion

Glucocorticoid-induced hypertension (GC-HT) is a prevalent clinical problem that is poorly understood. It has been commonly thought to be mediated by excess sodium and water reabsorption by the renal mineralocorticoid receptor. However, experimental and clinical data in both humans and animal models suggest important roles for the glucocorticoid receptor (GR) as well, in the pathogenesis as well as the maintenance of this hypertension. The GR is widely expressed in a number of organ systems relevant to blood pressure regulation, including the kidney, the brain and the vasculature (Goodwin and Geller, 2012). Although numerous basic science and also clinical studies in recent years addressed the question how GCs induce hypertension, precise mechanisms still remain unknown (Ong and Whitworth, 2011). It seems that there may be multiple interactions between GCs and the GR in several different tissues that result in an acute induction phase, mainly mediated through vascular effects (Goodwin and Geller, 2012). Thus, in the following, effects of the synthetic glucocorticoid DEX on target structures of the vasculature (whole rat aorta, rat aortic smooth muscle cells and human endothelial cells) are discussed.

5.1 *In vivo* Effects of Glucocorticoids on the Vascular System

5.1.1 Effects on Endothelial Function and Blood Pressure

NO derived from eNOS is crucial for the maintenance of normal blood pressure (Huang et al., 1995). GC-HT is accompanied by oxidative stress in the vessel wall whereby, amongst others, eNOS uncoupling is discussed as one relevant source of ROS generation (Cai and Harrison, 2000). Thus, the involvement of an uncoupled eNOS in DEX-induced hypertension (DEX-HT) was studied. Hypertension is a common manifestation of chronic DEX exposure (Ong *et al.*, 2009). This also could be shown previously in rat models of DEX treatment (Zhang *et al.*, 2004; Hu *et al.*, 2006). In the present study, blood pressure of DEX-treated Wistar Kyoto rats increased with the time of DEX treatment compared to control animals (Figure 4.1, top). However, this

effect was not significant with the number of animals (n=12) analyzed. Comparing the results of this work to studies done by other groups in the past, observed differences in obtained blood pressure data may be due to varying DEX treatment methods and the use of unequal rat strains. Hu *et al.* treated male Sprague Dawley rats (SD rats, body weight: 200 g, n=10) with 20 µg / kg / day DEX or saline (vehicle) subcutaneously for 14 days (Hu *et al.*, 2006). Zhang *et al.* on the other hand used a dose of 10 µg / kg / day DEX subcutaneously for 13 days. They also treated male SD rats with bodyweights of 213-297 g (Zhang *et al.*, 2004). In another study done by Mitchell *et al.*, male SD rats (body weight: 300-324 g) were subcutaneously implanted with a pellet containing DEX (5 mg / pellet resulting in a daily dose of 0.79 mg / kg), performing the experiment for a maximum of 15 days (Mitchell *et al.*, 2003). In the present study, Wistar Kyoto rats (WKY, 6 months of age, average body weight: 420 g) were treated orally, not subcutaneously, with water-soluble DEX for 12 days using a considerably lower dose of approximately 30 µg / kg / day based on the average water intake of the rats (60 ml / kg bodyweight / day); the animals had free access to (DEX-containing) water. To use such a low dose compared to Mitchell's study was a clear decision, since pre-experiments with higher DEX concentrations demonstrated toxic effects in the rats including changes in blood coagulation, massive weight loss and bad overall condition. Applying DEX orally instead of subcutaneously should prevent rats from stress situations and therefore possible falsification of analyzed data.

Endothelial function was assessed by acetylcholine-induced vasorelaxation of norepinephrine pre-contracted aortic rings. Surprisingly, the relaxation response was significantly improved in aorta rings taken from DEX treated WKY rats compared to controls (Figure 4.2, top). When aorta rings were pre-incubated with the NOS inhibitor L-NAME, relaxation capacity was only partially reduced (Figure 4.2, bottom). These results indicate that NO is not the only mediator of acetylcholine-induced relaxation under this experimental setting. Indeed, the relaxation response could also be partially inhibited by indomethacin (Figure 4.5), indicating the involvement of prostaglandins. Interestingly, in the presence of indomethacin, acetylcholine-induced relaxation was no longer different in rings from DEX-treated rats compared to control (Figure 4.5). These data suggest that the enhanced relaxation of DEX rats in response to acetylcholine observed in Figure 4.2 is likely to be mediated by an increased production of vasodilating prostaglandins. In agreement with this concept, the aortic expression of COX enzymes was upregulated by DEX treatment (Figure 4.10).

Norepinephrine-induced contraction of aortic rings was slightly smaller in DEX animals, even in the presence of L-NAME (Figure 4.3). Also here, the reduced contraction in DEX-treated rats might be attributed to enhanced prostaglandin synthesis. To find out the effect of DEX on endothelial NO release, we analyzed the effect of L-NAME on vasoconstriction. Endothelial cells continuously release NO. This basal NO production is a major endogenous vasodilator system counterbalancing the vasoconstriction produced by the sympathetic nervous system and the renin-angiotensin system. The counter regulation against peripheral vasodilatation by NO accounts for 69% of the basal norepinephrine release (Li and Förstermann, 2000). This is consistent with results from the present study showing that norepinephrine-induced contraction was markedly enhanced in the presence of L-NAME (Figure 4.3). This increase of norepinephrine-induced contraction by L-NAME, i.e. the L-NAME-induced contraction, is due to an inhibition of eNOS and thus a determinant of vascular NO production. As shown in Figure 4.4, L-NAME-induced contraction was smaller in aortic rings from DEX-treated rats, indicating that DEX treatment reduces vascular NO production.

Multiple mechanisms could contribute to a reduced endothelial NO bioactivity: reduced eNOS expression, inhibition in eNOS activity or eNOS uncoupling. Oxidative stress might play an important role in the reduction of NO bioactivity by DEX, because enhanced ROS production can not only induce eNOS uncoupling, but also accelerate NO inactivation by reaction of superoxide with NO.

5.1.2 Effects of GC on ROS Production And Oxidative Status in Rat Aorta

There is increasing evidence implicating vascular oxidative stress in the pathogenesis of hypertension, mediated by decreased NO bioavailability. Since antioxidants like tempol, apocynin, folic acid and aspirin prevent and / or reverse DEX-HT in rats, oxidative stress has also been implicated in hypertension caused by GCs (Ong *et al*., 2009). Also in cultured endothelial cells from human umbilical vein, elevated ROS production after DEX treatment could be demonstrated (Iuchi, 2003). The origin of O_2^- in vasculature has been the subject of much research. The activation of enzymes such as NADPH oxidase and xanthine oxidase has been implicated. There is considerable evidence showing that the activity and the expression of these enzymes can be enhanced by pathological stimuli (Moncada and Higgs, 2006). In 2009 Zafir and Banu

hypothesized that GCs cause oxidative damage by inducing an imbalance between the *in vivo* prooxidant and antioxidant status (Zafir and Banu, 2009).

In the present study expression levels of various pro- and anti-oxidative enzymes in the aorta were investigated. Furthermore, ROS measurements were performed in blood collected from the animals to access the oxidative status in the rat after DEX treatment. Between DEX-treated animals and controls no significantly altered ROS production could be identified under basal condition (Figure 4.6). When samples were additionally stimulated with PMA, a PKC activator and thus an activator of NADPH oxidases, the increase in ROS generation in whole blood samples of DEX-treated animals was highly significant (Figure 4.6).

NADPH oxidases are major sources of ROS in the heart as well as vasculature and appear to have an important role in the pathogenesis of several cardiovascular conditions (Sirker *et al.*, 2011). Nox activity has been detected in all layers of the vessel wall as well as in other key organs, such as the kidney and the central nervous system, that affect the regulation of blood pressure (Sirker *et al.*, 2011). Concomitantly, $p22^{phox}$, which has been described to co-localize with Nox1, Nox2 and Nox4, was found in all vascular cells (Brandes and Kreuzer, 2005). Since NADPH oxidases are the only enzymes whose single function is the production of ROS, an upregulation of Nox is assumed to be linked to cardiovascular disease states. After WKY rats were treated with DEX, a significant increase in mRNA expression could be observed for the NADPH oxidase isoforms Nox1 and Nox4 using qRT-PCR, while Nox2 and $p22^{phox}$ were not changed compared to control animals (Figure 4.7). In ACTH-induced hypertension Zhang and colleagues investigated that the Nox inhibitor apocynin prevented and even reversed hypertension in the rat, suggesting that superoxide production by NADPH oxidases plays an important role in ACTH-induced hypertension (Zhang *et al.*, 2005a).

Xanthine oxidase may be another potential source of enhanced oxidative stress due to GCs. Xanthine oxidoreductase (XOR) can exist in two different forms, xanthine dehydrogenase (XDH) or xanthine oxidase (XO) (Wallwork et al., 2003). XO is generated from XDH by proteolysis under severe conditions, such as ischemic injury, and thereby cause increased oxidative stress. XO donates electrons to molecular oxygen, thereby producing superoxide and hydrogen peroxide. Oxypurinol, an inhibitor of XO, has been shown to reduce O_2^- production and improve endothelium-dependent vascular relaxations to acetylcholine in blood vessels from hyperlipidemic animals

(Förstermann, 2010). In contrast to NADPH oxidases, the relative importance of XO for endothelial dysfunction is less certain. Recent experimental evidence has suggested that endothelial cells themselves can express XDH (and thus XO) and that this expression is regulated in a redox-sensitive way, dependent on the endothelial Nox (McNally *et al.*, 2003). Analyzing the mRNA expression level of XDH in aorta samples of DEX-treated Wistar Kyoto rats, a 2-fold increase could be detected (Figure 4.7). In 2003 Wallwork *et al.* observed significantly increased mean blood pressure and XO activity levels in cremaster muscle of DEX-treated male Wistar Kyoto rats compared to control animals (Wallwork et al., 2003). This effect could be reversed by administration of the XO inhibitor allopurinol. In contrast to that, effective inhibition of this pathway using allopurinol failed to alleviate hypertension induced by ACTH or DEX in the rat (Ong *et al.*, 2007; Zhang *et al.*, 2005a) suggesting that XO activity is not a major determinant of GC-HT in the rat.

Changes in the availability and activity of endogenous antioxidant enzymes, such as superoxide dismutase (SOD), catalase (Cat), thioredoxin (TXN) and glutathione-related enzymes, are seen in response to oxidative stress (Wassmann *et al.*, 2004). Interestingly, overexpression of Cat has protective effects in the cardiovascular system such as delayed development of atherosclerosis (Yang *et al.*, 2004) and inhibition of angiotensin II-induced aortic wall hypertrophy (Zhang *et al.*, 2005b). Rajashree and Puvanakrishnan found that hypertensive DEX-treated rats had decreased Cat and SOD levels in the heart (Rajashree and Puvanakrishnan, 1999). They also demonstrated a decrease followed by a subsequent increase in glutathione peroxidase (GPx) activity with DEX treatment. This finding goes in line with the here observed significant upregulation of GPx1 through DEX (Figure 4.8). This can be interpreted as counter regulation, since in apoE-deficient mice, the deficiency of GPx1 accelerates and modifies atherosclerotic lesion progression (Förstermann, 2010). Out of the investigated antioxidant enzymes GPx1 was the only one altered by DEX exposure. Whether SOD1-3 nor Cat or TXN1 / TXN2 were affected in their mRNA expression in rat aorta after the animals were treated with DEX (Figure 4.8). Furthermore, oxidative stress in calves induced by DEX was associated with activation of GPx (Carletti *et al.*, 2007). It is likely that there is an element of a compensatory induction, at transcriptional level, of antioxidant proteins and enzymes in response to ROS exposure (Crawford and Davies, 1994).

5.1.3 GC Effects on Vascular Inflammation

A reduced bioavailability of NO, either through enhanced inactivation and / or reduced synthesis, is seen in correlation with risk factors for cardiovascular disease (Förstermann and Li, 2012). Redox-sensitive inflammatory processes also contribute to vascular remodeling in hypertension (Fortuño *et al.*, 2005). Therefore the effect of DEX on the expression of different enzymes and factors involved in vascular inflammation was investigated. Among IL-6, ICAM-1 and the transcription factor NF-κB (nuclear factor kappa B), NF-κB was the only one being significantly upregulated in aorta samples of DEX-treated WKY rats. No effect could be shown for IL-6 or ICAM-1 (Figure 4.9). A just recently published paper investigated the relationship between inflammatory and apoptotic parameters and the severity and extent of target organ damage in patients with essential hypertension (Morillas et al., 2012). They identified elevated serum plasma levels of IL-6 in patients with target organ damage (like heart, kidney, and blood vessels) compared to hypertensive patients without organ damage. An increasing level of IL-6 was progressively associated with an increase in the number of organs damaged. Expression of ICAM-1 is increased in the aorta from aldosterone-infused rats. Furthermore, in an experimental model of angiotensin II-enhanced oxidative stress, where the role of Nox is clearly demonstrated, induction of ICAM-1 expression is associated with tissue hypertrophy (Fortuño *et al.*, 2005). The observation of NF-κB being upregulated in aorta samples of DEX-treated WKY rats in the present study goes in line with previous studies, where NF-κB has been found to be activated under oxidative stress conditions and leads to the expression of pro-inflammatory genes along with cytokine and chemokine production (Schramm *et al.*, 2012). Aside from modulating intracellular signaling pathways, ROS contributes to DNA, lipid and protein damage. ROS-induced DNA damage activates poly (ADP-ribose) polymerase (PARP), leading to PKC activation and a further increase in NF-κB activity (Schramm *et al.*, 2012).

Moreover, we analyzed the mRNA expression levels of cycloogyneases 1 and 2 (COX1+2). Endothelial COX is involved in the regulation of vascular tone, endothelial function and pressor reactivity to agonists (Ong *et al*., 2009). Prostacyclin and prostaglandin E2 have been found to be predominant products of COX metabolism and reduced bioavailability - of one or all of these protective endothelial factors - results in vascular dysfunction, a condition that has been documented in patients with

hypertension (Eatman *et al.*, 2011). Increased arachidonic acid metabolism by endothelial COX is a source of O_2^- as demonstrated in studies on cerebral arteries in cats and dogs (Ong *et al*., 2009). While the constitutively expressed isoform COX1 was upregulated by DEX in the current study, inducible COX2 showed the same tendency but this effect was not significant (Figure 4.10). The role of COX-related superoxide overproduction in DEX-HT has not been fully evaluated. Aspirin, a non-selective COX inhibitor with antioxidant properties, tended to prevent DEX-HT in rats but failed to reverse it (Zhang *et al.*, 2007). However, whether this effect is due to non-specific antioxidant properties or aspirin-induced stimulation of NO production via eNOS acetylation and increased cGMP, rather than inhibition of COX-related oxidative stress, remains speculative (Ong *et al*., 2009).

5.1.4 GC Effects on eNOS Functionality

Previous studies could demonstrate that DEX-HT in the rat was associated with downregulation of eNOS (Wallerath *et al.*, 1999; Mitchell et al., 2003) and vascular GCH1, the rate-limiting enzyme for *de novo* synthesis of BH_4 (Mitchell *et al.*, 2003). In a study performed by Thida *et al.* ACTH- and DEX-treated rats were further treated with the BH_4 precursor sepiapterin or N-nitro-L-arginine (NOLA), a NOS inhibitor, to investigate the role of eNOS uncoupling in GC-HT (Thida *et al.*, 2010). Because sepiapterin did not prevent ACTH- or DEX-induced hypertension and NOLA even exacerbated the situation, they concluded that eNOS uncoupling does not play a major role in the genesis of GC-HT in the rat. Investigating possible alterations of eNOS functionality in rat aorta after DEX treatment, in the present work mRNA expression levels of eNOS as well as the enzymes GCH1 and DHFR (both involved in BH_4 bioavailability) were analyzed via qRT-PCR. Whereas eNOS expression was slightly upregulated, neither GCH1 nor DHFR were affected by DEX (Figure 4.12). The extent to which DHFR regulates intracellular BH_4 levels and eNOS uncoupling *in vivo* remains unknown although numerous studies in cultured endothelial cells gained more insight (Crabtree and Channon, 2011). Analyses of the effect of DEX on the levels of total biopterin, BH_4 and BH_2 in aorta samples of treated rats were done by HPLC. Here a slightly lowered concentration of BH_4 and BH_2 as well as total biopterin could be observed but none of those effects was significant (Figure 4.11). Comparing the results of the present work to the study done by Mitchell *et al.* in 2003, the observed

differences in GCH1 expression may be due to varying DEX treatment methods. Mitchell *et al.* subcutaneously implanted rats with a pellet containing DEX (5 mg / pellet resulting in a daily dose of 0.79 mg / kg), performing the experiment for a maximum of 15 days (Mitchell *et al.*, 2003). In the present study, rats were orally treated with water-soluble DEX for 12 days using a considerably lower dose (0.03 mg / kg / day). To use such a low dose compared to previous studies was a clear decision, since pre-experiments with higher DEX concentrations demonstrated toxic effects in the rats including changes in blood coagulation, massive weight loss and bad overall condition. Despite the fact that intense research efforts have been made in this context, *in vivo* demonstration of eNOS uncoupling is still very difficult.

5.2 *In vitro* Effects of Glucocorticoids in Rat Aortic Smooth Muscle Cells

5.2.1 Effects of GC on ROS Production And Oxidative Status in A7r5 Cells

Extensive experimental evidence indicates that oxidative stress is involved in the pathogenesis of hypertension (Montezano and Touyz, 2012). After investigating the effect of DEX *in vivo*, in the next step, analyses were made in cultured rat aortic smooth muscles cells (A7r5). ROS measurements were conducted using two different detection methods, after incubation of A7r5 cells with DEX. A slightly elevated ROS production through DEX could be observed via chemiluminescence analysis (Figure 4.13). However, no change was detectable in fluorescence measurements (Figure 4.14). Furthermore, several pro- and anti-oxidative enzymes were analyzed via qRT-PCR to detect possible alterations in their mRNA expression. Xanthine Oxidase as source of ROS is implicated in the development of hypertension in spontaneously hypertensive and Dahl salt-sensitive rats. However, XO doesn't seem to be the major source of superoxide in rat DEX-HT as the inhibitor allopurinol failed to prevent / reverse DEX-HT despite lowering plasma uric acid as product of a functional XO (Ong *et al.*, 2007). In the present work, cells treated with DEX showed a significant upregulation of the mRNA expression level of XDH (Figure 4.23). The contribution of

this enzyme to oxidative stress linked to DEX-HT, however, is still uncertain. As NADPH oxidases are a major source of cardiovascular ROS and discussed as most promising target in correlation with GC-HT, this enzyme family is discussed in detail in 5.2.2 and 5.2.3. The most efficient enzymatic antioxidants in the vasculature include SOD, GPx and Cat (Chen *et al.*, 2012). Investigating the effect of DEX on anti-oxidative enzymes in A7r5 cells in course of the present work, out of the three different SOD isoforms only SOD2 was significantly altered. Here we could detect an upregulation of the mRNA expression, possibly as a counter regulation. SOD1 and SOD3 expression levels were not changed by DEX exposure. Furthermore, in contrast to SOD2, Cat and also GPx1 were both significantly downregulated, whereas neither of both TXN isoforms was affected by DEX (Figure 4.24).

5.2.2 GR-Dependent Effects of DEX on the mRNA Expression of Different Nox Isoforms

Being a major source of ROS in the vasculature, the involvement of NADPH oxidases in DEX-HT and eNOS uncoupling are intensively studied by numerous research groups. However, precise mechanisms and roles of different Nox isoforms are unclear, so far. In the present study the impact of DEX on the isoforms Nox1, Nox4 and the $p22^{phox}$ was investigated in cultured rat aortic smooth muscle cells (A7r5). Nox1 was massively upregulated after DEX incubation of A7r5 cells with increasing DEX concentrations, with a striking time- and concentration-dependent increase of Nox1 mRNA up to 130-fold (maximum after exposure to 100 nM DEX for 5 days) (Figure 4.15). Using the GR antagonist RU486, this effect was found indeed mediated by GR since it was prevented by RU486 (Figure 4.18). In contrast to that, expression analyses of Nox4 revealed a time- and concentration-dependent decrease of Nox4 mRNA (Figure 4.16). Also here the effect could be blocked by RU486, indicating that it is mediated by the GR (Figure 4.19). The mRNA expression level of subunit $p22^{phox}$ was not significantly altered over time after DEX treatment of A7r5 cells (Figure 4.17).

For activation, Nox1 is dependent on the subunit $p22^{phox}$ and is expressed at low levels in physiological conditions. Nox1-derived superoxide is increased in a stimulus-dependent manner, involving complex interactions between regulatory subunits and the redox chaperone protein disulfide isomerase (Montezano and Touyz, 2012). Nox1 expression / activity is increased in the vasculature in models of cardiovascular disease

such as hypertension and atherosclerosis, which goes in line with our own findings in the present study. In vascular smooth muscle cells Nox4, like Nox1, co-localizes with $p22^{phox}$ and is, unlike Nox1, constitutively active (Montezano and Touyz, 2012). While Nox1 produces superoxide, Nox4 is primarily a source of hydrogen peroxide (H_2O_2). The pathological role of Nox4 is unclear, although it has been implicated in hypertension, atherosclerosis and other cardiovascular disease states. Recent studies even suggest protective effects like enhanced vasodilation and thus reduced blood pressure (Montezano and Touyz, 2012) or protection of the vasculature during ischemic or inflammatory stress (Schröder *et al.*, 2012). In contrary to our own results, it was postulated previously that Nox4 mRNA was increased in various models of hypertension (Sedeek et al., 2009). In another study by Wind *et al.* Nox activity, as well as protein expression of its catalytic subunits Nox1 and Nox2, was increased in the aortas of spontaneously hypertensive rats, whereas the expression of Nox4 protein as the most abundant Nox isoform, was not significantly changed (Wind et al., 2010). They even could reverse oxidative stress and endothelial dysfunction by inhibition of Nox1 / Nox2. These findings are comparable to a study conducted last year by Briones *et al.* who could demonstrate Nox1 co-localization with Nox2 but not with Nox4 in rat vascular smooth muscle cells (VSMCs), implicating association between Nox1 and Nox2 but not between Nox1 and Nox4 (Briones *et al*., 2011). Their data highlight the complexity of Nox biology in VSMCs, emphasizing that more than one Nox member may be involved in Nox-mediated ROS production.

5.2.3 Influence of DEX on Nox1 via mRNA Stability And Transcription

As discussed in the previous section (5.2.2) Nox1 was found to be massively upregulated in A7r5 cells after DEX exposure. In the next step we wanted to investigate whether this is a transcriptional or post-transcriptional event. Therefore we incubated cells again with DEX for a total time of 24 h. Part of the cells were additionally incubated with the transcription inhibitor DRB for 18 or 24 h. Subsequent qRT-PCR analyses revealed a stabilizing effect of DEX on Nox1 mRNA, increasing the half-life of Nox1 transcripts (Figure 4.20). Treating A7r5 cells with DRB, ahead of as well as in combination with DEX, demonstrated transcription-dependency (Figure 4.21). After 6 h of DEX incubation the significant upregulation of Nox1 mRNA could be blocked with DRB (Figure 4.21, top). In cells treated with DEX for 24 h, the effect of

DEX was also partially blocked by DRB (Figure 4.21, bottom). In additional experiments, cells were transiently transfected with the pGl3_huNox1_6000 plasmid, carrying a 6000 bp-long fragment of the Nox1 promoter. Subsequently, transfected cells were treated with DEX for 24 h to analyze a possible effect on the activity of the exogenous Nox1 promoter. Luciferase measurements showed a significant decrease of Nox1 promoter activity after DEX treatment down to about 55 % (Figure 4.22). This discrepancy (blocking effect of DRB versus reduced activation of Nox1 promoter construct) could be explained by possibly different responses of the endogenous and the exogenous promoter. Whereas the transiently transfected plasmids are ‘‘naked’’ DNA and not packed into chromatin in the same way as genomic DNA, the endogenous promoter is subject to the control of epigenetic mechanisms. A discrepancy between promoter activities of transiently transfected luciferase constructs and endogenous transcription has been reported previously for eNOS (Rössig *et al.*, 2002).

5.3 Glucocorticoid Effects in Human Endothelial Cells

Since the endothelium is a major source of NO in the vasculature, loss of eNOS function and NO synthesis would result in endothelial dysfunction. Thus, regulation of eNOS and NO bioavailability become critical for the development and progression of vascular diseases, such as atherosclerosis and hypertension (Chatterjee and Catravas, 2008).

5.3.1 GC Effects on ROS Production And Oxidative Status in EA.hy 926 Cells

All mammalian cells including endothelial cells generate superoxide anions (O_2^-), which are inactivated mainly by SOD (Chatterjee and Catravas, 2008). Although, depending on the tissue, the enzymatic origin of oxygen radicals can vary. Both animal and human studies suggest that the primary enzymes responsible for ROS production in the vasculature are NADPH oxidases. In the past, studies revealed an upregulation of not only Nox but also COX in correlation with hypertension (Taddei *et al.*, 1998; Zalba *et al*., 2000).In the present study mRNA expression levels of several pro- and anti-oxidative enzymes were analyzed, demonstrating a significant downregulation of Nox4

after incubation of EA.hy 926 cells with the highest DEX concentration used (100 nM). On the other hand the prooxidant enzyme XDH was not altered by DEX (Figure 4.27). Furthermore also anti-oxidative enzymes were investigated after exposure to DEX. Whereas for Cat, SOD1 and GPx1 no significant change in mRNA expression could be found, TXN2 showed a concentration-dependent downregulation (Figure 4.28). As ROS scavenger also TXN has been recognized as a critical protective system, being present in endothelial cells as well as vascular smooth muscle. TXN acts via direct (antioxidant) and indirect (regulation of signal transduction) effects (Förstermann, 2010).

mRNA expression data alone are insufficient to judge the overall oxidant status in EA.hy 926 cells after DEX treatment. Therefore, we further analyzed the development of ROS in EA.hy 926 cells, additionally using the NOS inhibitor L-NAME to verify whether an uncoupled eNOS accounts for oxidative stress. Unfortunately, results from these experiments were inconsistent. Therefore, we employed two different approaches to address this issue. In the H_2DCFDA experiment (Figure 4.25), a tendency of increased ROS production in DEX-treated cells could be seen despite the high variation from experiment to experiment. In majority of the experiments performed, L-NAME was likely to reduce the enhanced ROS production by DEX (Figure 4.25). Also in Figure 4.26, L-NAME was likely to reduce ROS production in DEX-treated cells. Thus, because of the inconsistency of the results, it was impossible to draw a clear conclusion. In general, however, there was a tendency of eNOS uncoupling in DEX-treated cells. In supporting this idea, a previous study demonstrated overproduction of ROS and concomitant lowered NO availability in human umbilical vein endothelial cells (Iuchi *et al.*, 2003).

5.3.2 Effects of DEX on eNOS

Numerous diseases of the cardiovascular system lead to changes in eNOS expression. In the present study, an elevated eNOS mRNA expression level was seen at the lowest DEX concentration and shortest period of treatment tested (1 nM for 24 h). For higher DEX concentrations of 10 and 100 nM a decrease of eNOS mRNA could be observed (Figure 4.29). The upregulation of eNOS by 1 nM DEX was GR-dependent, since it could be reversed by the GR antagonist RU486 (Figure 4.31). In previous studies of our own group, reduction of eNOS was apparent not only on mRNA but also on protein expression level. This effect was prevented using the GR antagonist RU486, leading to the conclusion that expressional downregulation of eNOS may contribute to GC-HT (Wallerath *et al.*, 1999). In protein analyses performed in course of the current work a decreased eNOS expression could be detected after 72 h DEX incubation, as well (Figure 4.30). The constitutively expressed eNOS mRNA has a half-life of 10-35 h (Chatterjee and Catravas, 2008). Therefore, synthesis of the encoded protein is likely to persist long after gene expression has been repressed. Thus, altering the half-life of stable transcripts may be the most rapid and efficient effect of modulating mRNA levels and gene expression. In $eNOS^{-/-}$ mice treatment with GCs had no effect on blood pressure, demonstrating that the expressional downregulation of eNOS and the reduction in vascular NO production contribute to hypertension caused by GCs (Wallerath *et al.*, 2004). Besides eNOS expression, also changes in phosphorylation critically account for eNOS activity. Functional changes after $serine^{1177}$- and $threonine^{495}$-phosphorylation are the best-studied ones, although eNOS features numerous other potential phosphorylation sites. $Serine^{1177}$ is located within the reductase domain of eNOS. McCabe *et al.* could demonstrate an increased electron transport after phosphorylation of this specific amino acid. This leads to an amplified eNOS enzyme activity (McCabe *et al.*, 2000). There are several activators known that increase phosphorylation at site $serine^{1177}$. Shear stress can activate eNOS through enforced phosphorylation by AKT kinase and PKA (Boo *et al.*, 2002; Dimmeler *et al.*, 1999a), whereas VEGF, estrogens and insulin just stimulate the AKT kinase-mediated phosphorylation (Fleming *et al.*, 2001). Investigating the influence of DEX treatment on eNOS phosphorylation in EA.hy 926 cells, attempts to investigate $threonine^{495}$ phosphorylation were without results due to undetectable bands in the western blot assay. Concerning $serine^{1177}$ on the other hand, we were able to observe a massively decreased phosphorylation in a time- and concentration-dependent manner

(Figure 4.32). Specifically after 72 h of incubation the highest DEX concentration of 100 nM, eNOS phosphorylation at site serine^{1177} was reduced down to about 10 %. This observation leads us to the assumption that eNOS activity may be inhibited in GC-HT.

5.3.3 GC Effects on Level of Total Biopterin, BH_4 And BH_2

Tetrahydrobiopterin (BH_4) is an essential cofactor required for proper eNOS functionality. BH_4 is produced by two pathways, *de novo* synthesis and a regenerating salvage pathway (Mitchell and Webb, 2005) and is highly susceptible to oxidation. BH_4 bioavailability in cells reflects the balance between *de novo* BH_4 synthesis, loss of BH_4 by oxidation to BH_2 and the regeneration of BH_4 by the enzyme DHFR (Crabtree and Channon, 2011b). Suboptimal concentrations of BH_4 in the endothelium reduce the biosynthesis of NO; eNOS becomes enzymatically uncoupled and generates superoxide, thus contributing to oxidative stress and the pathogenesis of endothelial dysfunction. In 2009 Crabtree *et al.* demonstrated that DHFR activity is critical in regulating BH_4 / BH_2 ratio and hence eNOS coupling *in vitro*, particularly at low total biopterin availability (Crabtree *et al.*, 2009a). While Bendall *et al.* postulated that eNOS coupling is directly related to eNOS / BH_4 stoichiometry (Bendall *et al.*, 2005), Crabtree and his group pointed out that the intracellular BH_4 / BH_2 ratio, rather than absolute concentrations of BH_4, is the key determinant of eNOS uncoupling, even in the absence of exogenous oxidative stress (Crabtree *et al.*, 2009b). Interestingly, some previous studies have shown that DHFR levels or activity are diminished in experimental models of cardiovascular diseases, suggesting that insufficient recycling of BH_2 to BH_4 by DHFR is at least in part responsible for reduced BH_4 levels and accumulation of BH_2, leading to eNOS uncoupling (Crabtree and Channon, 2011a).

In the present study analyses of BH_4 bioavailability as well as levels of total biopterin and BH_2 were done via high-performance liquid chromatography (HPLC). After treatment of EA.hy 926 cells with DEX (1-100 nM) for 24 to 72 h a significant time- and concentration-dependent decrease was detectable for total biopterin as well as BH_4 (Figure 4.34). BH_2 showed a comparable tendency but this effect was not significant. Although both BH_4 and BH_2 levels were decreased by DEX, having a closer look at alterations in the BH_4 / BH_2 ratio, a shift for the benefit of BH_2 becomes apparent (Figure 4.35). A study published by Sugiyama *et al.* revealed increased ROS production

after siRNA-knockdown of DHFR but not GCH1 (Sugiyama *et al.*, 2009). This effect was abolished either by simultaneous siRNA-mediated knockdown of eNOS or by supplementation of BH_4. In contrast, addition of BH_2 increased ROS production and this effect was blocked by BH_4 supplementation. Similarly, in spontaneously hypertensive rats, BH_4 supplementation improves endothelial dysfunction (Heitzer *et al.*, 2000; Hong *et al.*, 2001). These data suggest that depletion of BH_4 is not sufficient to interfere with NO signaling, but rather that the concentration of intracellular BH_2 as well as the BH_4 / BH_2 ratio, together play a determining role in the redox regulation of eNOS-modulated endothelial responses (Sugiyama *et al.*, 2009). Furthermore another hypothesis, based on a computational model to simulate the kinetics of the biochemical pathways of eNOS for both NO and O_2^- production, suggests that eNOS uncoupling is a result of a decrease in BH_4 / total biopterin ratio. According to this hypothesis, a supplementation of BH_4 might only be effective when the BH_4 / total biopterin ratio increases (Kar and Kavdia, 2011).

5.3.4 GR-Dependent Effects of DEX on the *de novo* Pathway of BH_4 Synthesis (GCH1)

BH_4 biosynthesis occurs via the *de novo* pathway in a magnesium-, zinc- and NADPH-dependent reaction from GTP. In endothelial cells, the first and rate-limiting step in this pathway is GCH1 (GTP cyclohydrolase I). GCH1 activity regulation takes place at transcriptional and post-transcriptional levels (Schmidt and Alp, 2007). Some evidence suggests that GCH1 expression may be downregulated, and BH_4 synthesis reduced thereby, in certain pathological states. In a GC-induced rat model of hypertension, GCH1 mRNA levels were reduced and impaired endothelium-dependent relaxations could be restored by incubating vessels in sepiapterin (a BH_4 precursor molecule), suggesting reduced BH_4 bioavailability as a cause of eNOS uncoupling (Mitchell *et al.*, 2003). In 2008 Wang *et al.* found out that acute inhibition of GCH1 was associated with increased levels of superoxide as well as a significantly elevated BP in C57BL6 mice. They conclude that GCH1 maintains normal BP and endothelial function via BH_4 *in vivo* by preserving eNOS functionality and thus NO production (Wang *et al.*, 2008). Experiments performed in this work could confirm the GC effect on GCH1 expression described above. Compared to the corresponding control cells, a highly significant time- and concentration-dependent decrease of GCH1 mRNA was seen after DEX

incubation for 48 h (Figure 4.37). This effect of DEX on GCH1 expression could be reversed by RU486 indicating that the effect of DEX is GR-dependent (Figure 4.39). Regarding the effect of DEX on the GCH1 protein expression, results were comparable to mRNA analyses, but observed effects were only significant for the longest incubation time of 72 h (Figure 4.38). Interestingly, luciferase measurements of the GCH1 promoter activity after DEX treatment resulted in a significant increase (Figure 4.36). A discrepancy between the promoter activities of transiently transfected luciferase constructs and endogenous transcription has been reported previously for eNOS (Rössig *et al.*, 2002). In this study HDAC inhibition reduced eNOS on mRNA and protein expression level. eNOS promoter activity in transient transfection experiments, however, was paradoxically enhanced. The activity of transiently transfected promoter constructs does not necessarily reflect the activity of the endogenous promoter. Whereas the transiently transfected plasmids are ‘‘naked’’ DNA and not packed into chromatin in the same way as genomic DNA, the endogenous promoter underlies the control of epigenetic mechanisms.

5.3.5 GR-Dependent Effects of DEX on the Salvage Pathway of BH_4 Recycling (DHFR)

In addition to key roles in folate metabolism, constitutively active dihydrofolate reductase (DHFR) can reduce BH_2, regenerating BH_4. Thus, it is likely that net BH_4 bioavailability in cells reflects the balance between *de novo* BH_4 synthesis, loss of BH_4 by oxidation to BH_2 and the regeneration of BH_4 by DHFR, which is also known as salvage pathway (Crabtree and Channon, 2011b). However, whether DHFR is functionally important in maintaining eNOS coupling remains unclear. Pharmacological inhibition of DHFR activity by methotrexate, or genetic knockdown of DHFR by RNA interference, reduced intracellular BH_4 and increased BH_2 levels resulting in eNOS uncoupling in endothelial cells. In cells expressing eNOS with low biopterin levels, DHFR inhibition or knockdown further diminished the BH_4 / BH_2 ratio and exacerbated eNOS uncoupling (Crabtree *et al.*, 2009a). Furthermore, Crabtree *et al.* revealed a key role for DHFR in regulating the BH_4 / BH_2 ratio and eNOS coupling under conditions of low total biopterin availability *in vivo* (Crabtree *et al.*, 2009b). In another study they treated wild-type, BH_4-deficient (hph-1) and GCH1 overexpressing (GCH-Tg) mice with methotrexate to inhibit BH_4 recycling by DHFR. Methotrexate treatment resulted in a

substantial elevation in BH_2 and a decreased BH_4 / BH_2 ratio in the aortas of wild-type mice. These effects were magnified in hph-1 but diminished in GCH-Tg mice. Attenuated eNOS activity was observed in methotrexate-treated hph-1 but not wild-type or GCH-Tg mice, suggesting that inhibition of DHFR in BH_4-deficient states leads to eNOS uncoupling (Crabtree *et al.*, 2011a).

In the present study, DEX time- and concentration-dependently decreased the expression of DHFR mRNA (Figure 4.40) and protein (Figure 4.41) in EA.hy 926 cells. GR antagonist RU486 blocked the effect of DEX effects on DHFR, indicating the role of the glucocorticoid receptor (Figure 4.42). In studies postulating that sepiapterin supplementation restores impaired endothelium-dependent relaxations (Mitchell *et al.*, 2003) or lowers elevated blood pressure eNOS-dependently (Wang *et al.*, 2008), the scientists only concentrated on decreased GCH1 expression, whereas DHFR was not considered. As long as DHFR expression is maintained, sepiapterin supplementation can lead to an increased BH_2 level via sepiapterin reductase and subsequent transformation to BH_4. Our data on the DEX effect on DHFR mRNA and protein expression indicate that sepiapterin supplementation is not necessarily beneficial in DEX-treated animals due to the reduced level of total biopterin and the downregulation of DHFR. In supporting this hypothesis, a recent paper showed that administration of sepiapterin is not effective in recoupling eNOS in DOCA-salt-induced hypertension (Youn et al., 2012). This is believed to be due to an endothelium-specific loss in the enzyme sepiapterin reductase, whereas co-administration of BH_4 and apocynin (a Nox inhibitor) is highly efficient in recoupling eNOS. This is consistent with our observations that in DEX-induced hypertension, endothelial deficiency in DHFR might contribute to uncoupling of eNOS. These data indicate that therapeutical strategies targeting different enzymes involved in BH_4 metabolism might be necessary for eNOS functionality in different types of hypertension.

5.3.6 Effect of DEX on NO Production in Endothelial Cells

NO produced by eNOS is a key mediator of vascular homoeostasis. The enzyme has been implicated in a number of cardiovascular diseases and virtually every risk factor for these appears to be associated with a reduction in endothelial generation of NO (Moncada and Higgs, 2006). Thus, reduced bioavailability of NO is considered to be one of the most important factors associated with vascular disease (Chatterjee and Catravas, 2008) such as atherosclerosis and hypertension. This may be a result of both reduced NO synthesis and increased NO inactivation by ROS (Schmidt and Alp, 2007).

In the present study, DEX treatment reduced eNOS phosphorylation at Ser^{1177} and lowered levels of biopterin, BH_2 and BH_4 and also reduced BH_4 / BH_2 ratio in human endothelial cells. All these mechanisms may lead to a reduction of eNOS-mediated NO production. Indeed, in RFL-6 reporter cell assays a highly significant time- and concentration-dependent decrease in NO production was detected (Figure 4.43).

6 Summary

Glucocorticoids (GCs) are important hormones in the regulation of metabolic homeostasis. Synthetic GCs, such as dexamethasone (DEX), play a fundamental role in the treatment of inflammatory diseases. There are numerous side effects of a DEX therapy, e.g. the development of hypertension, in whose pathogenesis oxidative stress is a crucial factor. Although numerous studies in recent years addressed the question how GCs induce hypertension, precise mechanisms still remain unknown. An increased expression of Nox enzymes and an uncoupling of endothelial NO synthase (eNOS), the main sources of reactive oxygen species (ROS) in the vascular system, significantly contributes to the pathogenesis of cardiovascular diseases, thus a participation of these enzymes in GC-induced oxidative stress seemed likely. Therefore, we hypothesized that NADPH oxidases (Nox) and an uncoupled eNOS are most the promising enzymes among the numerous different pro- and anti-oxidative enzymes involved. Focusing on those two systems, the present study investigated the effect of DEX in both *in vivo* (WKY rats) as well as *in vitro* experiments (A7r5 and EA.hy 926 cells). Nox1, Nox4 and $p22^{phox}$ were found to be differentially regulated by DEX with Nox1 being upregulated, Nox4 downregulated and $p22^{phox}$ unchanged. This regulation seems to occur at both transcriptional and post-transcriptional levels. As Nox1 and Nox4 were reciprocally regulated by DEX, the net effect of the different Nox enzymes is uncertain. There is increasing evidence implicating vascular oxidative stress in the pathogenesis of glucocorticoid-induced hypertension (GC-HT), leading to decreased nitric oxide (NO) bioavailability. NO generated by the eNOS is an essential protective factor of the vasculature. A reduced NO bioavailability might be the consequence of a possibly uncoupled eNOS, triggered by elevated oxidative stress. Since tetrahydrobiopterin (BH_4) availability is a crucial regulator of eNOS activity and enzymatic coupling, this study addressed modifications in the supply of BH_4 through GCs. DEX treatment of EA.hy 926 cells caused a time- and concentration-dependent downregulation of eNOS on mRNA and protein level and diminished its phosphorylation at $serine^{1177}$. BH_4 as the major “coupling switch” can be synthesized endogenously by two different pathways, depending on GCH1 and DHFR as the rate

limiting enzymes. In a time- and concentration-dependent manner DEX decreased BH_4, BH_2 and total biopterin levels, as well as the BH_4 / BH_2 ratio. Both enzymes GCH1 and DHFR were downregulated on mRNA and also protein level, showing that GCs affect both BH_4-producing pathways. Also NO production was massively decreased after DEX treatment. In ROS measurements, we found a tendency of eNOS uncoupling. Clear evidence for eNOS uncoupling, however, could not be demonstrated under our experimental setting.

In summary, GC treatment leads to changes in both the vascular NADPH oxidase and the eNOS-NO system. DEX upregulates Nox1 in smooth muscle cells and reduces Nox4 in endothelial cells. In parallel, DEX decreases BH_4 availability and inhibits eNOS phosphorylation / activity. The ultimate contribution of Nox enzymes and uncoupled eNOS to oxidative stress in GC-HT needs to be clarified in future studies.

7 Zusammenfassung

Glukokortikoide (GCs) stellen wichtige Hormone in der Regulation der metabolischen Homöostase dar. Synthetische GCs, wie Dexamethasone (DEX), spielen eine essentielle Rolle in der Behandlung inflammatorischer Krankheiten. Jedoch sind unter einer Dexamethason-Therapie zahlreiche Nebenwirkungen bekannt, so z.B. auch die Entwicklung einer Hypertonie, in deren Pathogenese oxidativer Stress eine entscheidende Rolle spielt. Obwohl sich in den vergangenen Jahren zahlreiche Studien zum Ziel setzten die GC-induzierte Hypertonie (GC-HT) aufzuklären, sind die genauen Mechanismen bis heute unklar. Eine erhöhte Expression von NADPH Oxidasen (Nox) und eine Entkopplung der endothelialen NO Synthase (eNOS), die Hauptquellen reaktiver Sauerstoffspezies (ROS) im vaskulären System, tragen maßgeblich zur Pathogenese kardiovaskulärer Erkrankungen bei. Daher ist eine Beteiligung dieser Enzyme in GC-induziertem oxidativen Stress sehr wahrscheinlich. Folglich wurde die Hypothese aufgestellt, dass NADPH Oxidasen und eine entkoppelte eNOS die vielversprechendsten unter den zahlreichen involvierten pro- und anti-oxidativen Enzymen sind. Mit Fokus auf die oben genannten Systeme wurde in der vorliegenden Studie der Effekt von DEX mit Hilfe von *in vivo* (WKY Ratten) ebenso wie *in vitro* Experimenten (A7r5 und EA.hy 926 Zellen) untersucht. Dabei zeigte sich, dass Nox1, Nox4 und $p22^{phox}$ durch DEX unterschiedlich reguliert wurden. Nox1 wurde hoch-, Nox4 hingegen herunterreguliert, während $p22^{phox}$ unverändert blieb. Die Modufikation schien hierbei auf transkriptioneller und post-transkriptioneller Ebene stattzufinden. Durch die gegensätzliche Regulation von Nox1 und Nox4 bleibt die Nettowirkung der verschiedenen Nox Isoformen unklar. Immer mehr Studien bringen vaskulären oxidativen Stress mit der Pathogenese einer GC-HT in Zusammenhang, welche letztendlich zu einer verminderten Bioverfügbarkeit von Stickstoffmonoxid (NO) führt. Durch die eNOS produziertes NO stellt einen essentiellen Schutzfaktor der Blutgefäße dar. Eine verminderte NO-Bioverfügbarkeit könnte die Folge einer eNOS-Entkopplung darstellen, ausgelöst durch oxidativen Stress. Da die Verfügbarkeit von Tetrahydrobiopterin (BH_4) entscheident ist für die Aktivität und enzymatische Kopplung der eNOS, beschäftigt sich die vorliegende Arbeit mit GC-induzierten Veränderungen in der BH_4-Versorgung. Die Behandlung von EA.hy 926 Zellen mit DEX

führte zu einer zeit- und konzentrationsabhängigen Herunterregulation von eNOS auf mRNA- und Proteinebene. Gleichzeitig wurde die Phosphorylierung an Serine^{1177} vermindert. Als maßgeblicher "Kopplungs-Schalter" kann BH_4 endogen über zwei verschiedene Signalwege synthetisiert werden, welche durch die Enzyme GCH1 und DHFR reguliert werden. DEX führte zu einer zeit- und konzentrationsabhängigen Herunterregulation von BH_4, BH_2 und Biopterin, wobei ebenso das BH_4 / BH_2 -Verhältnis vermindert wurde. Beide Enzyme, GCH1 genauso wie DHFR, wurden auf mRNA- und Proteinebene herunterreguliert, was auf einen Effekt von GCs auf beide BH_4-produzierenden Signalwege schließen lässt. Nach Behandlung mit DEX wurde die Produktion von NO in Endothelzellen maßgeblich vermindert. In ROS-Messungen zeigte sich eine Tendenz hin zu einer eNOS-Entkopplung, jedoch war es mit unserem experimentellen Aufbau nicht möglich, diese endgültig zu beweisen.

Zusammenfassend lässt sich sagen, dass die Behandlung mit GCs zu Veränderungen in beiden untersuchten Systemen, den NADPH Oxidasen ebenso wie dem eNOS-NO System, führte. DEX erhöhte die Expression von Nox1 in glatten Muskelzellen und reduzierte die Nox4-Expression in Endothelzellen. Gleichzeitig verminderte DEX die Verfügbarkeit von BH_4 und inhibierte die Phosphorylierung / Aktivität von eNOS. Mithilfe weiterer Studien muss die endgültige Beteiligung von NADPH Oxidasen und einer eNOS-Entkopplung an oxidativem Stress in GC-HT abschließend aufgeklärt werden.

Bibliography

Ago, T. et al., 2004. Nox4 as the major catalytic component of an endothelial NAD(P)H oxidase. *Circulation*, 109(2), pp.227–233.

Aicher, A. et al., 2003. Essential role of endothelial nitric oxide synthase for mobilization of stem and progenitor cells. *Nature Medicine*, 9(11), pp.1370–1376.

Alheid, U. et al., 1987. Endothelium-derived relaxing factor from cultured human endothelial cells inhibits aggregation of human platelets. *Thrombosis Research*, 47(5), pp.561–571.

Alp, N. J. & Channon, K. M., 2004. Regulation of endothelial nitric oxide synthase by tetrahydrobiopterin in vascular disease. *Arteriosclerosis, Thrombosis, and Vascular Biology*, 24(3), pp.413–420.

Altenhöfer, S. et al., 2012. The NOX toolbox: validating the role of NADPH oxidases in physiology and disease. *Cellular and Molecular Life Sciences*, 69(14), pp.2327–2343.

Ambasta, R. K. et al., 2004. Direct interaction of the novel Nox proteins with p22phox is required for the formation of a functionally active NADPH oxidase. *Journal of Biological Chemistry*, 279(44), pp.45935–45941.

Arbiser, J. L. et al., 2002. Reactive oxygen generated by Nox1 triggers the angiogenic switch. *Proceedings of the National Academy of Sciences of the United States of America*, 99(2), pp.715–720.

Arnold, R. S. et al., 2007. Nox1 expression determines cellular reactive oxygen and modulates c-fos-induced growth factor, interleukin-8, and Cav-1. *American Journal of Pathology*, 171(6), pp.2021–2032.

Bachetti, T. et al., 2004. Arginase pathway in human endothelial cells in pathophysiological conditions. *Journal of Molecular and Cellular Cardiology*, 37(2), pp.515–523.

Bedard, K. & Krause, K.-H., 2007. The NOX family of ROS-generating NADPH oxidases: physiology and pathophysiology. *Physiological Reviews*, 87(1), pp.245–313.

Bendall, J. K. et al., 2005. Stoichiometric relationships between endothelial tetrahydrobiopterin, endothelial NO synthase (eNOS) activity, and eNOS coupling in vivo: insights from transgenic mice with endothelial-targeted GTP cyclohydrolase 1 and eNOS overexpression. *Circulation Research*, 97(9), pp.864–871.

Bengtsson, S. H. M. et al., 2003. Novel isoforms of NADPH oxidase in vascular physiology and pathophysiology. *Clinical and Experimental Pharmacology and Physiology*, (May), pp.849–854.

Berry, C. et al., 2001. Oxidative stress and vascular damage in hypertension. *Current Opinion in Nephrology and Hypertension*, 10(2), pp.247-255.

Biddie, S. C. et al., 2012. Dynamic regulation of glucocorticoid signalling in health and disease. *Rheumatology (Oxford, England)*, 51(3), pp.403–412.

Boo, Y. C. et al., 2002. Shear stress stimulates phosphorylation of endothelial nitric-oxide synthase at Ser1179 by Akt-independent mechanisms: role of protein kinase A. *Journal of Biological Chemistry*, 277(5), pp.3388–3396.

Bookout, A. L. et al., 2006. Anatomical profiling of nuclear receptor expression reveals a hierarchical transcriptional network. *Cell*, 126(4), pp.789–799.

Brandes, R. P. & Kreuzer, J., 2005. Vascular NADPH oxidases: molecular mechanisms of activation. *Cardiovascular Research*, 65(1), pp.16–27.

Briones, A. M. et al., 2011. Differential regulation of Nox1, Nox2 and Nox4 in vascular smooth muscle cells from WKY and SHR. *Journal of the American Society of Hypertension*, 5(3), pp.137–153.

Busse, R. et al., 1987. Endothelium-derived relaxant factor inhibits platelet activation. *Naunyn-Schmiedeberg's Archives of Pharmacology*, 336(5), pp.566–571.

Bánfi, B. et al., 2003. Two novel proteins activate superoxide generation by the NADPH oxidase NOX1. *Journal of Biological Chemistry*, 278(6), pp.3510–3513.

Cai, H. et al., 2001. Induction of Endothelial NO Synthase by Hydrogen Peroxide via a Ca2+/Calmodulin-Dependent Protein Kinase II/Janus Kinase 2-Dependent Pathway. *Arteriosclerosis, Thrombosis, and Vascular Biology*, 21(10), pp.1571–1576.

Cai, H. & Harrison, D. G., 2000. Endothelial Dysfunction in Cardiovascular Diseases: The Role of Oxidant Stress. *Circulation Research*, 87, pp.840-844.

Carletti, M. et al., 2007. Serum antioxidant enzyme activities and oxidative stress parameters as possible biomarkers of exposure in veal calves illegally treated with dexamethasone. *Toxicology in vitro : an International Journal Published in Association with BIBRA*, 21(2), pp.277–283.

Cayatte, A. J. et al., 1994. Chronic inhibition of nitric oxide production accelerates neointima formation and impairs endothelial function in hypercholesterolemic rabbits. *Arteriosclerosis, Thrombosis, and Vascular Biology*, 14(5), pp.753–759.

Chandel, N. S. et al., 2000. Role of oxidants in NF-kappa B activation and TNF-alpha gene transcription induced by hypoxia and endotoxin. *Journal of Immunology (Baltimore, Md.: 1950)*, 165(2), pp.1013–1021.

Chatterjee, A. & Catravas, J. D., 2008. Endothelial nitric oxide (NO) and its pathophysiologic regulation. *Vascular Pharmacology*, 49, pp.134–140.

Chen, A. F. et al., 2012. Free radical biology of the cardiovascular system. *Clinical Science (London, England : 1979)*, 123(2), pp.73–91.

Chen, W. et al., 2008. A possible biochemical link between NADPH oxidase (Nox) 1 redox-signalling and ERp72. *Biochemical Journal*, 416(1), pp.55–63.

Comini, L. et al., 1996. Aorta and skeletal muscle NO synthase expression in experimental heart failure. *Journal of Molecular and Cellular Cardiology*, 28(11), pp.2241–2248.

Cosentino, F. & Lüscher, T. F., 1999. Tetrahydrobiopterin and endothelial nitric oxide synthase activity. *Cardiovascular Research*, 43(2), pp.274–278.

Crabtree, M. J. et al., 2009. Critical role for tetrahydrobiopterin recycling by dihydrofolate reductase in regulation of endothelial nitric-oxide synthase coupling: relative importance of the de novo biopterin synthesis versus salvage pathways. *Journal of Biological Chemistry*, 284(41), pp.28128–28136.

Crabtree, M. J. et al., 2009. Quantitative regulation of intracellular endothelial nitric-oxide synthase (eNOS) coupling by both tetrahydrobiopterin-eNOS stoichiometry and biopterin redox status: insights from cells with tet-regulated GTP cyclohydrolase I expression. *Journal of Biological Chemistry*, 284(2), pp.1136–1144.

Crabtree, M. J. et al., 2008. Ratio of 5,6,7,8-tetrahydrobiopterin to 7,8-dihydrobiopterin in endothelial cells determines glucose-elicited changes in NO vs. superoxide production by eNOS. *American Journal of Physiology - Heart and Circulatory Physiology*, 294(4), pp.1530–1540.

Crabtree, M. J. & Channon, K. M., 2011. Synthesis and recycling of tetrahydrobiopterin in endothelial function and vascular disease. *Nitric Oxide: Biology and Chemistry*, 25(2), pp.81–88.

Crabtree, M. J. et al., 2011. Dihydrofolate reductase protects endothelial nitric oxide synthase from uncoupling in tetrahydrobiopterin deficiency. *Free Radical Biology & Medicine*, 50(11), pp.1639–1646.

Crawford, D. R. & Davies, K. J., 1994. Adaptive response and oxidative stress. *Environmental Health Perspectives*, 102, pp.25–28.

Cui, X. et al., 2006. Expression of NADPH Oxidase Isoform 1 (Nox1) in Human Placenta: Involvement in Preeclampsia. *Placenta*, 27, pp.422–431.

Dikalova, A. et al., 2005. Nox1 overexpression potentiates angiotensin II-induced hypertension and vascular smooth muscle hypertrophy in transgenic mice. *Circulation*, 112(17), pp.2668–2676.

Dimmeler, S. et al., 1999. Activation of nitric oxide synthase in endothelial cells by Akt-dependent phosphorylation. *Nature*, 399(6736), pp.601–605.

Dimmeler, S. & Zeiher, A. M., 1999. Nitric oxide - an endothelial cell survival factor. *Cell Death and Differentiation*, 6(10), pp.964–968.

Dodd, S. et al., 2010. ROS-mediated activation of NF-κB and Foxo during muscle disuse. *Muscle Nerve*, 41(1), pp.110–113.

Drexler, H. et al., 1991. Correction of endothelial dysfunction in coronary microcirculation of hypercholesterolaemic patients by L-arginine. *The Lancet*, 338(8782-8783), pp.1546–1550.

Eatman, D. et al., 2011. The involvement of prostaglandins in the contractile function of the aorta by aldosterone. *BMC Research Notes*, 4(1), pp.125.

Ellmark, S. H. M. et al., 2005. The contribution of Nox4 to NADPH oxidase activity in mouse vascular smooth muscle. *Cardiovascular Research*, 65(2), pp.495–504.

Esposito, F. et al., 2003. Protein kinase B activation by reactive oxygen species is independent of tyrosine kinase receptor phosphorylation and requires SRC activity. *Journal of Biological Chemistry*, 278(23), pp.20828–20834.

Fan, C. Y. et al., 2005. PKCdelta mediates up-regulation of NOX1, a catalytic subunit of NADPH oxidase, via transactivation of the EGF receptor: possible involvement of PKCdelta in vascular hypertrophy. *Biochemical Journal*, 390(Pt 3), pp.761–767.

Fan, C. Y. et al., 2005. Transactivation of the EGF receptor and a PI3 kinase-ATF-1 pathway is involved in the upregulation of NOX1, a catalytic subunit of NADPH oxidase. *FEBS Letters*, 579(5), pp.1301–1305.

Fleming, I. et al., 2001. Phosphorylation of Thr495 Regulates Ca2+/Calmodulin-Dependent Endothelial Nitric Oxide Synthase Activity. *Circulation Research*, 88(11), pp.e68–e75.

Fortuño, A. et al., 2005. Oxidative stress and vascular remodelling. *Experimental Physiology*, 90(4), pp.457–462.

Furchgott, R., 1988. Studies on relaxation of rabbit aorta by sodium nitrite: the basis for the proposal that the acid-activatable inhibitory factor from retractor penis is inorganic nitrite and the endothelium-derived relaxing factor is nitric oxide. *Vasodilatation: Vascular Smooth Muscle, Peptides, Autonomic Nerves and Endothelium, ed. Vanhoutte, P.M., New York: Raven Press*, pp.401–414.

Furchgott, R. F. et al., 1984. Endothelial cells as mediators of vasodilation of arteries. *Journal of Cardiovascular Pharmacology*, 6 Suppl 2, pp.S336–343.

Furchgott, R. F. & Zawadzki, J. V., 1980. The obligatory role of endothelial cells in the relaxation of arterial smooth muscle by acetylcholine. *Nature*, 288(5789), pp.373–376.

Förstermann, U. et al., 1991. Calmodulin-dependent endothelium-derived relaxing factor/nitric oxide synthase activity is present in the particulate and cytosolic fractions of bovine aortic endothelial cells. *Proceedings of the National Academy of Sciences of the United States of America*, 88(5), pp.1788–1792.

Förstermann, U. et al., 1995. Isoforms of nitric oxide synthase: Properties, cellular distribution and expressional control. *Biochemical Pharmacology*, 50(9), pp.1321–-1332.

Förstermann, U. et al., 1994. Nitric oxide synthase isozymes. Characterization, purification, molecular cloning, and functions. *Nitric Oxide: Biology and Chemistry*, pp.1121–1131.

Förstermann, U. et al., 1989. The cytosol of N1E-115 neuroblastoma cells synthesizes an EDRF-like substance that relaxes rabbit aorta. *Naunyn-Schmiedeberg's Archives of Pharmacology*, 340, pp.771–774.

Förstermann, U. & Kleinert, H., 1995. Nitric oxide synthase: expression and expressional control of the three isoforms. *Naunyn-Schmiedeberg's Archives of Pharmacology*, 352(4), pp.351–364.

Förstermann, U., 2010. Nitric oxide and oxidative stress in vascular disease. *Pflügers Archiv: European Journal of Physiology*, 459(6), pp.923–939.

Förstermann, U. & Li, H., 2012. Nitric Oxide: Biological Synthesis and Functions, *Gasotransmitters: Physiology and Pathophysiology*, Springer-Verlag Berlin Heidelberg, Book DOI 10.1007/978-3-642-30338-8, Book ISBN: 978-3-642-30337-1

Förstermann, U. & Münzel, T., 2006. Endothelial nitric oxide synthase in vascular disease: from marvel to menace. *Circulation*, 113(13), pp.1708–1714.

Förstermann, U. & Sessa, W. C., 2011. Nitric oxide synthases: regulation and function. *European Heart Journal*, 33(7), pp.829–837.

Gao, Y. T. et al., 2007. Oxygen metabolism by endothelial nitric-oxide synthase. *Journal of Biological Chemistry*, 282(39), pp.28557–28565.

Garg, U., 1989. Nitric Oxide-generating Vasodilators and 8-Bromo-Cyclic Guanosine Monophosphate Inhibit Mitogenesis and Proliferation of Cultured Rat Vascular Smooth Muscle Cells. *Journal of Clinical Investigation*, 83(May), pp.1774–1777.

Geiszt, M. et al., 2000. Identification of renox, an NAD(P)H oxidase in kidney. *Proceedings of the National Academy of Sciences of the United States of America*, 97(14), pp.8010–8014.

Geiszt, M., 2006. NADPH oxidases: new kids on the block. *Cardiovascular Research*, 71(2), pp.289–299.

Geiszt, M. & Leto, T. L., 2004. The Nox family of NAD(P)H oxidases: host defense and beyond. *Journal of Biological Chemistry*, 279(50), pp.51715–51718.

Goodwin, J. E. & Geller, D. S., 2012. Glucocorticoid-induced hypertension. *Pediatric Nephrology (Berlin, Germany)*, 27(7), pp.1059–1066.

Griendling, K. K., 2004. Novel NAD(P)H oxidases in the cardiovascular system. *Heart*, 90(5), pp.491–493.

Guzik, T. J. et al., 2004. Systemic regulation of vascular NAD(P)H oxidase activity and nox isoform expression in human arteries and veins. *Arteriosclerosis, Thrombosis, and Vascular Biology*, 24(9), pp.1614–1620.

Hanna, I.et al., 2004. Functional association of nox1 with p22phox in vascular smooth muscle cells. *Free Radical Biology and Medicine*, 37(10), pp.1542-1549.

Heitzer, T. et al., 2000. Tetrahydrobiopterin improves endothelium-dependent vasodilation by increasing nitric oxide activity in patients with Type II diabetes mellitus . *Diabetologia*, 43, pp.1435–1438.

Heitzer, T. et al., 2001. Endothelial Dysfunction, Oxidative Stress, and Risk of Cardiovascular Events in Patients With Coronary Artery Disease. *Circulation*, 104(22), pp.2673–2678.

Heitzer, T. et al., 2000. Tetrahydrobiopterin Improves Endothelium-Dependent Vasodilation in Chronic Smokers Evidence for a Dysfunctional Nitric Oxide Synthase. *Circulation Research*, 86, pp.e36-e41.

Helmcke, I. et al., 2009. Identification of structural elements in Nox1 and Nox4 controlling localization and activity. *Antioxidants & Redox Signaling*, 11(6), pp.1279–1287.

Higashi, Y. et al., 2002. Tetrahydrobiopterin enhances forearm vascular response to acetylcholine in both normotensive and hypertensive individuals. *Journal of Hypertension*, 15, pp.326–332.

Hilenski, L. L. et al., 2004. Distinct subcellular localizations of Nox1 and Nox4 in vascular smooth muscle cells. *Arteriosclerosis, Thrombosis, and Vascular Biology*, 24(4), pp.677–683.

Hink, U. et al., 2001. Mechanisms Underlying Endothelial Dysfunction in Diabetes Mellitus. *Circulation Research*, 88, pp.e14-e22.

Hogan, M. & Cerami, A., 1992. Advanced Glycosylation Endproducts Block the Antiproliferative Effect of Nitric Oxide Role in the Vascular and Renal Complications of Diabetes Mellitus. *Journal of Clinical Investigation*, (1110), pp.1110–1115.

Hong, H.-J. et al., 2001. Supplemention With Tetrahydrobiopterin Suppresses the Development of Hypertension in Spontaneously Hypertensive Rats. *Hypertension*, 38(5), pp.1044–1048.

Hu, L. et al., 2006. Apocynin but not L-arginine prevents and reverses dexamethasone-induced hypertension in the rat. *American Journal of Hypertension*, 19(4), pp.413–418.

Huang, P. L. et al., 1995. Hypertension in mice lacking the gene for endothelial nitric oxide synthase. *Nature*, 377(6546), pp.239–242.

Ignarro, L. et al., 1987. Endothelium-derived relaxing factor produced and released from artery and vein is nitric oxide. *Proceedings of the National Academy of Sciences*, 84, pp.9265–9269.

Ignarro, L. et al., 1988. Biochemical and pharmacological properties of endothelium-derived relaxing factor and its similarity to nitric oxide radical. *Vasodilatation: Vascular Smooth Muscle, Peptide, Autonomic Nerves and Endothelium, ed. Vanhoutte, P.M., New York: Raven Press*, pp.427–436.

Iuchi, T., 2003. Glucocorticoid Excess Induces Superoxide Production in Vascular Endothelial Cells and Elicits Vascular Endothelial Dysfunction. *Circulation Research*, 92(1), pp.81–87.

Janssens, S.et al., 1992. Cloning and expression of a cDNA encoding human endothelium-derived relaxing factor/nitric oxide synthase. *Journal of Biological Chemistry*, 267(21), pp.14519–14522.

John, S. et al., 2009. Kinetic complexity of the global response to glucocorticoid receptor action. *Endocrinology*, 150(4), pp.1766–1774.

Kamata, T., 2009. Roles of Nox1 and other Nox isoforms in cancer development. *Cancer Science*, 100(8), pp.1382–1388.

Kano, H. et al., 1999. A HMG-CoA reductase inhibitor improved regression of atherosclerosis in the rabbit aorta without affecting serum lipid levels: possible relevance of up-regulation of endothelial NO synthase mRNA. *Biochemical and Biophysical Research Communications*, 259(2), pp.414–419.

Kar, S. & Kavdia, M., 2011. Modeling of biopterin-dependent pathways of eNOS for nitric oxide and superoxide production. *Free Radical Biology & Medicine*, 51(7), pp.1411–1427.

Katsuyama, M. et al., 2005. Essential role of ATF-1 in induction of NOX1, a catalytic subunit of NADPH oxidase: involvement of mitochondrial respiratory chain. *Biochemical Journal*, 386(Pt 2), pp.255–261.

Katusic, Z. S. et al., 2009. Vascular protection by tetrahydrobiopterin: progress and therapeutic prospects. *Trends in Pharmacological Sciences*, 30(1), pp.48–54.

Kauser, K. et al., 2000. Role of endogenous nitric oxide in progression of atherosclerosis in apolipoprotein E-deficient mice. *American Journal of Physiology - Heart and Circulatory Physiology*, 278, pp.H1679–H1685.

Kerr, S. et al., 1999. Superoxide anion production is increased in a model of genetic hypertension: role of the endothelium. *Hypertension*, pp.1353–1358.

Kobayashi, T. & Kamata, K., 2001. Effect of chronic insulin treatment on NO production and endothelium-dependent relaxation in aortae from established STZ-induced diabetic rats. *Atherosclerosis*, 155(2), pp.313–320.

Krause, K.-H., 2004. Tissue distribution and putative physiological function of NOX family NADPH oxidases. *Japanese Journal of Infectious Diseases*, 57(5), pp.S28–29.

Kubes, P. et al., 1991. Nitric oxide: an endogenous modulator of leukocyte adhesion. *Proceedings of the National Academy of Sciences of the United States of America*, 88(11), pp.4651–4655.

Kuhlencordt, P. J. et al., 2001. Accelerated Atherosclerosis, Aortic Aneurysm Formation, and Ischemic Heart Disease in Apolipoprotein E/Endothelial Nitric Oxide Synthase Double-Knockout Mice. *Circulation*, 104(4), pp.448–454.

Kuroda, J. et al., 2005. The superoxide-producing NAD(P)H oxidase Nox4 in the nucleus of human vascular endothelial cells. *Genes to cells: Devoted to Molecular & Cellular Mechanisms*, 10(12), pp.1139–1151.

Lambeth, J. D., 2004. NOX enzymes and the biology of reactive oxygen. *Nature Reviews. Immunology*, 4(3), pp.181–189.

Lassègue, B. et al., 2001. Novel gp91phox Homologues in Vascular Smooth Muscle Cells : nox1 Mediates Angiotensin II-Induced Superoxide Formation and Redox-Sensitive Signaling Pathways. *Circulation Research*, 88(9), pp.888–894.

Lassègue, B. & Clempus, R. E., 2003. Vascular NAD(P)H oxidases: specific features, expression, and regulation. *American Journal of Physiology. Regulatory, Integrative and Comparative Physiology*, 285(2), pp.R277–297.

Laursen, J. et al., 2001. Endothelial regulation of vasomotion in apoE-deficient mice: implications for interactions between peroxynitrite and tetrahydrobiopterin. *Circulation*, pp.1282–1288.

Li, H. & Förstermann, U., 2000. Nitric oxide in the pathogenesis of vascular disease. *Journal of Pathology*, 190(3), pp.244–254.

Li, H. & Förstermann, U., 2009. Prevention of atherosclerosis by interference with the vascular nitric oxide system. *Current Pharmaceutical Design*, 15(27), pp.3133–3145.

Li, H. et al., 2002. Physiological mechanisms regulating the expression of endothelial-type NO synthase. *Nitric Oxide: Biology and Chemistry*, 7(2), pp.132–147.

Martyn, K. D. et al., 2006. Functional analysis of Nox4 reveals unique characteristics compared to other NADPH oxidases. *Cellular Signalling*, 18(1), pp.69–82.

McCabe, T.J . et al., 2000. Enhanced electron flux and reduced calmodulin dissociation may explain “calcium-independent” eNOS activation by phosphorylation. *Journal of Biological Chemistry*, 275(9), pp.6123–6128.

McNally, J. S. et al., 2003. Role of xanthine oxidoreductase and NAD(P)H oxidase in endothelial superoxide production in response to oscillatory shear stress. *American Journal of Physiology - Heart and Circulatory Physiology*, 285(6), pp.H2290–2297.

Michel, T. & Feron, O., 1997. Nitric Oxide Synthases: Which, Where, How, and Why? *Journal of Clinical Investigation*, 100(9), pp.2146–2152.

Ming, X.-F. et al., 2004. Thrombin stimulates human endothelial arginase enzymatic activity via RhoA/ROCK pathway: implications for atherosclerotic endothelial dysfunction. *Circulation*, 110(24), pp.3708–3714.

Mitchell, B. M. et al., 2003. GTP cyclohydrolase 1 downregulation contributes to glucocorticoid hypertension in rats. *Hypertension*, 41(3 Pt 2), pp.669–674.

Mitchell, B. M. & Webb, C., 2005. Glucocorticoid-Induced Hypertension and Tetrahydrobiopterin (BH4), a Common Cofactor for the Production of Vasoactive Molecules. *Current Hypertension Reviews*, 1(1), pp.1–6.

Mitsushita, J. et al., 2004. The superoxide-generating oxidase Nox1 is functionally required for Ras oncogene transformation. *Cancer Research*, 64(10), pp.3580–3585.

Moat, S. et al., 2006. Folic acid reverses endothelial dysfunction induced by inhibition of tetrahydrobiopterin biosynthesis. *European Journal of Pharmacology*, 530(3), pp.250258.

Moe, K. et al., 2006. Differential upregulation of Nox homologues of NADPH oxidase by tumor necrosis factor-α in human aortic smooth muscle and embryonic kidney cells. *Journal of Cellular and Molecular Medicine*, 10(1), pp.231239.

Mollnau, H., 2002. Effects of Angiotensin II Infusion on the Expression and Function of NAD(P)H Oxidase and Components of Nitric Oxide/cGMP Signaling. *Circulation Research*, 90(4), pp.58e–65.

Moncada S. et al., 1989. Biosynthesis of nitric oxide from L-arginine. A pathway for the regulation of cell function and communication. *Biochemical Pharmacology*, 38(11), pp.1709-1715.

Moncada, S. & Higgs, E., 2006. The discovery of nitric oxide and its role in vascular biology. *British Journal of Pharmacology*, 147, pp.S193–201.

Montezano, A. C. & Touyz, R. M., 2012. Oxidative stress, Noxs, and hypertension: Experimental evidence and clinical controversies. *Annals of Medicine*, 44, pp.S2–S16.

Morillas, P. et al., 2012. Inflammation and Apoptosis in Hypertension. Relevance of the Extent of Target Organ Damage. *Revista Espanola de Cardiologia*, Epub ahead of print.

Mueller, C. F. H. et al., 2005. ATVB in focus: redox mechanisms in blood vessels. *Arteriosclerosis, Thrombosis, and Vascular Biology*, 25(2), pp.274–278.

Munck, A. et al., 1984. Physiological functions of glucocorticoids in stress and their relation to pharmacological actions. *Endocrine Reviews*, 5(1), pp.25–44.

Murad, F. et al., 1978. Guanylate cyclase: activation by azide, nitro compounds, nitric oxide, and hydroxyl radical and inhibition by hemoglobin and myoglobin. *Advances in Cyclic Nucleotide Research*, 9, pp.145–158.

Nakaki, T. et al., 1990. Inhibition by nitric oxide and nitric oxide-producing vasodilators of DNA synthesis in vascular smooth muscle cells. *European Journal of Pharmacology*, 189(6), pp.347–353.

Oemar, B. et al., 1998. Reduced endothelial nitric oxide synthase expression and production in human atherosclerosis. *Circulation*, pp.2494–2498.

Ong, S. L. H. et al., 2007. Role of xanthine oxidase in dexamethasone-induced hypertension in rats. *Clinical and Experimental Pharmacology & Physiology*, 34(5-6), pp.517–519.

Ong, S. L. H. & Whitworth, J. A., 2011. How do glucocorticoids cause hypertension: role of nitric oxide deficiency, oxidative stress, and eicosanoids. *Endocrinology and Metabolism Clinics of North America*, 40(2), pp.393–407.

Ong, S. L. H. et al., 2009. Mechanisms of Dexamethasone-Induced Hypertension. *Current Hypertension Reviews*, 5(1), pp.61-74.

Park, H. et al., 2004. Sequential Activation of Phosphatidylinositol 3-Kinase, beta-Pix, Rac1, and Nox1 in Growth Factor-Induced Production of H2O2. *Molecular and Cellular Biology*, 24(10), pp.4384–4394.

Patterson, C.et al., 2000. The Oxidative Paradox : Another Piece in the Puzzle. *Circulation Research*, pp.1074–1076.

Pedruzzi, E. et al., 2004. NAD (P) H oxidase Nox-4 mediates 7-ketocholesterol-induced endoplasmic reticulum stress and apoptosis in human aortic smooth muscle cells. *Molecular and Cellular Biology*, 24(24), pp.10703–10717.

Pollock, J. S. et al., 1993. Characterization and localization of endothelial nitric oxide synthase using specific monoclonal antibodies. *American Journal of Physiology*, 265, pp.C1379–1387.

Pritchard, K.et al., 1995. Native low-density lipoprotein increases endothelial cell nitric oxide synthase generation of superoxide anion. *Circulation*, 77(3), pp.510-518.

Rajashree, S. & Puvanakrishnan, R., 1999. Dexamethasone induced alterations in the levels of proteases involved in blood pressure homeostasis and blood coagulation in rats. *Molecular and Cellular Biochemistry*, 197(1-2), pp.203–208.

Rapoport, R. M. et al., 1983. Endothelium-dependent relaxation in rat aorta may be mediated through cyclic GMP-dependent protein phosphorylation. *Nature*, 306(5939), pp.174–176.

Rössig, L. et al., 2002. Inhibitors of Histone Deacetylation Downregulate the Expression of Endothelial Nitric Oxide Synthase and Compromise Endothelial Cell Function in Vasorelaxation and Angiogenesis. *Circulation Research*, 91(9), pp.837–844.

Sasaki, K. et al., 2006. Ex vivo pretreatment of bone marrow mononuclear cells with endothelial NO synthase enhancer AVE9488 enhances their functional activity for cell therapy. *Proceedings of the National Academy of Sciences of the United States of America*, 103(39), pp.14537–14541.

Schmidt, T. S. & Alp, N. J., 2007. Mechanisms for the role of tetrahydrobiopterin in endothelial function and vascular disease. *Clinical Science (London, England : 1979)*, 113(2), pp.47–63.

Schramm, A. et al., 2012. Targeting NADPH oxidases in vascular pharmacology. *Vascular Pharmacology*, 56(5-6), pp.216–231.

Schröder, K. et al., 2012. Nox4 is a protective reactive oxygen species generating vascular NADPH oxidase. *Circulation Research*, 110(9), pp.1217–1225.

Schwemmer, M. et al., 2000. Cardiovascular dysfunction in hypercholesterolemia associated with enhanced formation of AT1-receptor and of eicosanoids. *Journal of Cardiovascular Pharmacology and Therapeutics*, 5(1), pp.59–68.

Schäfer, M. et al., 2003. Signaling of hypoxia-induced autonomous proliferation of endothelial cells. *FASEB journal : official publication of the Federation of American Societies for Experimental Biology*, 17(3), pp.449–451.

Searles, C. D., 2006. Transcriptional and posttranscriptional regulation of endothelial nitric oxide synthase expression. *American journal of physiology. Cell Physiology*, 291(5), pp.C803–816.

Sedeek, M. et al., 2009. Molecular mechanisms of hypertension: role of Nox family NADPH oxidases. *Current Opinion in Nephrology and Hypertension*, 18(2), pp.122–127.

Sendelbeck, L. R. & Yates, F. E., 1970. Adrenal cortical and medullary hormones in recovery of tissues from local injury. *American Journal of Physiology*, 219(4), pp.845–853.

Shinozaki, K. et al., 1999. Abnormal biopterin metabolism is a major cause of impaired endothelium-dependent relaxation through nitric oxide/O2- imbalance in insulin-resistant rat aorta. *Diabetes*, 48(12), pp.2437–2445.

Sirker, A. et al., 2011. NADPH oxidases in cardiovascular disease: insights from in vivo models and clinical studies. *Basic Research in Cardiology*, 106(5), pp.735–747.

Slater, A. F. et al., 1995. Signalling mechanisms and oxidative stress in apoptosis. *Toxicology Letters*, 82-83, pp.149–153.

So, A. Y.-L. et al., 2007. Determinants of cell- and gene-specific transcriptional regulation by the glucocorticoid receptor. *PLoS Genetics*, 3(6), pp.927-938.

Sorescu, D. et al., 2002. Superoxide Production and Expression of Nox Family Proteins in Human Atherosclerosis. *Circulation*, 105(12), pp.1429–1435.

Stein, B. & Eschenhagen, T., 1998. Increased expression of constitutive nitric oxide synthase III, but not inducible nitric oxide synthase II, in human heart failure. *Journal of the American College of Cardiology*, 32(5), pp.1179-1186.

Stroes, E. et al., 1997. Tetrahydrobiopterin restores endothelial function in hypercholesterolemia. *Journal of Clinical Investigation*, 99(1), pp.41–46.

Stuehr, D. et al., 2001. Oxygen reduction by nitric-oxide synthases. *Journal of Biological Chemistry*, 276(18), pp.14533–14536.

Stulak, J. M. et al., 2001. Impaired renal vascular endothelial function in vitro in experimental hypercholesterolemia. *Atherosclerosis*, 154(1), pp.195–201.

Sturrock, A. et al., 2006. Transforming growth factor-beta1 induces Nox4 NAD(P)H oxidase and reactive oxygen species-dependent proliferation in human pulmonary artery smooth muscle cells. *American Journal of Physiology. Lung Cellular and Molecular Physiology*, 290(4), pp.L661–L673.

Sugiyama, T. et al., 2009. Tetrahydrobiopterin Recycling, a Key Determinant of Endothelial Nitric-oxide Synthase-dependent Signaling Pathways in Cultured Vascular Endothelial Cells. *Journal of Biological Chemistry*, 284(19), pp.12691–12700.

Taddei, S. et al., 1998. Vitamin C Improves Endothelium-Dependent Vasodilation by Restoring Nitric Oxide Activity in Essential Hypertension. *Circulation*, 97(22), pp.2222–2229.

Takase, H. et al., 2000. Long-term effect of antihypertensive therapy with calcium antagonist or angiotensin converting enzyme inhibitor on serum nitrite/nitrate levels in human essential hypertension. *Arzneimittelforschung*, 50(6), pp.530–534.

Thannickal, V. J. & Fanburg, B. L., 2000. Reactive oxygen species in cell signaling. *American Journal of Physiology - Lung Cellular and Molecular Physiology*, 279, pp.1005–1028.

Thida, M. et al., 2010. Effects of Sepiapterin Supplementation and NOS Inhibition on Glucocorticoid-Induced Hypertension. *American Journal of Hypertension*, 23(5), pp.569-574.

Tiefenbacher, C. P. et al., 2000. Endothelial Dysfunction of Coronary Resistance Arteries Is Improved by Tetrahydrobiopterin in Atherosclerosis. *Circulation*, 102(18), pp.2172–2179.

Ting, H. H. et al., 1996. Vitamin C improves endothelium-dependent vasodilation in patients with non-insulin-dependent diabetes mellitus. *Journal of Clinical Investigation*, 97(1), pp.22–28.

Touyz, R. M. & Schiffrin, E. L., 2004. Reactive oxygen species in vascular biology: implications in hypertension. *Histochemistry and Cell Biology*, 122(4), pp.339–352.

Vásquez-Vivar, J. et al., 2002. The ratio between tetrahydrobiopterin and oxidized tetrahydrobiopterin analogues controls superoxide release from endothelial nitric oxide synthase: an EPR spin trapping study. *Biochemical Journal*, 739(362), pp.733–739.

Walker, B. R., 2007. Glucocorticoids and cardiovascular disease. *European Journal of Endocrinology*, 157(5), pp.545–559.

Wallerath, T. et al., 1999. Down-regulation of the expression of endothelial NO synthase is likely to contribute to glucocorticoid-mediated hypertension. *Proceedings of the National Academy of Sciences of the United States of America*, 96(23), pp.13357–13362.

Wallerath, T. et al., 2004. Dexamethasone lacks effect on blood pressure in mice with a disrupted endothelial NO synthase gene. *Nitric Oxide: Biology and Chemistry*, 10(1), pp.36–41.

Wallwork, C. et al., 2003. Xanthine oxidase activity in the dexamethasone-induced hypertensive rat. *Microvascular Research*, 66(1), pp.30–37.

Wang, S. et al., 2008. Acute inhibition of guanosine triphosphate cyclohydrolase 1 uncouples endothelial nitric oxide synthase and elevates blood pressure. *Hypertension*, 52(3), pp.484–490.

Wang, Y. et al., 2007. The role of the NADPH oxidase complex, p38 MAPK, and Akt in regulating human monocyte/macrophage survival. *American Journal of Respiratory Cell and Molecular Biology*, 36(1), pp.68–77.

Wassmann, S. et al., 2004. Modulation of oxidant and antioxidant enzyme expression and function in vascular cells. *Hypertension*, 44(4), pp.381–386.

Werner, E. R. et al., 2003. Tetrahydrobiopterin and Nitric Oxide: Mechanistic and Pharmacological Aspects. *Experimental Biology and Medicine*, 228, pp.1291-1302.

Werner-Felmayer, G. et al., 1993. Pteridine Biosynthesis in Human Endothelial Cells. *Journal of Biological Chemistry*, pp.1842–1846.

Wind, S. et al., 2010. Oxidative stress and endothelial dysfunction in aortas of aged spontaneously hypertensive rats by NOX1/2 is reversed by NADPH oxidase inhibition. *Hypertension*, 56(3), pp.490–497.

Wohlfart, P. et al., 2008. Antiatherosclerotic Effects of Small-Molecular-Weight Compounds Enhancing Endothelial Nitric-Oxide Synthase (eNOS) Expression and Preventing eNOS Uncoupling. *Journal of Pharmacology and Experimental Therapeutics*, 325(2), pp.370–379.

Wu, S. et al., 2005. Activation of AP-1 through reactive oxygen species by angiotensin II in rat cardiomyocytes. *Free Radical Biology and Medicine*, 39(12), pp.1601–1610.

Xu, W. et al., 2004. Increased arginase II and decreased NO synthesis in endothelial cells of patients with pulmonary arterial hypertension. *FASEB Journal*, 18(14), pp.1746–1748.

Yang, H. et al., 2004. Retardation of atherosclerosis by overexpression of catalase or both Cu/Zn-superoxide dismutase and catalase in mice lacking apolipoprotein E. *Circulation Research*, 95(11), pp.1075–1081.

Youn, J. Y. et al., 2012. Endothelium-specific sepiapterin reductase deficiency in DOCA-salt hypertension. *American journal of physiology. Heart and Circulatory Physiology*, 302(11), pp.H2243–2249.

Zafir, A. & Banu, N., 2009. Modulation of in vivo oxidative status by exogenous corticosterone and restraint stress in rats. *Stress (Amsterdam, Netherlands)*, 12(2), pp.167–177.

Zalba, G. et al., 2001. Oxidative Stress in Arterial Hypertension: Role of NAD(P)H Oxidase. *Hypertension*, 38(6), pp.1395–1399.

Zalba, G. et al., 2000. Vascular NADH/NADPH Oxidase Is Involved in Enhanced Superoxide Production in Spontaneously Hypertensive Rats. *Hypertension*, 35(5), pp.1055–1061.

Zhang, Y. et al., 2005. Apocynin but not allopurinol prevents and reverses adrenocorticotropic hormone-induced hypertension in the rat. *American Journal of Hypertension*, 18(7), pp.910–916.

Zhang, Y. et al., 2004. The antioxidant tempol prevents and partially reverses dexamethasone-induced hypertension in the rat. *American Journal of Hypertension*, 17(3), pp.260–265.

Zhang, Y. et al., 2007. Aspirin prevents and partially reverses adrenocorticotropic hormone-induced hypertension in the rat. *American Journal of Hypertension*, 20(11), pp.1222–1228.

Zhang, Y. et al., 2005. Vascular hypertrophy in angiotensin II-induced hypertension is mediated by vascular smooth muscle cell-derived H2O2. *Hypertension*, 46(4), pp.732–737.

Zou, M.-H., 2002. Oxidation of the zinc-thiolate complex and uncoupling of endothelial nitric oxide synthase by peroxynitrite. *Journal of Clinical Investigation*, 109(6), pp.817–826.

Publications

During the dissertation period, the following manuscripts for publication were generated:

Papers:

Tobias S*, Siuda D*, Daiber A, Schmidt H, Förstermann U, Li H (2012) "Effect of dexamethasone on vascular Nox1 expression" (in preparation)

Tobias S, Habermeier A, Daiber A, Siuda D, Reifenberg G, Xia N, Closs E, Förstermann U, Li H (2012) "Contribution of uncoupled endothelial nitric oxide synthase to dexamethasone-induced oxidative stress?" (in preparation)

Dellee U, **Tobias S**, Li H, Mildenberger E (2012) "Expression of NO synthases and redox enzymes in umbilical arteries from newborns born small, appropriate, and large for gestational age" (in revision)

Yang Q, Xue HM, Wong WT, Tian XY, Huang Y, Tsui SK, Ng PK, Wohlfart P, Li H, Xia N, **Tobias S**, Underwood MJ, He GW (2011) "AVE3085, an enhancer of endothelial nitric oxide synthase, restores endothelial function and reduces blood pressure in spontaneously hypertensive rats." Br J Pharmacol. 2011 Jul;163(5):1078-85

Spanier G, Xu H, Xia N, **Tobias S**, Deng S, Wojnowski L, Förstermann U, Li H (2009) "Resveratrol reduces endothelial oxidative stress by modulating the gene expression of superoxide dismutase 1 (SOD1), glutathione peroxidase 1 (GPx1) and NADPH oxidase subunit (Nox4)" J Physiol Pharmacol. 2009 Oct;60 Suppl 4:111-116

Meeting abstracts:

S. Tobias, A. Habermeier, A. Daiber, N. Xia, E. Closs, U. Förstermann, H. Li (2012) „Contribution of uncoupled endothelial nitric oxide synthase to dexamethasone-induced oxidative stress?“ (78. Jahrestagung der Deutschen Gesellschaft für Experimentelle und Klinische Pharmakologie und Toxikologie, Dresden, Deutschland)

S. Tobias, N. Xia, A. Daiber, U. Förstermann, H. Li (2011) “Effects of dexamethasone on rat vascular NADPH oxidases” (The 8th meeting on “Rat Genomics & Models” of the Cold Spring Harbor Laboratory, New York, USA)

U. Zillessen, **S. Tobias**, H. Li, E. Mildenberger (2011) „Expression von NO-Synthasen und pro- und anti-oxidativen Enzymen in Nabelschnurarterien von SGA-, AGA- und LGA-Neugeborenen” (25. Deutscher Kongress für Perinatale Medizin, Berlin, Deutschland)

S. Tobias, N. Xia, A. Rus, A. Daiber, U. Förstermann, H. Li (2011) „Dexamethasone upregulates Nox1 expression in vascular smooth muscle cells” (77. Jahrestagung der Deutschen Gesellschaft für Experimentelle und Klinische Pharmakologie und Toxikologie, Frankfurt a.M., Deutschland)

D. Siuda, N. Xia, **S. Tobias**, U. Förstermann, H. Li (2011) “Regulation of Nox1 expression by histone deacetylases in vascular smooth muscle cells“ (77. Jahrestagung der Deutschen Gesellschaft für Experimentelle und Klinische Pharmakologie und Toxikologie, Frankfurt a.M., Deutschland)

U. Zillessen, **S. Tobias**, H. Li, E. Mildenberger (2010) “Expression of NO synthases and redox enzymes in umbilical arteries from newborns born small, appropriate, and large for gestational age” (The 3rd Congress of the European Academy of Paediatric Societies, Kopenhagen, Dänemark)